Response to Referee #1:

We are grateful to the referee for her/his careful reading of the manuscript and for her/his corrections and suggestions. Responses to each individual comment that has been quoted […] are given here below.

General comments

1/ *[I have one general comment that relates to the simultaneous use of the linear trend with a VPSCxEESC proxy in the multi linear regression: How well can the linear O3 trend be determined at high latitudes (in winter/spring) when part of this change (through the EESC factor) is already included in the MLR? The combined effect of EESC and linear trends in polar regions is briefly addressed at L.690, but I could not find a discussion on the effect on the trends. This is in particular important in the light of the strong statements made: "To the best of our knowledge, these results represent the first detection of a significant recovery in the stratospheric and the total O3 columns over the Antarctic from one single satellite dataset."]*

As already found in previous studies and stated in the manuscript, "the PSC volume is multiplied by the EESC to account for the changes in the amount of inorganic stratospheric chlorine that activates the polar ozone loss". In other words, the EESC factor is used to decrease the "efficiency" of the VPSC in activating the O_3 loss.

Actually, there is no possible confusion in the MLR between the linear trend and the VPSC x EESC proxy that is non-linear by nature given the strong oscillations in VPSC. The effect of the change in EESC on the amplitudes of the annual oscillations in VPSC which variate from year to year is very weak with, hence, no tendency detectable at all in the VPSC x EESC proxy (see Figure 1 here below). Therefore, it could not compensate the linear trend adjustment at all.

2/ *[I have to say that I am skeptical about the robustness of the speeding up of the trends in recent years, given that these trends are evaluated over really short periods only. Although the authors have done the analysis with statistical rigor, linear trends over periods as short as 2 years (2015-2017) are prone to changes in atmospheric dynamics and circulation (or other factors) that may not be perfectly captured by the MLR proxies. I (strongly) suggest that the authors consider a more careful wording in the conclusions and abstract, stating the evidence for the speeding up of the trends, but also the inherent uncertainties.]*

The speeding up has been investigated by removing the natural variability adjusted over the whole IASI period in order to avoid the effect of short trend-like segments in natural variations on the trend determination.
However, it is true that the uncaptured variability from the MLR performed over the full IASI period might disproportionately affect the estimated trends over varying time periods, but, so might be the calculation of the associated uncertainty, accordingly. This is specifically addressed in Fig.12 of the paper that illustrates the time evolution of both trends and associated uncertainties over varying time periods.
We agree, however, that the comparison of trends calculated over different lengths of time period is not straightforward because the statistical error is not comparable across the fits. This is addressed in Figure 2 here below that represents the minimum amplitude of the estimated trend, by subtracting the associated uncertainty (accounting for the autocorrelation in the noise residuals) from the linear trend; it still shows the significant increase in O_3 change rate across the fits.
Another approach, as suggested by Referee #2, would consist in considering successive time segments of same length. Nevertheless, here again, the uncaptured variability might induce different systematic errors between the successive segments, e.g. in case of "trend-like" noise over a specific segment. The choice of the segment length is also complicated by limitations (long segments would smooth the progressive

acceleration, while short segment would induce larger uncertainty; the jump in September 2010 in the IASI dataset would misrepresent the trend calculated over short segments that encompass the jump period).
Finally, we believe that Fig.12 of the paper is the best alternative to represent the progressive acceleration in the O_3 recovery. Note also that we now consider the autocorrelation in the noise residuals in the uncertainty estimation illustrated in Fig.12.
Nevertheless, we agree that the IASI period is still relatively short to compare trends over successive segments of same length that are long enough to reduce the uncertainty.

Therefore, as suggested, we use, in the revised version, a more careful wording about the speeding up of the O_3 trends through the revised manuscript, especially in the abstract, in Section 4.4 and in the conclusions. For example, one can read now at the end of the abstract: "Additional years of IASI measurements would, however, be required to confirm the O_3 change rates observed in the stratospheric layers over the last years" and at the end of Section 4.4: "Nevertheless, we calculated that additional years of IASI measurements would help in confirming the changes in O_3 recovery and decline over the IASI period (e.g. ~ 4 additional years are required to verify the trends calculated over the 2015-2017 segment in the highest latitudes in LSt). In addition, a longer measurement period would be useful to derive trends over successive segments of same length that are long enough to reduce the uncertainty, in order to make the trend and its associated uncertainty more comparable across the fit."

The title of the manuscript has also been changed accordingly to: "Is the recovery of stratospheric O_3 speeding up in the Southern Hemisphere? An evaluation from the first IASI decadal record".
An alternative to that title would be: "First signs of a speeding up of stratospheric O_3 recovery in the Southern Hemisphere, contrasting with a decline in the Northern Hemisphere, as seen from IASI".

Finally, we have also found a bug in the calculation of the estimated trends through the manuscript. We apologize for this. The overall conclusions remain unchanged but the figures 8 to 12, and the numbers given in the text have been corrected accordingly.

Specific comments

1/ *[L.72: Is this true for both hemispheres, or only NH?]*

Ball et al. (2018) reports a decline in lower stratospheric O_3 between 60°S and 60°N. The polar regions are not included in that study due to limited latitude coverage of instruments merged in the data composites.

2/ *[L.83: "sensitive" does not seem the right word here. Sensitive to what?]*
Changed to "difficult".

3/ *[Section 2.2: It would be good to have an explicit formula for the MLR included here, in addition to the reference to eq. (1) in Wespes et al. (2016).]*

The MLR and the normalization equations are now included in the revised paper at the start of Section 2.2.

4/ *[L.210: A few more words on the GEO and PV proxies would be helpful. Although L.372 states that their contribution is generally small, their use in ozone trend studies is not common practice, so some reference to their purpose and how and why they improve the fit is justified. Are these proxies lat/lon dependent?]*

The use of the GEO and PV proxies is inherited from previous papers (e.g. Knibbe et al., 2014; Wespes et al., 2017) to account for the impact of tropopause height and of the mixing of tropospheric and stratospheric air masses, in particular, on the LSt O_3 variations. Their contributions into the LSt O_3 variations are found minor due to correlations with the annual harmonic term, as expected, but the proxies are kept in the MLR

for completeness. They are lat/lon dependent (2.5°x2.5° gridded; this is now mentioned in the revised Table 1), hence, their gridded adjusted coefficients are not comparable on a global basis; only the adjusted signals can be compared.

5/ *[L.357++: SF: energetic particle precipitation (solar protons and also electrons) can also lead to enhanced ozone destruction in the MUSt through NOx catalysed cycles. The main effect of a solar proton event in the MUSt is actually to decrease O3 (and only to second order to decrease O3 destruction).]*

Added as suggested. Note that the role of the solar proton event on the decrease of O_3 destruction, as mentioned in the paper, refers to the LSt where NO_x decrease active chlorine and bromine.

6/ *[L.380++: EPF: I am surprised that the correlation of IASI O3 with EPF is small at low latitudes: Weber et al. (2011) note a rather strong anti-correlation between tropical total ozone and extra-tropical EPF.]*

Weber et al. found a negative correlation between tropical total ozone and extra-tropical EPF at lower latitudes throughout the winter and early spring, while it goes to zero by early summer. On an annual basis, Fig. 5 of the paper shows a weak but negative contribution (up to ~ -5 DU) onto O_3 variations. The negative sign which indicates an opposite response in O_3 to change in EPF is in agreement with the negative correlation, but the absolute value of the "regression" coefficient does not refer to the absolute value of the "correlation" coefficient; it indicates how much the proxy explains/contributes to the O_3 variations, while the absolute value of the correlation coefficient (as shown in Weber et al., 2011) indicates the degree of linearity between 2 variables.

The weak adjusted negative regression coefficients for EPF might result from correlation/compensation effect between the annual cycle and EPF. Despite the year-to-year variations in the EPF proxy, which limit the compensation effect with the 1-yr harmonic term, correlation between the two covariates is expected given the annual oscillations in EPF. This is illustrated in Figure 3 below that compares the global distribution of the fitted coefficient for the 1-yr harmonic term with or without EPF included in the MLR. The global distributions are quite similar with absolute differences (< 5 DU) lower than the EPF regression coefficient, indicating a good overall discrimination, except at the tropics where the EPF contribution is the lowest. Hence, the compensation effect between the 1-yr term (that is the main contributor to O_3 variations) and EPF might underrepresent its contribution at the Tropics. Note however that the correlation between the EPF and 1-yr terms is taken into account in their associated uncertainties.

Some words of caution have been added in the revised Section 3 about a likely compensation between the annual harmonic term and the EPF proxy that also shows an annual oscillation in nature:
"Furthermore, given the annual oscillations in EPF, compensation by the 1-yr harmonic term (eq. 1, Section 2) is found (data not shown), but it remains weaker than the EPF contribution (data not shown), in particular at high latitudes where the EPF contribution is the largest."

The Weber et al. (2011) reference has been added in the revised version.

7/ *[L.474: suggestion "N.H. mode" -> NAO]*

Changed as suggested.

8/ *[L480: Just as a note: It may also be that large O3 changes impact on the AAO]*

We apologise but we do not understand what the referee means here.

9/ *[L.514: "if the influence of ENSO on stratospheric O3 measurements has been reported": the word "if" seems a bit out of place here as clearly the influence of ENSO on stratospheric O3 has been reported in the cited studies.]*

Changed to: "Indeed, the influence of ENSO on stratospheric O_3 measurements has already been reported in earlier studies (…), but it is the first time that …"

Technical corrections

[L.233: "EFP" -> "EPF"]

Corrected

Figures

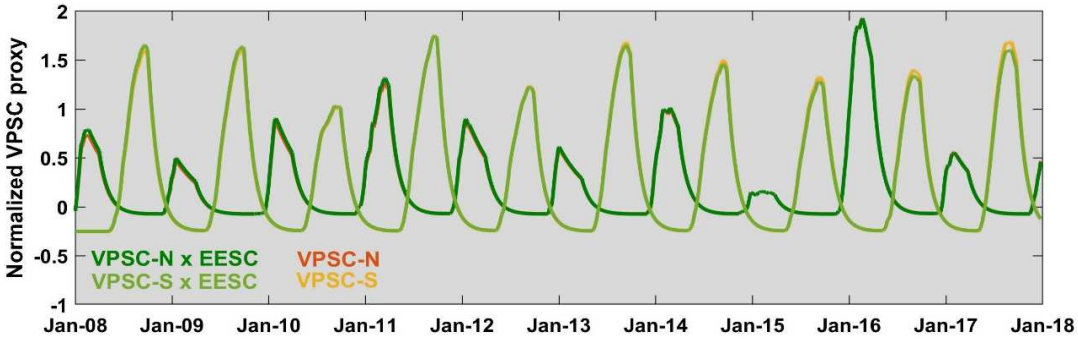

Figure 1: Normalized proxies as a function of time for the period covering January 2008 to December 2017 for the volume of polar stratospheric clouds multiplied or not by EESC and accumulated over time for the north and south hemispheres (VPSC-N and VPSC-S).

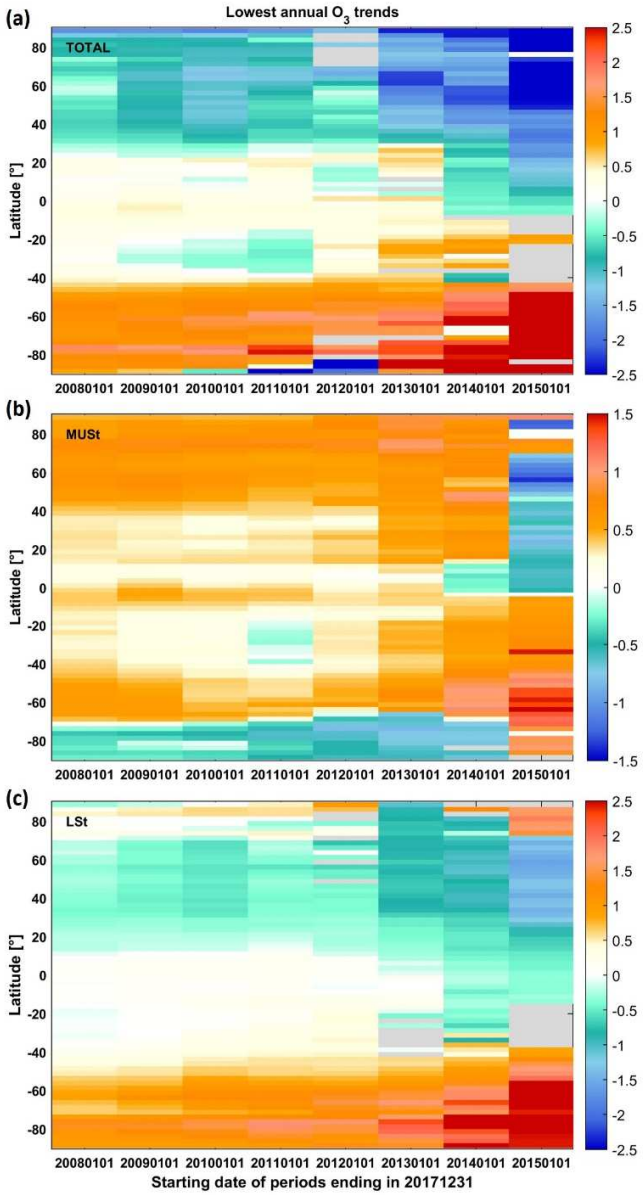

Figure 2: Evolution of estimated linear trend minus the associated uncertainty accounting for the autocorrelation in the noise residual (DU/yr; in the 95% confidence level) in (a) the total, (b) the MUSt and (c) the LSt O_3 columns (top to bottom panels, respectively), as a function of the covered IASI measurement period ending in December 2017, with all natural contributions estimated over the full IASI period (2008-2017).

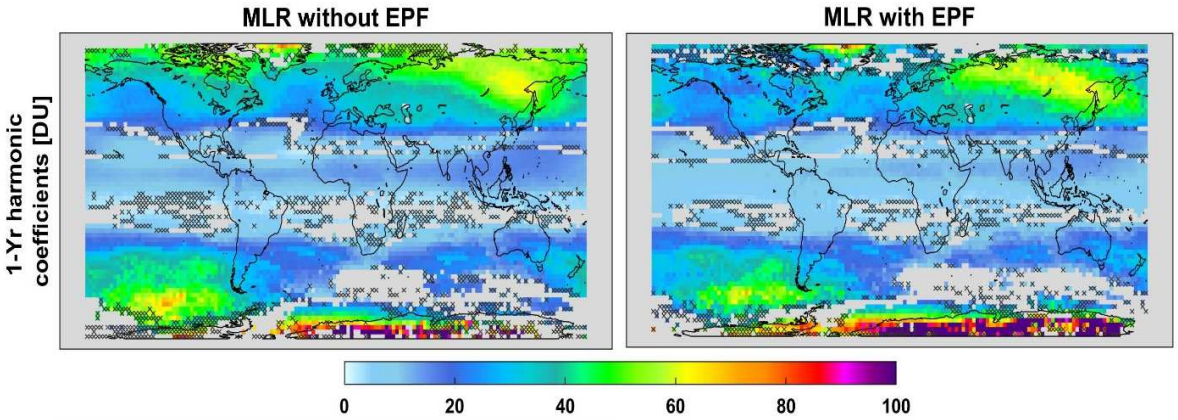

Figure 3: Global distribution of the annual regression coefficient estimates for the 1-yr harmonic term ($\sqrt{a_1^2 + b_1^2}$, in DU) in LSt obtained from the annual MLR without or with EPF (left and right panels, respectively).

Response to Referee #2:

We are grateful to the referee for her/his very careful reading of the manuscript and for her/his constructive comments and suggestions. Responses to each individual comment that has been quoted […] are given here below.

General comments

1/ *[This manuscript is largely an update of Wespes et al., 2016 but includes 4 more years of data.]*

This manuscript is indeed built on previous IASI studies, but we hope that the referee will appreciate that it is actually more than an update of Wespes et al., 2016, insofar as the regression model is more complex and here adapted to stratospheric studies with the inclusion of specific proxies (accounting for the aerosols, the volume of PSC and the Eliassen-Palm flux), and as the analysis is now performed at the global scale, not on a zonal basis, which allows us to better demonstrate the added value of the IASI dataset.

2/ [The manuscript is well written, though there are occasions where the wording is confusing, likely due to language issues]

We are grateful to the referee for suggesting a series of English style corrections in her/his technical comments below. They have all been included in the revised paper.

Major comments

1/ *[My primary comment concerns the analysis and conclusion that the ozone response to CFCs is changing in time. The authors base this conclusion on a series of linear fits over varying time periods, which show sharper trends (both positive and negative) in the most recent data relative to trends in the record from earlier start points. The series of trends is computed after the sources of natural variability, as fit over the full IASI time period to the most relevant proxies, are removed. Nevertheless there will still be variability in the time series that has not been perfectly captured by the regression model. If that variability has autocorrelation on a longer scale (months), a tendency for the data to be high or low at the beginning or end of the record, which might actually be due to uncaptured noise, will disproportionately affect the trend. If this is the case, such a variation at the end of the record will have successively more influence as the fit period gets shorter, as the end point of each fit is the same.]*

The referee is right; the uncaptured variability might disproportionately affect the estimated trends when calculated over varying time periods, but, so might be the calculation of the associated uncertainty. This is specifically addressed in Fig.12 of the paper that illustrates the time evolution of both trends and associated uncertainties over varying time periods.
We agree that the comparison of trends calculated over different lengths of time is not straightforward and that considering successive time segments of same length would make the statistical error more comparable across the fits. Nevertheless, there are limitations in using successive identical segments as discussed below in response to the referee's suggestions. We note finally that the uncaptured variability might also induce different systematic errors between segments (of same or different lengths), e.g. in case of "trend-like" noise over a specific segment.
In order to address this issue, we now consider the autocorrelation in the noise residuals in the uncertainty estimation illustrated in Fig.12.

As discussed below in response to the two next referee's comments, we believe that the results shown in the revised Fig.12 of the paper are the best way to represent the time evolution of the trends over the 10-

years IASI period. In addition to modifying the figure, we have taken care to better balance the findings through the revised manuscript, especially in the title, the abstract and the conclusions (see our responses here below).
Finally, we have also found a bug in the calculation of the estimated trends through the manuscript. We apologize for this. The overall conclusions remain unchanged but the Figures 8 to 12, and the numbers given in the text have been corrected accordingly.

2/ *[If I understand correctly, the associated uncertainty plots in Fig. 12 tell us that each trend is different from zero trend at the 95% level, but that does not mean that the trend fit over the last 2 years is different from the trend fit over the last three years or last 4 years at the 95% level. For example in the SH high latitude LST the initial trend is _ 1 DU/yr with uncertainty of say 0.25 DU/yr (difficult to tell exact numbers from the contour plots) and the final trend is approaching 2.5 DU/yr with an uncertainty of close to 1.5 DU/yr, meaning the initial and final trends are not statistically significantly different or only barely so, depending on the exact numbers.]*

We would like to point out that the exact numbers are given in Section 4.4 of the manuscript, specifically for the SH high latitude LSt: "In the LSt, a clear speeding up in the southern polar O_3 recovery is observed with amplitude ranging from ~1.5±0.4 DU/yr over 2008-2017 to ~5.5±2.5 DU/yr over 2015-2017 on latitudinal averages." Hence, the reader could appreciate that the initial and the final trends are statistically different from each other, despite the larger amplitude of the uncertainty over the shorter periods. This is further illustrated in Figure 1 here below which represents the lowest amplitude of the estimated trend, by subtracting, from the absolute value of the linear trend, the associated uncertainty that includes the autocorrelation in the noise residual.

The colorscale in the revised Fig.12 has been modified to avoid the saturation in order to address the comment on the lack of clarity. In addition, the uncertainty now accounts for the autocorrelation in the noise residuals and, hence, the uncertainty values are corrected accordingly throughout the manuscript.

3/ *[I believe a more appropriate approach would be to fit trend segments over the same length of time, with varying start and end points. The authors could compare the time evolution of trends over 2-yr segments, 3-yr segments, 4-yr segments and longer. The 2-yr segments would be the trend fit from 2008-2009, 2009-2010, 2010-2011,… 2015-2017. 3-yr segments would be 2008-2010, 2009-2011,…, 2014-2017 and 4-yr 2008-2011, 2009-2012, …, 2014-2017, and so on. In this way both the start and end point will vary, and each fit has the same length, such that the uncertainty is similar across the fits. If the results show consistent changes in time in the fit trends that are greater than the inherent uncertainty, this would indicate a change may be taking place. As the segments get longer (4-yr +) the change in trend will be less from segment to segment, but so will the uncertainty threshold that must be met to show significant change. So the authors can check for consistency in the trends within each segment length vs. time and consistency between 2-yr, 3-yr, 4-yr etc… segment results to determine if there is a shift in the ozone change rate.]*

We are grateful to the referee for this interesting suggestion. However, there are some limitations in using that approach:

- By fitting long segments, we would compare trends that are estimated over similar periods; i.e. for instance, 8-yr segments would imply comparing trends over 2008-2015 *vs* 2010-2017, which would smooth a progressive acceleration in the ozone change rate over the 10-year IASI period.
- By fitting short segments, we would induce a large uncertainty on the trend estimate (because of few data points and a hardly detectable trend from the noise) and, hence, less-conclusive results.
- The jump that occurs in September 2010 in the IASI dataset could over-represents disproportionally the estimated trends when they are calculated over short segments that encompass the jump period.

To follow the referee's suggestion, we have therefore investigated if the change rate in IASI O_3 could be inferred from segments that are long enough to lead low uncertainty and limit the jump effect. This is illustrated on Figure 2 here below that shows the trend evolution over 6-year, 7-year and 8-years segments in the LSt. Despite the smoothing of the trends over long periods, the progressive acceleration remains observed, especially in the Southern mid-latitudes. The results are also quite consistent with the revised Fig. 12, which gives more confidence in the speeding up observed in IASI LSt O_3.

Given the limitations discussed above, we believe that Fig.12 of the paper is the best way to represent the progressive acceleration in the O_3 recovery. Nevertheless, we agree that the IASI period is still relatively short to compare trends over successive segments of same length that are long enough to reduce the uncertainty. In addition, we calculate that the largest trend amplitudes derived over the last years of the IASI measurements would actually require a longer detection length than the covered time segments. Therefore, as suggested by the referee#1, we use, in the revised version, a more careful wording about the speeding up of the O_3 trends through the manuscript, especially in the abstract, in Section 4.4 and in the conclusions.

For example, one can read now at the end of the abstract: "Additional years of IASI measurements would, however, be required to confirm the O_3 change rates observed in the stratospheric layers over the last years" and at the end of Section 4.4: "Nevertheless, we calculated that additional years of IASI measurements would help in confirming the changes in O_3 recovery and decline over the IASI period (e.g. ~ 4 additional years are required to verify the trends calculated over the 2015-2017 segment in the highest latitudes in LSt). In addition, a longer measurement period would be useful to derive trends over successive segments of same length that are long enough to reduce the uncertainty, in order to make the trend and its associated uncertainty more comparable across the fit."

The title of the manuscript has also been changed accordingly to: "Is the recovery of stratospheric O_3 speeding up in the Southern Hemisphere? An evaluation from the first IASI decadal record".
An alternative to that title would be: "First signs of a speeding up in stratospheric O_3 recovery in the Southern Hemisphere, contrasting with a decline in the Northern Hemisphere, as seen from IASI".

4/ *[I also believe showing some example time series of the data being fit, after the other variations have been removed, would be very useful in this particular analysis.]*

We thank the referee for that suggestion. Some typical examples of gridded daily time series in the S.H. mid-latitudes in the LSt, after the fitted natural variations have been removed, are provided in the Figure 3 here below. The residuals clearly show positive trends. The fitted significant trends over varying periods ending in 2017 are superimposed. The trend values and associated uncertainties are also indicated for a conclusive evaluation of the significant O_3 change rate in stratosphere. While the speeding up is significant from the zonally averaged trends (see the revised Fig. 12 and the Figure 1 here below), it is more hardly but still detectable over individual gridded time series. Examples have been added in the revised Supplement.

5/ *[Finally, when doing this analysis, is the VPSC term also removed, or is this term considered part of the ozone response to CFCs and thus left in the time series? Similarly, in reference to the jump in the data in September 2010, although this may be small relative to the full trend, does this jump influence the results of the time dependent trend analysis shown in Fig. 12, or has it's effects been removed before fitting these trends?]*

All the adjusted proxies, including the VPSC term, have been kept fixed (or removed) in the trend analysis over varying time periods, so that any changes in the adjusted O_3 drivers (including in VPSCxEESC) over

time do not influence the trend estimation. It is now clearly mentioned in the revised manuscript that VPSC is removed as well:
"…the ozone response to each natural driver *(including VPSC)* taken from their adjustment over the whole IASI period (2008-2017; Section 3, Fig.5) is kept fixed."

On the contrary, for consistency with Chapter 4, the jump found in the IASI data in September 2010 has not been removed from the trend analysis shown in Fig.12 and, hence, it could influence the trends calculated over the periods starting before the jump only (i.e. 2008-2017, 2009-2017 and 2010-2017). However, the jump is of positive sign and, hence, it does not contribute at all to the acceleration observed in the IASI O_3 change rates over the 10-year period. It would even mask it when comparing the trends estimated over periods starting before *vs* after the jump. This has been added in Section 4.4:
"The jump found in the IASI O_3 records on September 2010 (see Section 2.1) is not taken into account in the regression; hence, it might over-represent the trend estimated over periods that start before the jump only (i.e. 2008-2017, 2009-2017, 2010-2017)."

Minor comments

1/ *[Can the authors say more about the difference between fitting a daily record and a monthly mean record? I know this was addressed in the 2016 paper, but I am particularly interested in the error analysis. Is the daily autocorrelation similar to the monthly autocorrelation? For long-term trends, the uncertainty is more impacted by correlations in the residual on longer time scales rather than day to day variations. Is the lag-1 autocorrelation term used to scale the uncertainty similar when considering daily data and monthly data?]*

The autocorrelation coefficients at various lags corresponding to a daily mean record *vs* a monthly mean record were examined for the 2 stratospheric layers (cfr Figure 4 here below for the latitudinal distributions of the lag-1 to -4 autocorrelation terms in daily *vs* monthly data fitting in the MUSt). As expected, the lag-1 autocorrelation term appears to be the most important in all cases (daily and monthly) and is found to be much larger in the daily than the monthly mean records. This means that the correction of the uncertainty estimate, by the autocorrelations in the noise residual, is larger when adjusting daily data, i.e. the uncertainty associated to the fitted trend is much more impacted by the autocorrelation when fitting a daily record, but, as shown in the 2016 paper, it is compensated by a better quality adjustment, which, hence, reduces the amplitude of the uncertainty in daily *vs* monthly data records.

2/ *[Although I appreciate not wanting to add too much to the paper, I think it would help the reader to repeat the basic equations defining the multivariate model in this paper. At different times three different papers are referenced for equations concerning the model. I think it would be easier to just include all relevant equations in this paper, including the normalization equation.]*

The MLR and the normalization equations are now included in the revised paper at the start of Section 2.2.

3/ *[Very little is said about the seasonal cycle, though the model description includes terms for the annual and 6-month harmonics (pg 5.). Can the authors comment on the seasonal cycle, and particularly do they see the seasonal cycle interacting with EPF and VPSC, which are both also correlated and look very seasonal in nature. Similarly on the interaction between EPF and VPSC, in Fig. 7a in the NH high latitudes the ozone variability explained by the proxies for EPF and VPSC are similar and well above the variability of the actual IASI ozone. Is this another way of showing that the two terms falsely depict variability that isn't in the actual data, but that variability cancels when the terms are added? Have the authors tried fitting to one or the other of the terms, rather than both terms? Particularly in the Austral Spring, where the authors believe the VPCS signal is real, is the amplitude of that signal sensitive to whether or not EPF and/or the seasonal cycle are fit?]*

Correlation between the annual cycle and EPF is of course expected. In several previous papers, the harmonic terms are even used to adjust the effects of the Brewer-Dobson circulation in addition to the seasonal cycle of insolation, but then the interannual variability is not captured. However, the EPF and VPSC proxies show sufficiently year-to-year variations to limit the compensation effect between each other and with the 1-yr harmonic term.

In order to verify this, as suggested by the referee, an annual MLR without including EPF has been performed to better evaluate the possible discrimination between the EPF, VPSC and 1-yr harmonic terms. This is illustrated for LSt in Figure 5 here below that represents the global distributions of the adjusted coefficients for the 1-yr harmonic ($\sqrt{a_1^2 + b_1^2}$) and the VPSC regression coefficients from the annual MLR without EPF *vs* the reference one. We show that the global distributions of the VPSC regression coefficients between the two MLRs are similar, which indicates a good discrimination between the two parameters on an annual basis. For the 1-yr coefficients, the overall global distributions look similar with, however, some expected but small differences relative to the EPF contribution, especially over the high latitudes where the EPF contribution is the largest. In addition, it is worth noting that the likely correlation between the VPSC, EPF and 1-yr terms is taken into account in their associated uncertainties.

Some words of caution have been added in the revised Section 3 about a possible correlation between the annual harmonic term and the EPF proxy:
"Furthermore, given the annual oscillations in EPF, compensation by the 1-yr harmonic term (eq. 1, Section 2) is found (data not shown), but it remains weaker than the EPF contribution, in particular at high latitudes where the EPF contribution is the largest."

We would like to point out that the likely correlation between VPSC and EPF was already mentioned in the paper in Sections 2.2 and 3 which describe the proxies and their adjustment: "Correlations between VPSC and EPF are possible since the same method is used to build these cumulative proxies". They can indeed compensate each other by construction given the opposite sign of their regression coefficients. However, we highlight the physical meaning behind the sign of their regression coefficients and the differences between the spatial distributions of their regression coefficients (see Fig.5 of the manuscript), which indicate a discrimination between these two variables.

On a seasonal basis, the austral spring is the period when VPSC is the largest and dominates over EPF in the S.H.; this is consistent with the role of PSCs on the polar O_3 depletion chemistry and the smallest EP influence due the formation of the O_3 hole, in comparison with the N.H. However, a compensation effect might indeed explain the large similar VPSC and EPF variability in the N.H. high latitudes in fall, as it was already mentioned in the paper: "The strong VPSC influence found at high northern latitudes in fall (Fig. 7a) are likely due to compensation effects with EPF as pointed out above."

The good discrimination in austral spring and the compensation effect in the N.H. fall are verified in the Figure 6 here below that compares the latitudinal distribution of the 2σ O_3 variability in VPSC, from the seasonal MLR with or without including EPF. The amplitude of the variation explained by VPSC are similar between the two seasonal MLRs in the Austral spring, while, not in the N.H. fall. The results in Figures 5 and 6 here demonstrate a good discrimination between the two covariates yearly and in the Austral spring.

In the revised version, we now mention:
"The strong VPSC influence found at high northern latitudes in fall (Fig. 7a) are due to compensation effects with EPF as pointed out above and verified from sensitivity tests (data not shown)."

Finally, we believe that it does not make sense to remove both the 1-yr harmonic term and EPF from the MLR model; the annual cycle that is caused by solar insolation which is the main driver of the observed O_3 variability will no longer be represented, which will lead to erroneous results.

4/ *[Can the authors discuss comparisons between IASI total ozone and other sources of satellite total ozone measurements? It is difficult to compare trend values presented here with previous studies (Weber et al for example) because of the different time periods fit, and zonal mean vs high spatial resolution gridded trends. Have IASI total ozone trends been directly compared to trends from any of the other total ozone satellite records? It would be very useful to also see how the data themselves compare in total ozone, either through reference to previous work or in a comparison plot in this manuscript.]*

Performing comparisons between O_3 trends derived from IASI *vs* other satellite instruments would be of course interesting for evaluating the inferred trends and the relevance of the current datasets to carry out trend studies. However, it is a significant endeavour that is beyond the scope of the present study. Actually, this will be specifically addressed in the frame of the recently started Ozone_CCI+ program where the IASI O_3 trends will be compared to those estimated from GOME-2 (both onboard the Metop platforms) over exactly the same time period and using the same MLR model/method. In that way, the bias resulting from different time periods, spatial/temporal samplings and trend calculations will be excluded.

5/ *[Can the authors address how the seasonal averages are constructed? In particular, the authors specifically investigate the JJA trends over the South Pole and Antarctica, but it appears from Fig. 4a there is very little is any coverage in the deep winter at polar latitudes, but that coverage increases with latitude towards the equator. Are the JJA averages for each grid point made with any available data, or is a threshold set, and does the coverage vary with latitude in the polar regions in Figure 10 and 11?]*

The distributions of seasonal trends provided in Fig. 10a and 11a of the paper do not correspond to averages; instead they represent the adjusted seasonal trend parameters for each grid cell (see our response to the technical comment [*L270-272*] below). It is true, however, that the coverage vary with latitude in the polar regions since only the daytime measurements are used in the paper (as mentioned in Section 2.1). This explains the gap (grey cells) over the polar regions during both austral and northern winters in Fig. 10a and 11a of the paper, in comparison with the other periods (Fig. 10b and 11b) and the annual trend distributions (Fig. 8 of the paper).

Technical comments

1/ [*The use of the absolute value signs around the trend values was a bit confusing. I can see this when talking about the amount of time needed to detect a trend of |x| DU yr-1 because this can be a positive or negative trend, but in other cases the authors state the trend is positive or negative, and in that case it is unclear why the absolute value designation is needed. For example on page 15, the absolute value bars are not needed in lines 561 and 564. In line 591, is this a positive trend of 1.5 DU/yr or do you mean positive or negative? If the authors do not mean to say this value can be positive or negative, I would suggest removing the absolute value bars and just stating positive or negative (such as in line 594, positive is stated so the bars can be removed, to me at least the bars imply positive or negative).*]

The consistency in using the absolute value bars has been checked through the manuscript. The absolute bars are now only used when discussing the detectability of a specified trend (i.e. when the trend can be of both positive and negative values); in other cases, the sign is specified.

2/ [*L12 should this be > 25hPa or < 25hPa? Since the units are in hPa I suggest it is < as in 25 hPa and lower pressures. L34 in a lesser -> to a lesser. L41 introduce O3 after ozone. L43 gas. In the stratosphere*

L45 for regulating -> to regulate. L45 introduce chlorofluorocarbons here, at first use of CFCs. L47-48 suggest These latter are the origin of the massive -> CFCs cause. L46-54: In general, I don't think the timing is correct is this introduction to the phase out of the CFCs. At the time the Vienna Convention was ratified, and the MP for that matter, it was not yet proven that CFCs were the cause. The Vienna Convention was ratified based on the theory that CFCs could cause ozone destruction; I don't believe the Farman paper was even released yet. All this to say, even though this is just an introductory paragraph I think it is important to be precise on the history, the implication in the wording is that the ozone hole was discovered first and everything else was a reaction to that discovery. L56 Suggest removing first phrase, and start sentence as A recovery from… L59 This is decline of CFCs in the stratosphere, correct? L61 confirmed -> identified. L67 polar region -> polar regions. L68 No reliable estimates of long-term trend -> Statistically significant long-term recovery in total O3 column on a global scale has not yet been observed, likely because… L71 low -> lower. L75 I believe there are other references here as well. Check Wargan, K., C. et al. Recent decline in lower stratospheric ozone attributed to circulation changes. Geophys. Res. Lett., 45, no. 10, 5166-5176, doi:10.1029/2018GL077406. L81 controversy -> uncertainty. L82 sensitive -> difficult. L109 applied on -> applied to. L110 remove 'of'. L172 and contrasts with -> rather than]

Thank you for these corrections. The text has been revised as suggested. Note in particular the following points:

- O_3 was already introduced in the abstract.
- The timing in the introduction has been corrected in the revised version. The Farman et al. paper was accepted (28 March 1985) just after the Vienna Convention (22 March 1985).
- Wargan et al. (2018) has been added in the introduction.

3/ [L*178-180 the effect of the jump is found small enough to explain the trend? I'm not sure what the authors mean here.]*

Changed to:
"The estimated amplitude of the jump is found to be relatively small in comparison to that of the decadal trends derived in Section 4, hence, it cannot explain the tendency in the IASI dataset. Therefore, the jump is not taken into account in the MLR."

4/ [*L192 In order to unambiguously -> In an effort to unambiguously (we try to separate unambiguously, but it is never perfect). L209 of the mixing*]

Done as suggested.

5/ [*L270-272 I'm not sure what the authors are trying to say here. Including the equations would help here. There is already a seasonal cycle in the original model, so it is not clear how the seasonal terms are added. Is this the equivalent of 4 separate runs, one for each season? Equations would also clarify how the seasonal MLR is used after the annual MLR is run.]*

As it is stated in the paper, the seasonal MLR replace the annual functions with 4 seasonal functions, i.e. by adjusting 4 coefficients (one for each seasonal functions for the main proxies, instead of only one coefficient per annual function in the annual MLR). Hence, in the seasonal MLR, the explanatory variables are split into four seasonal functions ($x_{spr} X_{norm,spr} + x_{sum} X_{norm,sum} + x_{fall} X_{norm,\,fall} + x_{w\mathrm{int}} X_{norm,w\mathrm{int}}$) that are simultaneously and independently adjusted. There is only one run (as for the annual MLR) with 4 adjusted parameters per proxy. Note that this is not to be confused with the seasonal cycle (harmonic terms) which is treated exactly the same way in both the annual and seasonal formulation of the MLR model (only one annual coefficient is adjusted for each harmonic function). Hence, the seasonal MLR is not equivalent to 4 separate runs. The seasonal MLR takes into account the different influence of the geophysical processes

onto O_3 across the seasons, while the annual model is more constrained by the adjustment of year-round proxies which, hence, induces larger systematic errors.

The sentence has been rewritten in the revised version to:
"In the seasonal formulation of the MLR model, the main proxies ($x_j X_{norm,j}$; with x_j , the regression coefficient and $X_{norm,j}$ the normalized proxy) are split into four seasonal functions ($x_{spr} X_{norm,spr} + x_{sum} X_{norm,sum} + x_{fall} X_{norm,fall} + x_{wint} X_{norm,wint}$) that are independently and simultaneously adjusted for each grid cell."

6/ [*L285-288 suggest for clarity not switching the order of the reported results, in L288 LSt goes first and in 291 MUSt is reported first. L302 counteracted -> counteracting (this may occur in other places as well in the text). L 321 suggest adjusted signal of the proxies -> reconstructed proxies. L333 shows up as a typical… L347 MUSt, (remove 'n'). L360 records -> values. L392 deployment ->formation. L414 remove 'have'. L460 in the case of prolonged…*]

Done as suggested.

7/ [*L555 I do not see polar trends reaching 2.5 DU/yr in the MUSt? The trends are positive in the NH pole but negative over Antarctica, and the scale only goes to 2 DU/yr. L560 The authors call out the similarity between the MUSt and LSt with both showing high positive trends at southern polar latitudes, but again at the pole the MUSt trend appears negative, though the trends at southern high latitudes are positive. This description seems a bit confusing and doesn't seem to match Figure 8.*]

Some cells were indeed characterized by trends of 2.5 DU/yr even if the color scale is saturated at 2 DU/yr for clarity. From Fig.8a of the manuscript, one can see that the trends in MUSt are positive almost everywhere, except over Antarctica, with the largest values over the northern polar region and around Antarctica for the S.H.
"(except over Antarctica)" has been added in the revised text to exclude this from the discussion.
Note that the Fig. 8 and the corresponding values given in the text have been revised to correct a bug, as mentioned above.

8/ [*L596 an additional _ 7 years. L599 suggest The longer required measurement periods at high latitudes is due to the larger residuals in the regression fits (i.e. largest sigma e) at these latitudes (see Fig 4 a and b). L613 is there a reason the authors occasionally switch to DU per decade? If not, I suggest keeping DU per year. At first I could not understand why such a large value of 15 was used, then I saw it was DU per decade. L623-624 again it seems the increase in total ozone at high southern latitudes is dominated by the LSt result over the pole though both layers contribute in the latitude bands surrounding Antarctica, comparing to the results in Fig. 8.*]

Done as suggested.

9/ [*L652 summer -> austral winter. L674 over Antarctica (remove 'the'). L696 Salomon -> Solomon*]

Done as suggested.

10/ [*L686 what makes the negative trends here unrealistic?, It seems that the large positive trends off the coast of Antarctica have a similar detection length. I see that there is a bit more uncertainty in the fit in the negative trend region, but to say they are unrealistic requires more specific evidence, such as a time series showing the failure of the fit. I suggest the authors either provide more evidence or simply note that the*

area of higher negative trends is associated with a higher residual from the model. Could it also be something that is happening in the troposphere that is affecting the total ozone trend.]

"unrealistic" has been replaced by "higher"; The large positive trends around Antarctica have a shorter detection length.

11/ [*L705 This is just a suggestion, but to make the interpretation for the reader easier, could the authors provide the relevant IASI mean ozone values (or climatological values) so the readers can translate between DU/yr and % per dec when comparing results from other studies.*]

The trend in IASI TOC is now given in %/dec as well.

12/ [*L766 suggest However, a longer period of IASI measurements is needed to unequivocally demonstrate a positive trend in the IASI record. L775 additional measurements for the trend to be unequivocal. L781 suggest These results verify the efficacy of the ban on ozone depleting substances imposed by the Montreal Protocol and it's amendments throughout the stratosphere… L788 and it likely -> which likely. L807 in the near future. L809 extent -> extend*]

Done as suggested.

Figures

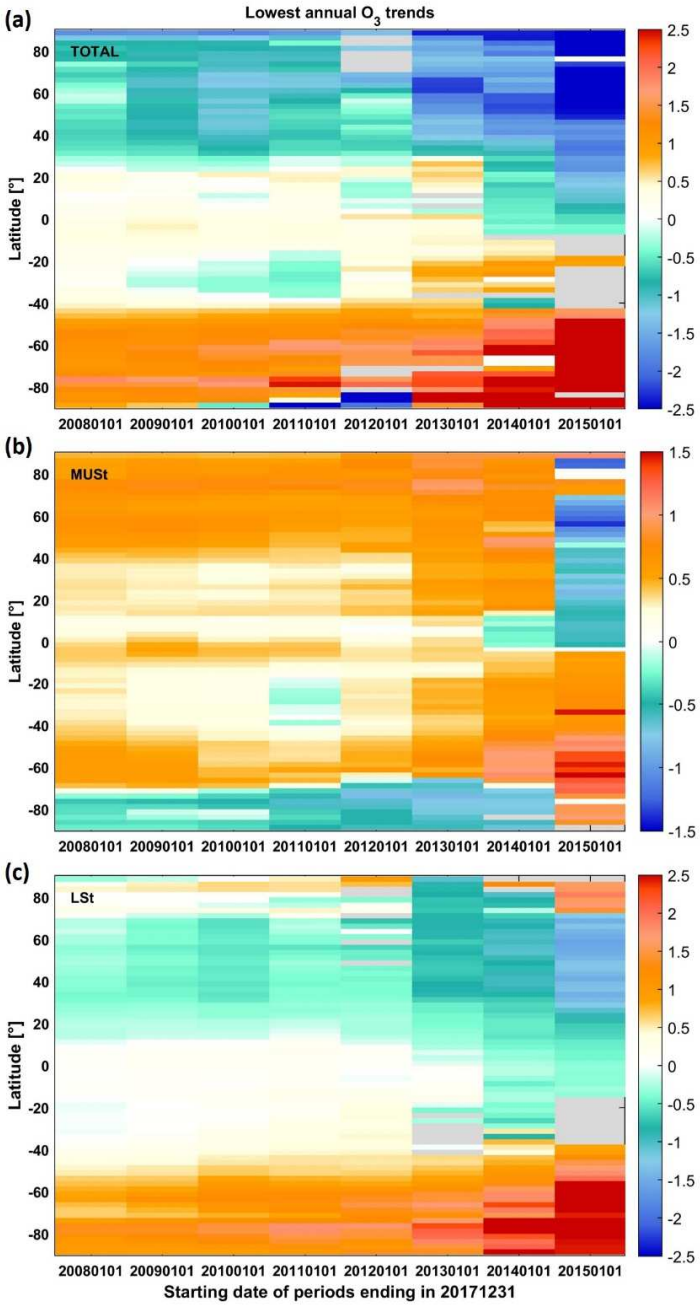

Figure 1: Evolution of estimated linear trend minus the associated uncertainty accounting for the autocorrelation in the noise residual (DU/yr; in the 95% confidence level) in (a) the total, (b) the MUSt and (c) the LSt O_3 columns, as a function of the covered IASI measurement period ending in December 2017, with all natural contributions estimated over the full IASI period (2008-2017).

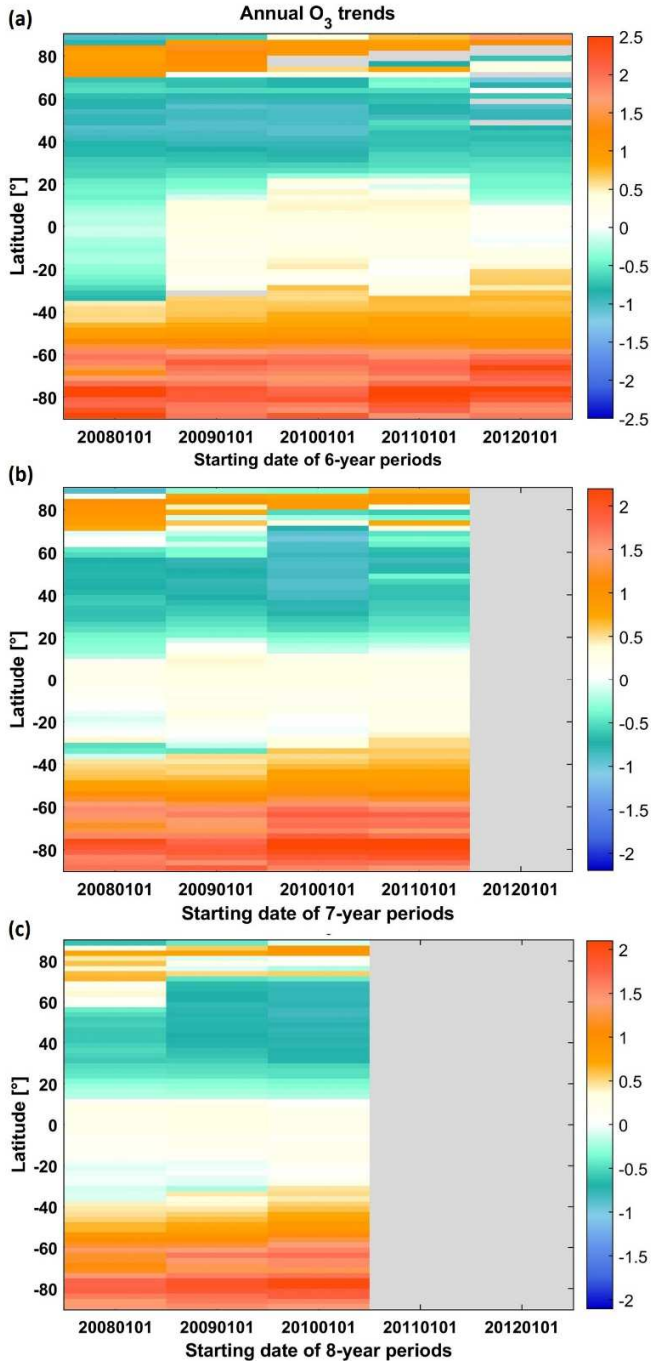

Figure 2: Evolution of estimated linear trend (DU/yr) in the LSt O_3 columns, over (a) 6-year, (b) 7-year and (c) 8 years segments of IASI measurements, with all natural contributions estimated over the full IASI period (2008-2017).

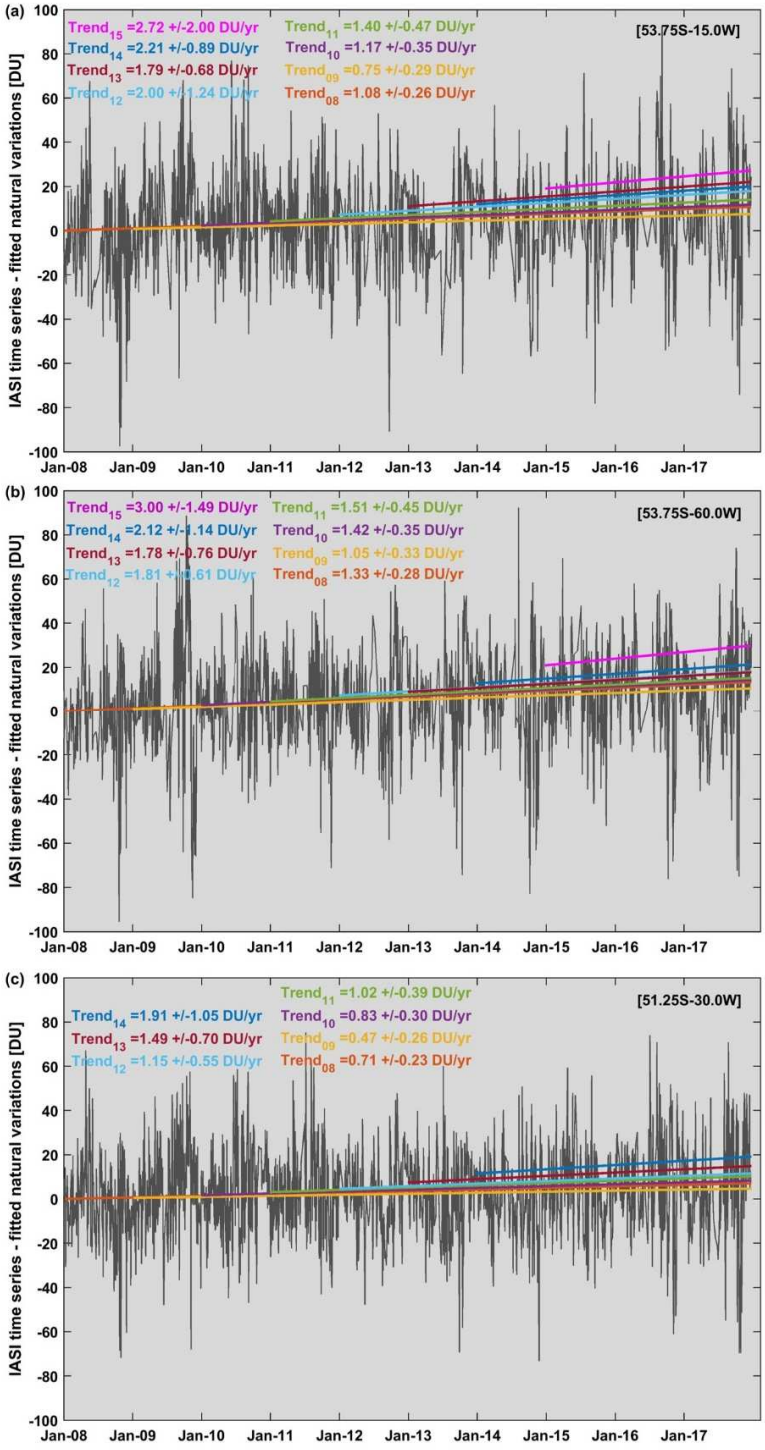

Figure 3: Example of gridded daily time series of O_3 measured by IASI in the LSt over the period 2008-2017 with all the contributions to O_3 variations adjusted from MLR over the full IASI period removed, except for the trend (in DU). The significant fitted trends calculated over varying time periods from a single linear regression are superimposed. The trend values with associated uncertainties (in the 95% confidence level; in DU/yr) are indicated.

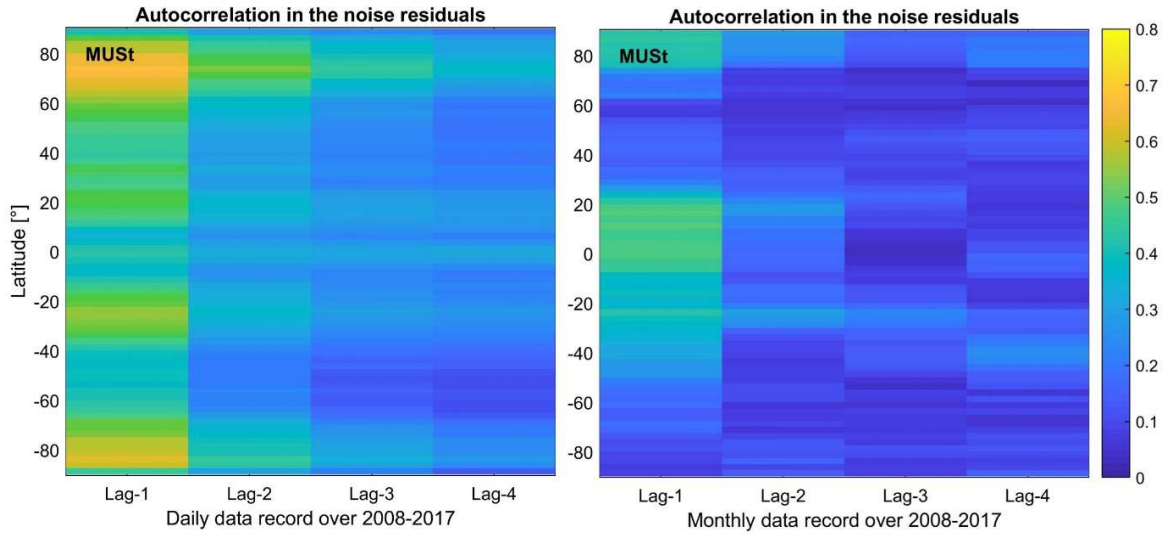

Figure 4: Latitudinal distribution of the lag-1 to -4 autocorrelation terms in the noise residuals when fitting a daily mean (left panel) *vs* a monthly mean (right panel) record in the MUSt over 2008-2017.

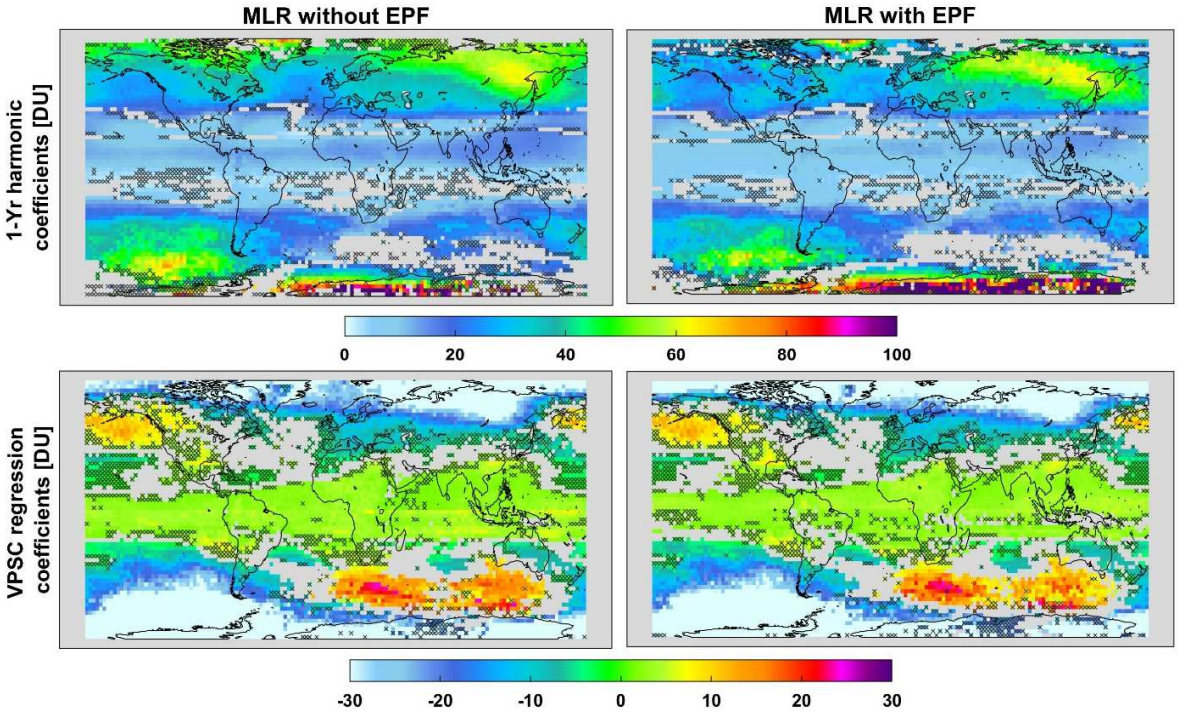

Figure 5: Global distributions of the annual regression coefficient estimates (in DU) for the 1-yr harmonic term ($\sqrt{a_1^2 + b_1^2}$, top panels) and for the VPSC proxy (bottom panels) in LSt obtained from the annual MLR without or with EPF (left and right panels).

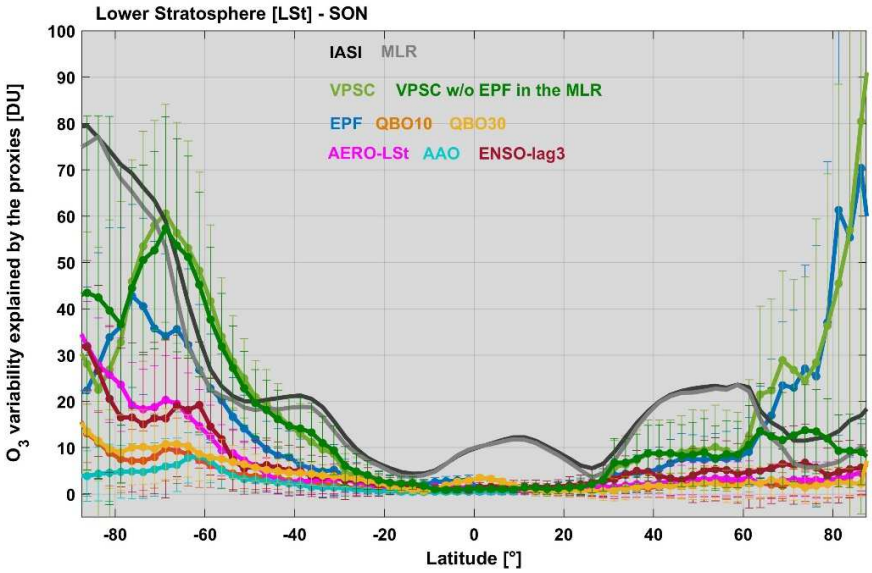

Figure 6: Same as Fig.7 of the paper for the austral spring periods (SON) in LSt, with, superimposed, the 2σ O_3 variability due to variations in VPSC from the seasonal MLR without EPF (dark green).

List of relevant changes made in the manuscript:

Title:

"Is the recovery of stratospheric O_3 speeding up in the Southern Hemisphere? An evaluation from the first IASI decadal record"

Abstract:

- **L. 14: "**(MUSt; <25hPa)"

- **L. 40-41:** "Additional years of IASI measurements would, however, be required to confirm the O_3 change rates observed in the stratospheric layers over the last years."

Introduction:

- **L. 48-56:** "In the 1980s, the scientific community motivated decision-makers to regulate the use of chlorofluorocarbons (CFCs), after the unexpected discovery of the springtime Antarctic ozone hole (Chubachi, 1984; Farman et al., 1985) that was suspected to be induced by continued use of CFCs (Molina and Rowland, 1974; Crutzen, 1974); The O_3 depletion was later verified from measurements at other Antarctic sites (e.g. Farmer et al., 1987) and from satellite observations (Stolarski et al., 1986), and explained by the role of CFC's on the massive destruction of O_3 following heterogeneous reactions on the surface of polar stratospheric clouds (Solomon, 1986; 1999 and references therein)."

Section 2.1:

- **L. 185-187:** "The estimated amplitude of the jump is found to be relatively small in comparison to that of the decadal trends derived in Section 4, hence, it cannot explain the tendency in the IASI dataset. Therefore, the jump is not taken into account in the MLR."

Section 2.2:

- **L. 200-213:** "we have applied to the 2.5°x2.5° gridded daily MUSt and LSt O_3 time series, a MLR model that is similar to that previously developed for tropospheric O_3 studies from IASI (see Wespes et al., 2017; 2018) but here adapted to fit the stratospheric variations:

$$O_3(t) = Cst + x_{j=1} \cdot trend + \sum_{n=1:2} \left[a_n \cdot \cos(n\omega t) + b_n \cdot \sin(n\omega t) \right] + \sum_{j=2}^{m} x_j X_{norm,j}(t) + \varepsilon(t) \quad (1)$$

where *t* is the number of days, x_1 is the trend coefficient in the data, $\omega = 2\pi/365.25$, a_n, b_n, x_j are the regression coefficients of the seasonal and non-seasonal variables and $\varepsilon(t)$ is the residual variation (assumed to be autoregressive with time lag of 1 day). $X_{norm,j}$ are the *m* chosen explanatory variables, commonly called "proxies", which are normalized over the study period (2008 – 2017) with:

$$X_{norm}(t) = 2\left[X(t) - X_{median}\right] / \left[X_{\max} - X_{\min}\right] \quad (2)"$$

- **L. 286-289:** "In the seasonal formulation of the MLR model, the main proxies ($x_j X_{norm,j}$; with x_j the regression coefficient and $X_{norm,j}$ the normalized proxy) are split into four seasonal functions ($x_{spr} X_{norm,spr} + x_{sum} X_{norm,sum} + x_{fall} X_{norm,fall} + x_{wint} X_{norm,wint}$) that are independently and simultaneously adjusted for each grid cell (Wespes et al., 2017)."

Section 3:

- **L. 388-389:** "… while it enhances the O_3 destruction in the MUSt through NO_x catalysed cycles,…"

- **L. 419-422:** "Furthermore, given the annual oscillations in EPF, compensation by the 1-yr harmonic term (eq. 1, Section 2) is found, but it remains weaker than the EPF contribution (data not shown), in particular at high latitudes where the EPF contribution is the largest."

- **L. 429-432: "**The strong VPSC influence found at high northern latitudes in fall (Fig. 7a) are due to compensation effects with EPF as pointed out above and verified from sensitivity tests (not shown)."

Section 4.1:

- **L. 576-577:** "…the MUSt shows significant positive trends larger than 1 DU/yr poleward of ~35°N/S (except over Antarctica)."

- **L. 625-627:** "The longer required measurement period at high latitudes is due to the larger noise residuals in the regression fits (i.e. largest σ_ε) at these latitudes (see Fig.4 a and b)."

Section 4.2:

- **L. 650-652: "**In addition, the increase in total O_3 at high southern latitudes is dominated by the LSt, although both layers positively contribute around Antarctica, comparing to the trend distributions in Fig. 8."

Section 4.3:

- **L. 677-680: "**Here we investigate the respective contributions of the LSt and the MUSt to the TOC recovery over the Southern latitudes during spring and also during winter when the minima in O_3 levels occur in the MUSt (down to ~60 DU in polar regions), in comparison with the Northern latitudes."

Section 4.4:

- **L. 743-747: "**The linear trend term only is adjusted over variable measurement periods that all end in December 2017, by using a single linear iteratively reweighted least squares regression applied on gridded daily IASI time series after all the sources of natural variability fitted over the full IASI period are removed (typical examples of linear trend adjustment can be found in the Fig. S2 of the supplementary materials).**"**

- **L. 747-750: "**The discontinuity found in the MUSt IASI O_3 records on September 2010 (see Section 2.1) is not taken into account in the regression; hence, it might over-represent the trends estimated over periods that start before the jump (i.e. 2008-2017, 2009-2017, 2010-2017)."

- **L. 750-753: "**The zonally averaged results are displayed in Fig. 12 for the statistically significant total, MUSt and LSt O_3 trends and their associated uncertainty (accounting for the autocorrelation in the noise residuals; in the 95% confidence level) estimated from an annual regression."

- **L. 769-773: "**Overall, the larger annual significant trend amplitudes derived over the last few years of total, MUSt and LSt O_3 measurements, compared with those derived from the whole studied period (Sections 4.1 and 4.2) and from earlier studies, translate to trends that remain detectable over the increasing uncertainty associated to the shorter and shorter time segments (see Fig. S3 of the supplementary materials), especially in both LSt and total O_3 in the S.H."

- **L. 775-781: "**Nevertheless, we calculated that additional years of IASI measurements would help in confirming the changes in O_3 recovery and decline over the IASI period (e.g. ~ 4 additional years are required to verify the trends calculated over the 2015-2017 segment in the highest latitudes in LSt). In addition, a longer measurement period would be useful to derive trends over successive segments of same length that are long enough to reduce the uncertainty, in order to make the trend and its associated uncertainty more comparable across the fit.**"**

Conclusion:

- **L. 837-839:** "Even if the acceleration cannot be categorically confirmed yet, it is of particular urgency to understand its causes for apprehending its possible impact on the O_3 layer and on future climate changes."

- **L. 842-843**: "… which translate to trend values that would be categorically detectable in the next few years on an annual basis."

Table 1:

- **EPF:** "Vertical component of Eliassen-Palm flux crossing 100 hPa, averaged over 45°-75° for each hemisphere and accumulated over the 3 or 12 last months depending on the time period and the latitude (see text for more details) (*daily*)"
- **PV and GEO:** "… (2.5°x2.5° gridded) …"

Throughout the manuscript:

- The absolute bars are now only used when discussing the detectability of a specified trend (i.e. when the trend can be of both positive and negative values); in other cases, the sign is specified.

- Figures 8 to 12 have been corrected. Hence, the values referring to these figures have been changed accordingly in the revised text.

References:

- **L. 1155-1156:** "Farmer, C. B., G. C. Toon, P. W. Shaper, J. F. Blavier, and L. L. Lowes, Stratospheric trace gases in the spring 1986 Antarctic atmosphere, Nature, 329, 126–130, 1987."

- **L. 1404-1405: "**Solomon, S., R. R. Garcia, F. S. Rowland, and D. J. Wuebbles, On the depletion of Antarctic zone, Nature, 321, 755–758, 1986."

- **L. 1422-1424**: “Stolarski, R. S., A. J. Krueger, M. R. Schoeberl, R. D. Mc-Peters, P. A. Newman, and J. C. Alpert, Nimbus 7 satellite measurements of the springtime Antarctic ozone decrease, Nature, 322, 808–811, 1986.“

- **L. 1489-1492**: “Weber, M., Dikty, S., Burrows, J. P., Garny, H., Dameris, M., Kubin, A., Abalichin, J., and Langematz, U.: The Brewer-Dobson circulation and total ozone from seasonal to decadal time scales, Atmos. Chem. Phys., 11, 11221-11235, https://doi.org/10.5194/acp-11-11221-2011, 2011.”

Supplementary Materials:

- Figures S2 and S3 with their associated description have been added in the Supplement.

~~Evidence from IASI of a speeding up in stratospheric O_3 recovery in the Southern Hemisphere contrasting with a decline in the Northern Hemisphere~~

Is the recovery of stratospheric O_3 speeding up in the Southern Hemisphere? An evaluation from the first IASI decadal record

Catherine Wespes[1], Daniel Hurtmans[1], Simon Chabrillat[2], Gaétane Ronsmans[1], Cathy Clerbaux[3,1] and Pierre-François Coheur[1]

[1]Université Libre de Bruxelles (ULB), Faculté des Sciences, Chimie Quantique et Photophysique, Bruxelles, Belgique
[2] Belgian Institute for Space Aeronomy, Brussels, Belgium
[3] LATMOS/IPSL, Sorbonne Université, UVSQ, CNRS, Paris, France

Abstract

In this paper, we present the global fingerprint of recent changes in the mid-upper stratospheric (MUSt; <~~>~25hPa) ozone (O_3) in comparison with the lower stratospheric (LSt; 150-25 hPa) O_3 derived from the first 10 years of the IASI/Metop-A satellite measurements (January 2008 – December 2017). The IASI instrument provides vertically-resolved O_3 profiles with very high spatial and temporal (twice daily) samplings, allowing to monitor O_3 changes in these two regions of the stratosphere. By applying multivariate regression models with adapted geophysical proxies on daily mean O_3 time series, we discriminate anthropogenic trends from various modes of natural variability, such as the El Niño/Southern Oscillation – ENSO. The representativeness of the O_3 response to its natural drivers is first examined. One important finding relies on a pronounced contrast between a positive LSt O_3 response to ENSO in the extra-tropics and a negative one in the tropics, with a delay of 3 months, which supports a stratospheric pathway for the ENSO influence on lower stratospheric and tropospheric O_3. In terms of trends, we find an unequivocal O_3 recovery from the available period of measurements in winter/spring at mid-high latitudes for the two stratospheric layers sounded by IASI (>~35°N/S in the MUSt and >~45°S in the LSt) as well as in the total columns at southern latitudes (>~45°S) where the increase reaches its maximum. These results confirm the effectiveness of the Montreal protocol and its amendments, and represent the first detection of a significant recovery of O_3 concurrently in the lower, in the mid-upper stratosphere and in the total column from one single satellite dataset. A significant decline in O_3 at northern mid-latitudes in the LSt is also detected, especially in winter/spring of the northern hemisphere. Given counteracting trends in LSt and MUSt at these latitudes, the decline is not categorical in total O_3. When freezing the regression coefficients determined for each natural driver over the whole IASI period but adjusting a trend, we calculate a significant speeding up in the O_3 response to the decline of O_3 depleting substances (ODS) in the total column, in the LSt and, ~~in~~to a lesser extent, in the MUSt, at high southern latitudes over the year. Results also show a~~A~~ small significant acceleration of the O_3 decline at northern mid-

latitudes in the LSt and in the total column ~~is also highlighted~~ over the last years. That, specifically, needs urgent investigation for identifying its exact origin and apprehending its impact on climate change. Additional years of IASI measurements would, however, be required to confirm the O_3 change rates observed in the stratospheric layers over the last years.

1 Introduction

Ozone is a key radiatively active gas of the Earth atmosphere, in both the troposphere and the stratosphere. While, in the troposphere, O_3 acts as a strong pollutant and an important greenhouse gas, in the stratosphere and, more particularly, in the middle-low stratosphere, it forms a protective layer for life on Earth against harmful solar radiation. In the 1980s, the scientific community motivated decision-makers to regulate the use of chlorofluorocarbons (CFCs)~~CFCs~~, after the unexpected discovery of the springtime Antarctic ozone hole (Chubachi, 1984; Farman et al., 1985) that was suspected to be induced by continued use of ~~chlorofluorocarbons (~~CFCs~~;~~ (Molina and Rowland, 1974; Crutzen, 1974); The O_3 depletion was later verified from measurements at other Antarctic sites (e.g. Farmer et al., 1987) and from satellite observations (Stolarski et al., 1986), and explained by the ~~These latter are at the origin of~~ role of CFC's on the massive destruction of O_3 following heterogeneous reactions on the surface of polar stratospheric clouds (Solomon, 1986; ~~Solomon,~~ 1999 and references therein). The world's nations reacted to that human-caused worldwide problem by ratifying the International Vienna Convention for the Protection of the Ozone Layer in 1985 and the Montreal Protocol in 1987 with its later amendments, which forced the progressive banning of these ozone depleting substances (ODS) in industrial applications by early 1990s with a total phase-out of the most harmful CFCs by the year 2000.

~~Ozone is very sensitive to changes in (photo-)chemistry, therefore a~~A recovery from O_3 depletion is expected in response to the Montreal Protocol and its amendments, but with a delayed period due to the long residence time of halocarbons in the atmosphere (Hofmann et al., 1997; Dhomse el al., 2006; WMO, 2007; 2011). The decline ~~in~~of CFCs in the stratosphere was only initiated about 10 years after their phasing out (Anderson et al., 2000; Newman et al., 2006; Solomon et al., 2006 ; Mäder et al., 2010; WMO, 2011; 2014). The early signs of ozone response to that decline were ~~confirmed~~ identified in several studies that reported first a slowdown in stratospheric ozone depletion (e.g. Newchurch et al., 2003; Yang et al., 2008), followed by a leveling off of upper stratospheric (e.g. WMO, 2007) and total O_3 (e.g. WMO, 2011; Shepherd et al., 2014) depletion since the 2000's. A significant onset of recovery was identified later for upper stratospheric O_3 (e.g. WMO, 2014; 2018; Harris et al., 2015). Only a few studies have shown evidence for increasing total column O_3 in polar regions during springtime (e.g. Salby et al., 2011; Kuttippurath et al., 2013; Shepherd et al., 2014; Solomon et al., 2016). ~~No reliable estimates of long-term trend in total O_3 columns (TOC) at global scale have been reported yet~~ Statistically significant long-term recovery in total O_3 column (TOC) on a global scale has not

yet been observed, likely because of counteracting trends in the different vertical atmospheric layers. Ball et al. (2018) have found that a continuing O_3 decline prevails in the lower stratosphere since 1998, leading to a slower increase in total O_3 than expected from the effective equivalent stratospheric chlorine (EESC) decrease. However, the reported decline is not reproduced by the state-of-the-art models and its exact reasons are still unknown (Ball et al., 2018). Wargan et al. (2018) and Galytska et al. (2019) recently ~~suggested~~ reported that the decline in the extratropical lower stratosphere and tropical mid-stratosphere is dynamically controlled by variations in the tropical upwelling.

Although recent papers based on observational datasets and statistical approaches agree that we currently progress towards an emergence into ozone recovery (e.g. Pawson et al., 2014; Harris et al., 2015; Steinbrecht et al., 2017; Sofieva et al., 2017; Ball et al., 2018; Weber et al., 2018), trend magnitude and trend significance over the whole stratosphere substantially differ from one study to another and, consequently, they are still subject to uncertainty ~~controversy~~ (Keeble et al., 2018). A clear identification of the onset of O_3 recovery is very ~~sensitive~~ difficult due to concurrent sources of O_3 fluctuations (e.g. Reinsel et al., 2005; WMO, 2007, 2011). They include: changes in solar ultraviolet irradiance, in atmospheric circulation patterns such as the quasi-biennial oscillation (QBO; Baldwin et al., 2001) and the El Niño–Southern Oscillation (ENSO; e.g. Randel et al., 2009), in temperature, in ODS emissions and volcanic eruptions (e.g. Mt Pinatubo in 1991 and Calbuco in 2015) with their feedbacks on stratospheric temperature and dynamics (e.g. Jonsson et al., 2004). Furthermore, the differences in vertical/spatial resolution and in retrieval methodologies (inducing biases), possible instrumental degradations (inducing drifts), and use of merged datasets into composites, likely explain part of the trend divergence between various studies. Merging may be performed on deseasonalized anomalies, which offers the advantage of removing instrumental biases between the individual data records (Sofieva et al., 2017) but large differences remain in anomaly values between the independent datasets, as well as large instrumental drifts and drift uncertainty estimates that prevent deriving statistically accurate trends (Harris et al., 2015; Hubert et al., 2016).

In this context, there is a pressing need for long-duration, high-density and homogenized O_3 profile dataset to assess significant O_3 changes in different parts of the stratosphere and their contributions to the total O_3.

In this paper, we exploit the high frequency (daily) and spatial coverage of the IASI satellite dataset over the first decade of the mission (January 2008 – December 2017) to determine global patterns of reliable trends in the stratospheric O_3 records, separately in the Mid-Upper Stratosphere (MUSt) and the Lower Stratosphere (LSt). This study is built on previous analysis of stratospheric O_3 trends from IASI, estimated on latitudinal averages over a shorter period (2008-2013) (Wespes et al., 2016). A multivariate linear regression (MLR) model (annual and seasonal formulations) that is similar to that previously used for tropospheric O_3 studies from

IASI (Wespes et al., 2017; 2018), but adapted here for the stratosphere with appropriate drivers, is applied ~~on~~to gridded daily mean O_3 time series in the MUSt and the LSt. The MLR model is evaluated in terms of its performance and ~~of~~ its ability to capture the observed variability in Section 2, in terms of representativeness of O_3 drivers in Section 3 and in terms of adjusted trends in Section 4. The minimum numbers of years of IASI measurements that is required to indeed detect the adjusted trends from MLR in the two layers is also estimated in Section 4 that ends with an evaluation of the trends detectable in polar winter and spring and with an evaluation of a speeding up in the O_3 changes.

2 Dataset and methodology

2.1 IASI O_3 data

The Infrared Atmospheric Sounding Interferometer (IASI) is a nadir-viewing Fourier transform spectrometer designed to measure the thermal infrared emission of the Earth-atmosphere system between 645 and 2760 cm^{-1}. Measurements are taken from the polar sun-synchronous orbiting meteorological Metop series of satellites, every 50 km along the track of the satellite at nadir and over a swath of 2200 km across track. With more than 14 orbits a day and a field of view of four simultaneous footprints of 12 km at nadir, IASI provides global coverage of the Earth twice a day at about 09:30 AM and PM mean local solar time.

The Metop program consists of a series of three identical satellites successively launched to ensure homogenous measurements covering more than 15 years. Metop-A and –B have been successively launched in October 2006 and September 2012. The third and last satellite was launched in November 2018 onboard Metop-C. In addition to its exceptional spatio-temporal coverage, IASI also provides good spectral resolution and low radiometric noise, which allows the measurement of a series of gas-phase species and aerosols globally (e.g. Clerbaux et al., 2009; Hilton et al., 2012; Clarisse et al., 2018).

For this study, we use the O_3 profiles retrieved by the Fast Optimal Retrievals on Layers for IASI (FORLI-O_3; version 20151001) near-real time processing chain set up at ULB (See Hurtmans et al, 2012 for a description of the retrieval parameters and the FORLI performances). The FORLI algorithm relies on a fast radiative transfer and a retrieval methodology based on the Optimal Estimation Method (Rodgers, 2000) that requires a priori information (a priori profile and associated variance-covariance matrix). The FORLI-O_3 a priori consists of one single profile and one covariance matrix built from the global Logan/Labow/McPeters climatology (McPeters et al., 2007). The profiles are retrieved on a uniform 1 km vertical grid on 41 layers from surface to 40 km with an extra layer from 40 km to the top of the atmosphere considered at 60 km. Previous characterization of the FORLI-O_3 profiles (Wespes et al., 2016) have demonstrated a good vertical sensitivity of IASI to the O_3 measurement with up to 4 independent levels of information

on the vertical profile in the troposphere and the stratosphere (MUSt; LSt; upper troposphere-lower stratosphere – UTLS – 300-150 hPa; middle-low troposphere − MLT – below 300 hPa). The two stratospheric layers that show distinctive patterns of O_3 distributions over the IASI decade (Fig. 1a) are characterized by high sensitivity (DOFS > 0.85; Fig. 1b) and low total retrieval errors (<5%; see Hurtmans et al., 2012; Wespes et al., 2016). The decorrelation between the MUSt and the LSt is further evidenced in Fig. 1d that shows low correlation coefficients (< 0.4) between the mean absolute deseasonalized anomalies (as calculated in Wespes et al., 2017) in the two layers (Fig. 1c). Note that the highest correlation coefficients over the Antarctic (~0.4) are due to the smaller vertical sensitivity of the IASI measurements over cold surface (Clerbaux et al., 2009). The latest validation exercises for the FORLI-O_3 product have demonstrated a high degree of precision with excellent consistency between the measurements taken from the two IASI instruments on Metop-A and -B, as well as a good degree of accuracy with biases lower than 20% in the stratospheric layers (Boynard et al., 2018; Keppens et al. 2017). Thanks to these good IASI-FORLI performances, large-scale dynamical modes of O_3 variations and long-term O_3 changes can be differentiated in the four retrieved layers (Wespes et al., 2016). The recent validations have, however, reported a drift in the MUSt FORLI-O_3 time series from comparison with O_3 sondes in the northern hemisphere (N.H.) (~3.53±3.09 DU.decade^{-1} on average over 2008–2016; Boynard et al., 2018) that was suggested to result from a pronounced discontinuity ("jump") rather than from a progressive change. Further comparisons with CTM simulations from the Belgian Assimilation System for Chemical ObsErvations (BASCOE; Chabrillat et al., 2018; Errera et al., 2019) confirm this jump that occurred on 15 September 2010 over all latitudes (see Fig. S1 of the supplementary materials). The discontinuity is suspected to result from updates in level-2 temperature data from Eumetsat that are used as inputs into FORLI (see Hurtmans et al., 2012). Hence, the apparent drift reported by Boynard et al. (2018) likely results from the jump ~~and contrasts with~~ rather than from a progressive "instrumental" drift. This is verified by the absence of drift in the O_3 time series after the jump (non-significant drift of -0.38±2.24 DU.decade^{-1} on average over October 2010 – May 2017; adapted from Boynard et al., 2018). This is in line with the excellent stability of the IASI Level-1 radiances over the full IASI period (Buffet et al., 2016). From the IASI-BASCOE comparisons, the amplitude of the jump has been estimated as lower than 2.0 DU in the 55°S–55°N latitude band and 4.0 DU in the 55°–90° latitude band of each hemisphere. The ~~effect~~ estimated amplitude of the jump is found to be relatively small in comparison to that of the decadal ~~on the calculation of significant~~ trends derived in Section 4 ~~is found small enough to~~, hence, it cannot explain the tendency in the IASI dataset~~rend.~~; ~~t~~Therefore, ~~this estimated~~the jump is not taken into account in the MLR. The jump values will be, however, considered in the discussion of the O_3 trends (Section 4).

Finally, the present study only uses the daytime measurements (defined with a solar zenith angle to the sun < 83°) from the IASI-A (aboard Metop-A) instrument that fully covers the first decade of the IASI mission. The daytime measurements are characterized by a higher vertical sensitivity (e.g. Clerbaux et al., 2009). Quality flags developed in previous IASI studies (e.g. Boynard et al.,

2018) were applied a posteriori to exclude data with a poor spectral fit, with less reliability or with cloud contamination.

2.2 Multivariate regression model

In ~~order~~ an effort to unambiguously discriminate anthropogenic trends in O_3 levels from the various modes of natural variability (illustrated globally in Fig.1c as deseasonalized anomalies), we have applied to the 2.5°x2.5° gridded daily MUSt and LSt O_3 time series, a MLR model that is similar to that previously developed for tropospheric O_3 studies from IASI (see ~~Eq. 1 and 2 in~~ Wespes et al., 2017; 2018) but here adapted to fit the stratospheric variations:

$$O_3(t) = Cst + x_{j=1} \cdot trend + \sum_{n=1:2} \left[a_n \cdot \cos(n\omega t) + b_n \cdot \sin(n\omega t) \right] + \sum_{j=2}^{m} x_j X_{norm,j}(t) + \varepsilon(t) \quad (1)$$

where t is the number of days, x_1 is the trend coefficient in the data, $\omega = 2\pi/365.25$, a_n, b_n, x_j are the regression coefficients of the seasonal and non-seasonal variables and $\varepsilon(t)$ is the residual variation (assumed to be autoregressive with time lag of 1 day). $X_{norm,j}$ are the m chosen explanatory variables, commonly called "proxies", which are normalized over the study period (2008 – 2017) with:

$$X_{norm}(t) = 2\left[X(t) - X_{median}\right] / \left[X_{\max} - X_{\min}\right] \quad (2)$$

In addition to harmonic terms that represent the 1-yr and 6-month variations, the MLR model includes the anthropogenic O_3 response through a linear trend (LT) term and a set of ~~explanatory variables (commonly called "~~proxies~~")~~ to parameterize the geophysical processes influencing the abundance of O_3 in the stratosphere. The MLR uses an iterative stepwise backward elimination approach to retain, at the end of the iterations, the most relevant proxies (with a 95% confidence level) explaining the O_3 variations (e.g. Mäder et al., 2007). Table 1 lists the selected proxies, their sources and their temporal resolutions. The proxies describe the influence of the Quasi-Biennial Oscillation (QBO; visible from the deseasonalized anomaly maps in Fig.1c with a typical band-like pattern around the Equator) at 10 hPa and 30 hPa, of the North Atlantic and the Antarctic Oscillations (NAO and AAO), of the El Niño/Southern Oscillation (ENSO), of the volcanic aerosols (AERO) injected into the stratosphere, of the strength of the Brewer-Dobson circulation (BDC) with the Eliassen-Palm flux (EPF), of the polar O_3 loss driven by the volume of polar stratospheric clouds (VPSC), of the tropopause height variation with the geopotential height (GEO) and of the mixing of tropospheric and stratospheric air masses with the potential vorticity (PV). The main proxies in terms of their influence on O_3 are illustrated in Fig. 2 over the period of the IASI mission. The construction of the EPF, VPSC and AERO proxies, which

are specifically used in this study, is explained hereafter, while the description of the other proxies can be found in previous IASI studies (Wespes et al., 2016; 2017).

The EPF proxy consists of the normalized upward component of the EP flux crossing 100 hPa and spatially averaged over the 45°-75° latitude band for each hemisphere. The fluxes are calculated from the NCEP/NCAR 2.5°x2.5° gridded daily reanalysis (Kalnay et al., 1996) over the IASI decade. The VPSC proxy is based on the potential volume of PSCs given by the volume of air below the formation temperature of nitric acid trihydrate (NAT) over 60°-90° north and south and calculated from the ERA-Interim reanalysis and from the MLS climatology of nitric acid (I. Wohltmann, private communication; Wohltmann et al., 2007; and references therein). The PSC volume is multiplied by the EESC to account for the changes in the amount of inorganic stratospheric chlorine that activates the polar ozone loss. The O_3 build-up and the polar O_3 loss are highly correlated with wintertime accumulated EP flux and PSC volume, respectively (Fusco and Salby, 1999; Randel et al., 2002; Fioletov and Shepherd, 2003 and Rex et al., 2004). These cumulative EP flux and PSC effects on O_3 levels are taken into account by integrating the EPF and VPSC proxies over time with a specific exponential decay time according to the formalism of Brunner et al. (2006; see Eq. 4). We set the relaxation time scale to 3 months everywhere, except during the wintertime build-up phase of O_3 in the extratropics (from October to March in the N.H. and from April to September in the southern hemisphere - S.H.) when it is set to 12 months. For ~~EFP~~EPF, it accounts for the slower relaxation time of extratropical O_3 in winter due to its longer photochemical lifetime. For VPSC, the 12-month relaxation time accounts for a stronger effect of stratospheric chorine on spring O_3 levels: the maximum of the accumulated VPSC (Fig. 2) coincides with the maximum extent of O_3 hole that develops during springtime and that lasts until November. Note that correlations between VPSC and EPF are possible since the same method is used to build these cumulative proxies. VPSC and EPF are also dynamically anti-correlated to some extent since a strong BDC is connected with warm polar stratospheric temperatures and, hence, reduced PSC volume (e.g. Wohltmann et al., 2007).

The AERO proxy is derived from aerosol optical depth (AOD) of sulfuric acid only. That proxy consists of latitudinally averaged (22.5°N-90°N – AERO-N, 22.5°S-90°S – AERO-S and 22.5°S-22.5°N – AERO-Eq) extinction coefficients at 12 µm calculated from merged aerosol datasets (SAGE, SAM, CALIPSO, OSIRIS, 2D-model-simulation and Photometer; Thomason et al., 2018) and vertically integrated over the two IASI stratospheric O_3 columns (AERO-MUSt and AERO-LSt). Fig.2 shows the AERO proxies (AERO-N, AERO-S and AERO-Eq) corresponding to the AOD over the whole stratosphere (150-2 hPa), while Fig.3 represents the latitudinal distribution of the volcanic sulfuric acid extinction coefficients integrated over the whole stratosphere (top panel) and, separately, over the MUSt (middle panel) and the LSt (bottom panel) from 2005 to 2017. The AOD distributions indicate the need for considering one specific AERO proxy for each latitudinal band (AERO-N, AERO-S and AERO-Eq) and for each vertical layer (AERO-MUSt and AERO-LSt). Note that, as an alternative proxy to AERO, the surface

area density of ambient aerosol, that represents the aerosol surface available for chemical reactions, has been tested, giving similar results.

Note also that, similarly to what has already been found for tropospheric O_3 from IASI (Wespes et al., 2016), several time-lags for ENSO (1-, 3- and 5-month lags; namely, ENSO-lag1, ENSO-lag3 and ENSO-lag5) are also included in the MLR model to account for a possible delay in the O_3 response to ENSO at high latitudes.

Finally, autocorrelation in the noise residual ε (t) (see Eq. 1 in Wespes et al., 2016) is accounted for in the MLR analysis with time lag of one day to yield the correct estimated standard errors for the regression coefficients. They are estimated from the covariance matrix of the regression coefficients and corrected at the end of the iterative process by the autocorrelation of the noise residual. The regression coefficients are considered significant if they fall in the 95% confidence level (defined by 2σ level).

In the seasonal formulation of the MLR model, the main proxies ($x_j X_{norm,j}$; with x_j, the regression coefficient and $X_{norm,j}$ the normalized proxy) are split ~~replaced by~~ into four ~~explanatory variables~~seasonal functions ($x_{spr} X_{norm,spr} + x_{sum} X_{norm,sum} + x_{fall} X_{norm,fall} + x_{wint} X_{norm,wint}$) that are independently and simultaneously adjusted for each grid cell (~~see Section 2.2 in~~ Wespes et al., 2017). Hence, the seasonal MLR adjusts 4 coefficients (instead of one in the annual MLR) to account for the seasonal O_3 response to changes in the proxy. If that method avoids to over-constrain the adjustment by the year-round proxies and, hence, reduces the systematic errors, the smaller daily data points covered by the seasonal proxies translate to a lower significance of these proxies. This is particularly true for EPF and VPSC that compensate each other by construction. As a consequence, the annual MLR is performed first in this study and, then, complemented with the seasonal one when it is found helpful for further interpreting the observations.

Figure 4 shows the latitudinal distributions of the O_3 columns in the two stratospheric layers over the IASI decade (first panels in Fig.4 a and b), as well as those simulated by the annual MLR regression model (second panels) along with the regression residuals (third panels). The root mean square error (*RMSE*) of the regression residual and the contribution of the MLR model into the IASI O_3 variations (calculated as $\frac{\sigma\left(O_3^{\text{Fitted\_model}}(t)\right)}{\sigma\left(O_3(t)\right)}$ where σ is the standard deviation relative to the regression model and to the IASI time series; bottom panels) are also represented (bottom panels). The results indicate that the model reproduces ~25-85% and ~35-95% of the daily O_3 variations captured by IASI in the MUSt and the LSt, respectively, and that the residual errors are generally lower than 10% everywhere for the two layers, except for the spring O_3 hole region

in the LSt. The *RMSE* relative to the IASI O_3 time series are lower than 15~~20~~ DU and 20~~15~~ DU at global scale in the MUSt~~LSt~~ and the LSt~~MUSt~~, respectively, except around the S.H. polar vortex in the LSt (~30 DU). On a seasonal basis (figure not shown), the results are only slightly improved: the model explains from ~35-90% and ~45-95% of the annual variations and the *RMSE* are lower than ~12 DU and ~23 DU everywhere, in the MUSt and the LSt, respectively. These results verify that the MLR models (annual and seasonal) reproduce well the time evolution of O_3 over the IASI decade in the two stratospheric layers and, hence, that they can be used to identify and quantify the main O_3 drivers in these two layers (see Section 3).

The MLR model has also been tested on nighttime FORLI-O_3 measurements only and simultaneously with daytime measurements, but this resulted in a lower quality fit, especially in the MUSt over the polar regions. This is due to the smaller vertical sensitivity of IASI during nighttime measurements, especially over cold surface, which causes larger correlations between stratospheric and tropospheric layers (e.g. 40-60% at high northern latitudes versus ~10-20% for daytime measurements based on deseasonalized anomalies) and, hence, which mixes counteracting~~ed~~ processes from these two layers. For this reason, only the results for the MLR performed on daytime measurements are presented and discussed in this paper.

3 Drivers of O_3 natural variations

Ascribing a recovery in stratospheric O_3 to a decline in stratospheric halogen species requires first identifying and quantifying natural cycles that may produce trend-like segments in the O_3 time series, in order to prevent any misinterpretation of those segments as signs of O_3 recovery. The MLR analysis performed in Section 2.2 that was found to give a good representation of the MUSt and LSt O_3 records shows distinctive relevant patterns for the individual proxies retained in the regression procedure, as represented in Fig. 5. The fitted drivers are characterized by significant regional differences in their regression coefficients with regions of in-phase relation (positive coefficients) or out-of-phase relation (negative coefficients) with respect to the IASI stratospheric O_3 anomalies. The areas of significant drivers (in the 95% confidence limit) are surrounded by non-significant cells when accounting for the autocorrelation in the noise residual. Figures 6 a and b respectively represent the latitudinal ~~distribution~~ averages of the fitted regression coefficients for the significant proxies showing latitudinal variation only in the O_3 response (namely, QBO, EPF, VPSC, AERO and ENSO) and of the contribution of these drivers into the O_3 variability (calculated as the product of the 2σ variability of each proxy by its corresponding fitted coefficient, i.e. the 2σ variability of the ~~adjusted signal of the~~reconstructed proxies). The 2σ O_3 variability in the IASI measurements and in the fitted MLR model are also represented (black and grey lines, respectively). Figure 7 displays the same results as Fig. 6b but for the austral spring and winter periods only (using the seasonal MLR).

The PV and GEO proxies are generally minor components (not shown here) with relative contributions smaller than 10% and large standard errors (>80%), except in the tropics where the contribution for GEO reaches 40% in the LSt due to the tropopause height variation. Each other adjusted proxy (QBO, SF, EPF, VPSC, AERO, ENSO, NAO and AAO) is an important contributor to the O_3 variations, depending on the layer, region, and season as described next:

1. QBO - The QBO at 10hPa and 30hPa are important contributors around the Equator for the two stratospheric layers. It shows up as a typical band-like pattern of high positive coefficients confined equatorward of ~15°N/S where the QBO is known to be a dominant dynamical modulation force associated with strong convective anomalies (e.g. Randel and Wu, 1996; Tian et al., 2006; Witte et al., 2008). In that latitude band, QBO10 and QBO30 explain up to ~8 DU and ~5 DU, respectively, of the MUSt and LSt yearly O_3 variations (see Fig. 5 and 6b; i.e. relative contributions up to ~50% and ~40% for QBO10/30 in MUSt and LSt O_3, respectively). The QBO is also influencing O_3 variations poleward of 60°N/S with a weaker correlation between O_3 and equatorial wind anomalies as well as in the sub-tropics with an out-of-phase transition. That pole-to-pole QBO influence results from the QBO-modulation of extra-tropical waves and its interaction with the BDC (e.g. Fusco and Salby, 1999). A pronounced seasonal dependence is observed in the out-of-phase sub-tropical O_3 anomalies in the MUSt, with the highest amplitude oscillating between the hemispheres in their respective winter (~5 DU of O_3 variations explained by QBO10/30 at ~20°S during JJA and at ~20°N during DJF; see Fig. 7b for the JJA period in the MUSt~~n~~ the DJF period is not shown), which is in agreement with Randel and Wu (1996). The amplitude of the QBO signal is found to be stronger for QBO30 than for QBO10 in the LSt, which is in good agreement with studies from other instruments for the total O_3 (e.g. Baldwin et al., 2001; Steinbrecht et al., 2006; Frossard et al., 2013; Coldewey-Egbers et al., 2014) and from IASI in the troposphere (Wespes et al., 2017). The smaller amplitude of O_3 response to QBO10 in the LSt compared to the MUSt is again in agreement with previous studies that reported changes in phase of the QBO10 response as a function of altitude with a positive response in the upper stratosphere and destructive interference in the mid-low stratosphere (Chipperfield et al., 1994; Brunner et al., 2006).

2. SF - In the MUSt layer, the solar cycle O_3 response is one of the strongest contributors and explains globally between ~2 and 15 DU of in-phase O_3 variations (i.e. higher O_3 ~~records~~ values during maximum solar irradiance) with the largest amplitude over the highest latitude regions (see Fig. 5; relative contribution up to ~20%). The solar influence in LSt is more complex with regions of in-phase and out-of-phase O_3 variations. The impact of solar variability on stratospheric O_3 abundance is due to a combination of processes: a modification in the O_3 production rates in the upper stratosphere induced by changes in spectral solar irradiance (e.g. Brasseur et al., 1993), the transport of solar

proton event-produced NO_y from the mesosphere down to the mid-low stratosphere where it decreases active chlorine and bromine and, hence, O_3 destruction (e.g. Jackman et al., 2000; Hood and Soukharev, 2006; and references therein) while it enhances the O_3 destruction in the MUSt through NO_x catalysed cycles, and its impact on the lower stratospheric dynamics including the QBO (e.g. Hood et al., 1997; Zerefos et al., 1997; Kodera and Kuroda, 2002; Hood and Soukharev, 2003, Soukharev and Hood, 2006). As for the QBO, the strong SF dependence at polar latitudes in the LSt with zonal asymmetry in the O_3 response reflects the influence of the polar vortex strength and of stratospheric warmings, and are in good agreement with previous results (e.g. Hood et al., 1997; Zerefos et al., 1997; Labitzke and van Loon, 1999; Steinbrecht et al., 2003; Coldewey-Egbers et al., 2014). It is also worth noting that because only one solar cycle is covered, the QBO and SF effects could not be completely separated because they have a strong interaction (McCormack et al., 2007).

3. EPF - The vertical component of the planetary wave Eliassen-Palm flux entering the lower stratosphere corresponds to the divergence of the wave momentum that drives the meridional residual Brewer-Dobson circulation. In agreement with previous studies (e.g. Fusco and Salby, 1999; Randel et al., 2002; Brunner et al., 2006; Weber et al., 2011), fluctuations in the BDC are shown to cause changes on stratospheric O_3 distribution observed from IASI: EPF largely positively contributes to the LSt O_3 variations at high latitudes of both hemispheres where O_3 is accumulated because of its long chemical lifetime, with amplitude ranging between ~20 and 100 DU (see Fig. 5 and 6; i.e. relative contribution of ~35-150%). The influence of the EPF decreases at lower latitudes where a stronger circulation induces more O_3 transported from the tropics to middle-high latitudes and, hence, a decrease in O_3 levels particularly below 20 km (Brunner et al., 2006). The influence of EP fluxes in the Arctic is the smallest in summer (see Fig.7; <~35 DU *vs* ~70 DU in fall; the two other seasons are not shown) due to the later O_3 build-up in polar vortices. In the S.H., because of the ~~deployment~~formation of the O_3 hole, the EP influence is smaller than in the N.H. and the seasonal variations are less marked. In the MUSt, the O_3 response attributed to variations in EPF is positive in both hemispheres, with a much lower amplitude than in the LSt (up to ~20-35 DU). The region of out-of-phase relation with negative EPF coefficients over the high southern latitudes (Fig. 5b) is likely attributable to the influence of VPSC that has correlations with EPF by construction (see Section 2.2). Furthermore, given the annual oscillations in EPF, compensation by the 1-yr harmonic term (eq. 1, Section 2) is found, but it remains weaker than the EPF contribution (data not shown), in particular at high latitudes where the EPF contribution is the largest.

4. VPSC - Identically to EPF, VPSC is shown to mainly contribute to O_3 variations in LSt over the polar regions (~55 DU or 40% in the N.H. *vs* ~60 DU or 85% in the S.H. on a

longitudinal average; see Fig. 6b) but with an opposite phase (Fig. 5 and 6a). The amplitude of the O_3 response to VPSC reaches its maximum over the southern latitudes during the spring (~60 DU; see Fig.7a for the austral spring period), which is consistent with the role of PSCs on the polar O_3 depletion when there is sufficient sunlight. The strong VPSC influence found at high northern latitudes in fall (Fig. 7a) are ~~likely~~ due to compensation effects with EPF as pointed out above and verified from sensitivity tests (not shown). Note also that the VPSC contribution into MUSt reflects the larger correlation between the two stratospheric layers over the southern polar region (Section 2.1, Fig. 1d).

5. AERO - Five important volcanic eruptions with stratospheric impact occurred during the IASI mission (Kasatochi in 2008, Sarychev in 2009, Nabro in 2011, Sinabung in 2014 and Calbuco in 2015; see Fig.3). The two major eruptions of the last decades, El Chichon (1982) and Mt. Pinatubo (1991), which ~~have~~ injected sulfur gases into the stratosphere, have been shown to enhance PSCs particle abundances (~15-25 km altitude), to remove NO_x (through reaction with the surface of the sulfuric aerosol to form nitric acid) and, hence, to make the ozone layer more sensitive to active chlorine (e.g. Hofmann et al., 1989; Hofmann et al., 1993; Portmann et al., 1996; Solomon et al., 2016). Besides this chemical effect, the volcanic aerosols also warm the stratosphere at lower latitudes through scattering and absorption of solar radiation, which further induces indirect dynamical effects (Dhomse et al., 2015; Revell et al., 2017). Even though the recent eruptions have been of smaller magnitude than El Chichon and Mt. Pinatubo, they produced sulphur ejection through the tropopause into the stratosphere (see Section 2.2, Fig.2 and Fig.3), as seen with AOD reaching $5x10^{-4}$ over the stratosphere (150-2 hPa), especially following the eruptions of Nabro (13.3°N, 41.6°E), Sinabung (3.1°N, 98.3°E) and Calbuco (41.3°S, 72.6°W). In the LSt, the regression supports an enhanced O_3 depletion over the Antarctic in presence of sulfur gases with a significantly negative annual O_3 response reaching ~25 DU (i.e. relative contribution of ~20% into O_3 variation; see Fig. 5b). On the contrary, enhanced O_3 levels in response to sulfuric acid are found in the MUSt with a maximum impact of up to10 DU (i.e. relative contribution of ~20% into the O_3 variation; see Fig. 5a) over the Antarctic. The change in phase in the O_3 response to AERO between the LSt (~15-25 km) and the MUSt (~25-40 km) over the Antarctic, as well as between polar and lower latitudes in the LSt (see Fig.5 and 6a), agree well with the heterogeneous reactions on sulfuric aerosol surface which reduce the concentration of NO_x to form nitric acid, leading to enhanced O_3 levels above 25 km but leading to decreased O_3 levels due to chlorine activation below 25 km (e.g. Solomon et al., 1996). On a seasonal basis, the depletion due to the presence of sulfur gases reaches ~30 DU on a longitudinal average, over the S.H. polar region during the austral spring (see Fig.7a) highlighting the link between volcanic gases converted to sulfate aerosols and heterogeneous polar halogen chemistry.

6. NAO – The NAO is an important mode of global climate variability, particularly in northern winter. It describes large-scale anomalies in sea level pressure systems between the sub-tropical Atlantic (Azores; high pressure system) and sub-polar (Iceland; low pressure system) regions (Hurrell, 1995). It disturbs the location and intensity of the North Atlantic jet stream that separates these two regions depending on the phase of NAO. The positive (negative) phase of the NAO corresponds to larger (weaker) pressure difference between the two regions leading to stronger westerlies (easterlies) across the mid-latitudes (Barnston and Livezey, 1987). The two pressure system regions are clearly identified in the stratospheric O_3 response to NAO, particularly in the LSt, with positive regression coefficients above the Labrador-Greenland region and negative coefficients above the Euro-Atlantic region (Fig. 5b). Above these two sectors, the positive phase induces, respectively, an increase and a decrease in LSt O_3 levels. The negative phase is characterized by the opposite behaviour. That NAO pattern is in line with previous studies (Rieder et al., 2013) and was also observed from IASI in tropospheric O_3 (Wespes et al., 2017). The magnitude of annual LSt O_3 changes attributed to NAO variations reaches ~20 DU over the in-phase Labrador region (i.e. contribution of 25% relative to the O_3 variations), while a much lower contribution is found for the MUSt (~4 DU or ~10%). The NAO coeffficient in the LSt also shows that the influence of the NAO extends further into northern Asia in the case of prolonged NAO phases. The NAO has also been shown to influence the propagation of waves into the stratosphere, hence, the BDC and the strength of the polar vortex in the N.H. mid-winter (Thompson and Wallace, 2000; Schnadt and Dameris, 2003; Rind et al., 2005). That connection between the NAO and the BDC might explain the negative anomaly in the O_3 response to EPF in the LSt over northern Asia which matches the region of negative response to the NAO.

7. AAO - The extra-tropical circulation of the S.H. is driven by the Antarctic oscillation that is characterized by geopotential height anomalies south of 20°S, with high anomalies of one sign centered in the polar region and weaker anomalies of the opposing sign north of 55°S (Thompson and Wallace, 2000). This corresponds well to the two band-like regions of opposite signs found for the regression coefficients of adjusted AAO in the LSt (negative coefficients centered in Antarctica and positive coefficient north of ~40°S; see Fig.5b). Similarly to the NAO~~N.H. mode~~, the strength of the residual mean circulation and of the polar vortex in the S.H. are modulated by the AAO through the atmospheric wave activity (Thompson and Wallace, 2000; Thompson and S~~o~~olomon, 2001). During the positive (negative) phase of the AAO, the BDC is weaker (stronger) leading to less (more) O_3 transported from the tropics into the southern polar region, and the polar vortex is stronger (weaker) leading to more (less) O_3 depletion inside. This likely explains both the positive AAO coefficients in the region north of ~40°S (contribution < ~5 DU or ~10%) and the negative coefficients around and over the Antarctic

(contribution reaching ~10 DU or ~15%; exception is found with positive coefficients over the western Antarctic). The dependence of O_3 variations to the AAO in the MUSt is lower than ~7 DU (or ~15%).

8. ENSO - Besides the NAO and the AAO, the El Nino southern oscillation is another dominant mode of global climate variability. This coupled ocean-atmosphere phenomenon is governed by sea surface temperature (SST) differences between high tropical and low extra-tropical Pacific regions (Harrison and Larkin, 1998). Domeisen et al. (2019) have recently reviewed the possible mechanisms connecting the ENSO to the stratosphere in the tropics and the extratropics of both hemispheres. The ozone response to ENSO is represented in Fig. 5 only for the ENSO-lag3 proxy which is found to be the main ENSO proxy contributing to the observed O_3 variations. While in the troposphere, previous works have shown that the ENSO influence mainly results in a high contrast of the regression coefficients between western Pacific/Indonesia/North Australia and central/eastern Pacific regions caused by reduced rainfalls and enhanced O_3 precursor emissions above western Pacific (called "chemical effect") (e.g. e.g. Oman et al., 2013; Valks et al., 2014; Ziemke et al., 2015; Wespes et al., 2016; and references therein), the LSt O_3 response to ENSO is shown here to translate into a strong tropical-extratropical gradient in the regression coefficients with a negative response in the tropics and a positive response at higher latitudes (~5 DU and ~10 DU, respectively, on longitudinal averages; see Fig. 6a). In the MUSt, ENSO is globally a smaller out-of-phase driver of O_3 variations (response of ~5 DU). The decrease in LSt O_3 during the warm ENSO phase in the tropics (characterized by a negative ENSO lag-3 coefficient reaching 7 DU (or 35%), respectively, in the LSt; see Fig. 5) is consistent with the ENSO-modulated upwelling via deep convection in the tropical lower stratosphere and, hence, increased BD circulation (e.g. Randel et al., 2009). The in-phase accumulation of LSt O_3 in the extra-tropics (contribution reaching 15 DU or 20%; see Fig. 5) is also consistent with enhanced extra-tropical planetary waves that propagate into the stratosphere during the warm ENSO phase, resulting in sudden stratospheric warmings and, hence, in enhanced BDC and weaker polar vortices (e.g. Brönnimann et al., 2004; Manzini et al., 2006; Cagnazzo et al., 2009). The very pronounced link between stratospheric O_3 and the ENSO related dynamical pathways with a time lag of about 3 months is one key finding of the present work. Indeed, ~~if~~ the influence of ENSO on stratospheric O_3 measurements has already been reported in earlier studies (Randel and Cobb, 1994; Brönnimann et al., 2004; Randel et al., 2009; Randel and Thompson, 2011; Oman et al., 2013; Manatsa and Mukwada, 2017; Tweedy et al., 2018), but it is the first time that a delayed stratospheric O_3 response is investigated in MLR studies. A 4- to 6-month time lag in O_3 response to ENSO has similarly been identified from IASI in the troposphere (Wespes et al., 2017), where it was explained not only by a tropospheric pathway but also by a specific stratospheric pathway similar to that modulating stratospheric O_3 but with further impact downward onto

tropospheric circulation (Butler et al., 2014; Domeisen et al., 2019). Furthermore, the 3-month lag identified in the LSt O_3 response is fully consistent with the modelling work of Cagnazzo et al. (2009) that reports a warming of the polar vortex in February-March following a strong ENSO event (peak activity in November-December) associated with positive O_3 ENSO anomaly reaching ~10 DU in the Arctic and negative anomaly of ~6-7 DU in the Tropics. We find that the tropical-extra-tropical gradient in O_3 response to ENSO-lag3 is indeed much stronger in spring with contributions of ~20-30 DU (see Fig.7a for the austral spring period *vs* winter).

Overall, although the annual MLR model underestimates the O_3 variability at high latitudes (>50°N/S) by up to 5 DU, particularly in the MUSt (see Fig. 6b), we conclude that it gives a good overall representation of the sources of O_3 variability in the two stratospheric layers sounded by IASI. This is particularly true for the spring period (see Fig. 7) which was studied in several earlier works to reveal the onset of Antarctic total O_3 recovery (Salby et al., 2011; Kuttippurath et al., 2013; Shepherd et al., 2014; Solomon et al., 2016; Weber et al., 2018), despite the large O_3 variability due to the hole formation during that period (~80 DU). It is also interesting to see from Fig.7 that the broad O_3 depletion over Antarctica in the LSt is attributed by the MLR to VPSC (up to 60 DU of explained O_3 variability on a latitudinal average). Following these promising results, we further analyze below the O_3 variability in response to anthropogenic perturbations, assumed in the MLR model by the linear trend term, with a focus over the polar regions.

4 Trend analysis

4.1 10-year trend detection in stratospheric layers

The distributions of the linear trend estimated by the annual regression are represented in Fig. 8a for the MUSt and the LSt (left and right panels). In agreement with the early signs of O_3 recovery reported for the extra-tropical mid- and upper stratosphere above ~25-10 hPa (>25-30 km; Pawson et al., 2014; Harris et al., 2015; Steinbrecht et al., 2017; Sofieva et al., 2017; Ball et al., 2018), the MUSt shows significant positive trends larger than 1 DU/yr poleward of ~35°N/S (except over Antarctica). The corresponding decadal trends (>10 DU/decade) are much larger than the discontinuity of ~2-4 DU encountered in the MUSt record on 15 September 2010 and discussed in section 2.1. The tropical MUSt also shows positive trends but they are weaker (<0.8 DU/yr) or not significant. The largest increase is observed in polar O_3 with amplitudes reaching ~2.05 DU/yr. The mid-latitudes also show significant O_3 enhancement which can be attributed to airmass mixing after the disruption of the polar vortex (Knudsen and Grooss, 2000; Fioletov and Shepherd, 2005; Dhomse, 2006; Nair et al., 2015).

As in the MUSt, the LSt is characterized in the southern polar latitudes by significantly positive and large trends (between ~ ~~|~~1.0~~|~~ and ~~|~~2.5~~|~~ DU/yr). In the mid-latitudes, the lower stratospheric trends are significantly negative, i.e. opposite to those obtained in the MUSt. This highlights the independence between the two O_3 layers sounded by IASI in the stratosphere. Poleward of 25°N the negative LSt trends range between ~ ~~-|~~0.5~~|~~ and ~~-|2.0~~1.7|~~ DU/yr. Negative trends in lower stratospheric O_3 have already been reported in extra-polar regions from other space-based measurements (Kyrölä et al., 2013; Gebhardt et al., 2014; Sioris et al., 2014; Harris et al., 2015; Nair et al., 2015; Vigouroux et al., 2015; Wespes et al., 2016; Steinbrecht et al., 2017; Ball et al., 2018) and may be due to changes in stratospheric dynamics at the decadal timescale (Galytska et al., 2019). These previous studies, which were characterized by large uncertainties or resulted from composite-data merging techniques, are confirmed here using a single dataset. The negative trends which are observed at lower stratospheric middle latitudes are difficult to explain with chemistry-climate models (Ball et al., 2018). It is also worth noting that the significant MUSt and LSt O_3 trends are of the same order as those previously estimated from IASI over a shorter period (from 2008 to 2013) and latitudinal averages (see Wespes et al., 2016). This suggests that the trends are not very sensitive to the natural variability in the IASI time series, hence, supporting the significance of the O_3 trends presented here.

The sensitivity of IASI O_3 to the estimated trend from MLR is further verified in Fig. 8b that represents the global distributions of relative differences in the *RMSE* of the regression residuals obtained with and without a linear trend term included in the MLR model ($(RMSE_{\_w/o\_LT} - RMSE_{\_with\_LT})/RMSE_{\_with\_LT} \times 100$; in %). An increase of ~1.0-4.0% and ~0.5-2.0% in the *RMSE* is indeed observed for both the MUSt and the LSt, respectively, in regions of significant trend contribution (Fig. 8a), when the trend is excluded. This demonstrates the significance of the trend in improving the performance of the regression. Another statistical method that can be used for evaluating the possibility to infer, from the IASI time period, the significant positive or negative trends in the MUSt and the LSt, respectively, consists in determining the expected year when these specified trends would be detectable from the available measurements (with a probability of 90%) by taking into account the variance (σ_ε^2) and the autocorrelation (Φ) of the noise residual according to the formalism of Tiao et al. (1990) and Weatherhead et al. (1998). Such a method has already been used for evaluating the trends derived from IASI in the troposphere (Wespes et al., 2018). It represents a more drastic and conservative method than the standard MLR. The results are displayed in Fig. 8c for an assumed specified trend of |1.5| DU/yr, which corresponds to a medium amplitude of trends derived here above from the MLR over the mid-polar regions (Fig. 8a). In the MUSt, we find that ~2-3 additional years of IASI measurements would be required to unequivocally detect a ~~positive~~ trend of |1.5| DU/yr (with probability 0.90) over high latitudes (detectable from ~2020-2022 ± 6-12 months) whereas it should already be detectable over the mid- and lower latitudes (from ~2015 ± 3-6 months). In the LSt, an additional ~7 years (± 1-2 years) of IASI measurements would be required to

categorically identify the probable decline derived from the MLR in northern mid-latitudes, and even more to measure the enhancement in the southern polar latitudes. The longerest required measurement period ~~over the~~ at high latitudes is ~~explained by~~due to the largerest noise residuals in the regression fits (i.e. largest σ_ε) ~~in the IASI data~~at these latitudes (see Fig.4 a and b). Note that a larger specified trend amplitude would obviously require a shorter period of IASI measurement. We find that only ~2 additional years would be required to detect a specified trend of |2.5| DU/yr which characterizes the LSt at ~~mid~~ high latitudes (data not shown).

4.2 Stratospheric contributions to total O_3 trend

The effect on total O_3 of the counteracting trends in the northern mid-latitudes and of the constructive trends in the southern polar latitudes ~~trends derived~~ in the two stratospheric layers sounded by IASI is now investigated.

Figure 9 represents the global distributions of the contribution of the MUSt and the LSt into the total O_3 columns (Fig.9a; in %), of the adjusted trends for the total O_3 (Fig. 9b in DU/yr) and of the estimated year for a |1.5| DU/yr ~~per decade~~ trend detection with a probability of 90% (Fig. 9c). While no significant change or slightly positive trends in total O_3 after the inflection point in 1997 have been reported on an annual basis (e.g; Weber et al., 2018), Fig. 9b shows clear significant changes: negative trend at northern mid- and high latitudes (up to ~2.0 DU/yr north of 30°N) and positive trend over the southern polar region (up to ~3.0 DU/yr south of 45~~0~~°S). Although counteracting trends between lower and upper stratospheric O_3 have been pointed out in the recent study of Ball et al. (2018) to explain the non-significant recovery in total O_3, we find from IASI a dominance of the LSt decline that translates to negative trends over some regions of the N.H. mid- and high latitudes in TOC (Fig. 9b). This is explained by the contributions of 45-55% from the LSt to the total column, *vs* ~30-40% from the MUSt (Fig. 9a) in the mid- and polar regions over the whole year. In addition, the increase in total O_3 at high southern latitudes is dominated by the LSt, although both layers positively contribute around Antarctica, comparing to the trend distributions in Fig. 8~~significant positive trends over the high southern latitudes in both the MUSt and the LSt explains the largest total O_3 enhancement in polar region~~. Note that most previous ozone trends studies, including Ball et al. (2018), excluded the polar regions due to limited latitude coverage of some instruments merged in the data composites.

While the annual MLR shows a significant dominance of LSt trends over MUSt trends in the northern mid-latitudes and significant constructive trends in the southern latitudes, total O_3 trends are not ascribed with complete confidence according to the formalism of Tiao et al. (1990) and Weatherhead et al. (1998) discussed in Section 4.1. The detectability of a specified trend of |1.5| DU/yr (Fig. 9c), which corresponds to the medium trend derived from MLR in mid-high

latitudes of both hemispheres (Fig. 9b), would need several years of additional measurements to be unequivocal from IASI on an annual basis (from ~2022-2024 over the mid-latitudes and from ~2035 over the polar regions). A higher trend amplitude of ~|2.5| DU/yr derived from the MLR would be observable from ~2020-2025 (figure not shown).

The use of the annual MLR could translate to large systematic uncertainties on trends (implying large σ_ε), which induces a longer measurement period required to yield significant trends. These uncertainties could be reduced on a seasonal basis, by attributing different weights to the seasons, which would help in the categorical detection of a specified trend. This is investigated in the subsection below by focusing on the winter and the spring periods.

4.3 Trends in ~~polar~~ spring and winter

The reports on early signs of total O_3 recovery (Salby et al., 2011; Kuttippurath et al., 2013; Shepherd et al., 2014; Solomon et al., 2016; Kuttippurath and Nair, 2017; Weber et al., 2018) have all focused on the Antarctic region during spring, when the ozone hole area is at its maximum extent, i.e. the LSt O_3 levels at minimum values. Here we investigate the respective contributions of the LSt and the MUSt to the TOC recovery over the Southern latitudes ~~Pole~~during spring ~~-~~and also ~~at the~~ during ~~JJA~~ winter ~~period because~~ when the minima in O_3 levels occur in the MUSt ~~over Antarctica occur later in summer~~ (down to ~60 DU in polar regions), in comparison with the Northern latitudes. Figures 10 and 11, respectively, show the S.H. and the N.H. distributions of the estimated trends from seasonal MLR (left panels) and of the corresponding year required for a significant detection of |3.0| DU increase per ~~decade~~ year (right panels) during their respective winter (JJA and DJF; Fig. 10a and 11a) and spring (SON and MAM; Fig. 10b and 11b) for the total, MUSt and LSt O_3 (top, middle and bottom panels, respectively). Fig. 10 a and b clearly show significant positive trends over Antarctica and the southernmost latitudes of the Atlantic and Indian oceans, with amplitudes ranging between ~1-5 DU/yr over latitudes south of ~35-40°S in total, MUSt and LSt O_3 (~3.~~9~~6±~~1~~2.7 DU/yr, ~~2.7~~3.0±1.~~0~~3 DU/yr, ~~3.3~~3.6±~~2.6~~3.1 DU/yr and ~~4.4~~3.7±1.~~9~~7 DU/yr, ~1.~~6~~3±0.~~6~~7 DU/yr, ~3.~~4~~7±1.~~4~~6 DU/yr, on spatial averages, respectively over JJA and SON, for the three O_3 columns). These trends over 10 years are much larger than the amplitude of the discontinuity in the MUSt time series (section 2.1) and than the trends estimated in Sections 4.1 (see Fig.8 for the MUSt and the LSt) and 4.2 (see Fig.9 for TOC) over the whole year. In MUSt, significant positive trends are observed during each season over the mid- and polar latitudes of both hemispheres (Fig. 10 and 11 for the winter and spring periods; the other seasons are not shown here) but more particularly in winter and in spring where the increase reaches a maximum of ~4 DU/yr. In the LSt, the distributions are more complex: the trends are significantly negative in the mid-latitudes of both hemispheres, especially in winter~~,~~ and in spring of the N.H., while in spring of the S.H., some mid-latitude regions also show near-zero or even positive trends. The southern

polar region shows high significant positive trends in winter/spring (see Fig.10). For the total O_3 at mid-high latitudes, given the mostly counteracting trends detected in the LSt and in the MUSt and the dominance of the LSt over the MUSt (~45-55% from the LSt vs ~30-40% from the MUSt into total O_3 over the whole year; ~~except over the Antarctica in spring as discussed above~~), these latitudes are governed by negative trends, especially ~~with the highest decline~~ in spring of the N.H. High significant increases are detected over polar regions in winter/spring of both hemispheres but more particularly in the S.H. where the LSt and MUSt trends are both of positive sign.

The substantial winter/spring positive trends observed in MUSt, LSt and total O_3 levels at high latitudes of the S.H. (and of the N.H. for the MUSt) are furthermore demonstrated to be detectable from the available IASI measurement period (see Fig. 10, right panels: an assumed increase of |3.0| DU/yr is detectable from 2016 ± 6 months and from 2018 ± 1 year in the MUSt and the LSt, respectively). The positive trend of ~4 DU/yr measured in polar total O_3 in winter/spring would be observable from ~2018-2020 ± 1-2 year and the decline of ~~|~~-3~~|~~ DU/yr in winter/spring of the N.H. in LSt would be detectable from ~2018-2020 ± 9 months (not shown here). Note that the ~~unrealistic~~ higher negative trends found above the Pacific at highest latitudes (see Fig. 10) correspond to the regions with longest required measurement period for significant trend detection and, hence, point to poor regression residuals. About ~50% and ~35% of the springtime MUSt and LSt O_3 variations, respectively, are due to anthropogenic factors (estimated by VPSC×EESC proxy and linear trend in MLR models). This suggests that O_3 changes especially in the LSt are mainly governed by dynamics, which contributes to a later projected trend-detection year in comparison with the MUSt (Fig. 10 and 11) and which may hinder the O_3 recovery process.

Overall, the large positive trends estimated concurrently in LSt, MUSt and total O_3 over the Antarctic region in winter/spring likely reflect the healing of the ozone layer with a decrease of polar ozone depletion (Salomon et al., 2016) and, hence, demonstrate the efficiency of the Montreal protocol. To the best of our knowledge, these results represent the first detection of a significant recovery in the stratospheric and the total O_3 columns over the Antarctic from one single satellite dataset.

4.4 Speeding up in O_3 changes

Positive trends in total O_3 have already been determined earlier by Solomon et al. (2016) and by Weber et al. (2018) over Antarctica during September over earlier periods (~2.5±1.5DU/yr over 2000-2014 and 8.2±6.2%/dec over 2000-2016, respectively). The larger trends derived from the IASI records (see Fig.10b; ~3.~~9~~7±1.7 DU/yr or ~14.4±5.8%/dec on average in TOC during SON) suggest that the O_3 response could be speeding up due to the accelerating decline of O_3 depleting substances (ODS) resulting from the Montreal Protocol. This has been investigated

here by estimating the change in trend in MUSt, LSt and total O_3 over the IASI mission. Knowing that the length of the measurement period is an important criterion for reducing systematic errors in the trend coefficient determination (i.e. the specific length of natural mode cycles should be covered to avoid any possible compensation effect between the covariates), the ozone response to each natural driver (including VPSC) taken from their adjustment over the whole IASI period (2008-2017; Section 3, Fig.5) is kept fixed. The linear trend term only is adjusted over variable measurement periods that all end in December 2017, by using a single linear iteratively reweighted least squares regression applied on gridded daily IASI time series after all the sources of natural variability fitted over the full IASI period are removed (typical examples of linear trend adjustment can be found in the Fig. S2 of the supplementary materials). The discontinuity found in the MUSt IASI O_3 records on September 2010 (see Section 2.1) is not taken into account in the regression; hence, it might over-represent the trends estimated over periods that start before the jump (i.e. 2008-2017, 2009-2017, 2010-2017). The zonally averaged results are displayed in Fig. 12 for the statistically significant total, MUSt and LSt O_3 trends and their associated uncertainty (accounting for the autocorrelation in the noise residuals; in the 95% confidence level) estimated from an annual regression. Note that the results are only shown for periods starting before 2015 as too short periods induce too large standard errors. In the LSt, a clear speeding up in the southern polar O_3 recovery is observed with amplitude ranging from ~1.5±0.43 DU/yr over 2008-2017 to ~65.5±32.5 DU/yr over 2015-2017 on ~~latitudinal~~ zonal averages. Similarly, a speeding of the O_3 decline at northern mid-latitudes is found with values ranging between ~-0.7±0.2 DU/yr over 2008-2017 and ~-2.58±1.25 DU/yr over 2015-2017. In the MUSt, a weaker increase is observed over the year around ~60° latitude of the S.H. (from ~~1.0~~0.8±0.~~1~~2 DU/yr over 2008-2017 to ~~3.5~~2.5±~~2.0~~1.3 DU/yr over 2015-2017). Given the positive acceleration in both LSt and MUSt O_3 in the S.H., this is where the total O_3 record is characterized by the largest significant recovery (from ~~1.5~~1.7±0.37 DU/yr over 2008-2017 to ~8.05±3.5 DU/yr over 2015-2017). Surprisingly, the speeding up in the O_3 decline in the N.H. is more pronounced in the total O_3 (from ~-1.0±0.24 DU/yr over 2008-2017 to ~-~~3.5~~5.0±~~1.5~~2.5 DU/yr over 2015-2017) compared to the LSt, despite the opposite trend in MUSt O_3. This could reflect the O_3 decline observed in the northern latitudes in the troposphere (~~|~~0.5~~|~~ DU/yr over 2008-2016; cfr Wespes et al., 2018) which is included in the total column.

Overall, the larger annual significant trend amplitudes derived over the last few years of total, MUSt and LSt O_3 measurements, compared with those derived from the whole studied period (Sections 4.1 and 4.2) and from earlier studies, translate to trends ~~that are categorically detectable over the covered period~~that remain detectable over the increasing uncertainty associated to the shorter and shorter time segments (see Fig. S3 of the supplementary materials), especially in both LSt and total O_3 in the S.H. This demonstrates that we progress towards a significant emergence and speeding up of O_3 recovery process in the stratosphere over the whole year. Nevertheless, we calculated that additional years of IASI measurements would help in confirming the changes in O_3 recovery and decline over the IASI period (e.g. ~ 4 additional years

are required to verify the trends calculated over the 2015-2017 segment in the highest latitudes in LSt). In addition, a longer measurement period would be useful to derive trends over successive segments of same length that are long enough to reduce the uncertainty, in order to make the trend and its associated uncertainty more comparable across the fit.

5 Summary and conclusion

In this study, we have analysed the changes in stratospheric O_3 levels sounded by IASI-A by examining the global pictures of natural and anthropogenic sources of O_3 changes independently in the lower (150-25 hPa) and in the mid-upper stratosphere (<25 hPa). We have exploited to that end a multi-linear regression model that has been specifically developed for the analysis of stratospheric processes by including a series of drivers known to have a causal relationship to natural stratospheric O_3 variations, namely SF, QBO-10, QBO-30, NAO, AAO, ENSO, AERO, EPF and VPSC. We have first verified the representativeness of the O_3 response to each of these natural drivers and found for most of them characteristic patterns that are in line with the current knowledge of their dynamical influence on O_3 variations. One of the most important finding related to the O_3 driver analysis relied on the detection of a very clear time lag of 3 months in the O_3 response to ENSO in the LSt, with a pronounced contrast between an in-phase response in the extra-tropics and an out-of-phase response in the tropics, which is consistent with the ENSO-modulated dynamic. The 3-month lag observed in the lower stratosphere is also coherent with the 4- to -6 months lag detected from a previous study in the troposphere (Wespes et al., 2017) and further supports the stratospheric pathway suggested in Butler et al. (2014) to explain an ENSO influence over a long distance. The representativeness of the influence of the O_3 drivers was also confirmed on a seasonal basis (e.g. high ENSO-lag3 effect in spring, strong VPSC and AERO influences during the austral spring …). These results have verified the performance of the regression models (annual and seasonal) to properly discriminate between natural and anthropogenic drivers of O_3 changes. The anthropogenic influence has been evaluated with the linear trend adjustment in the MLR. The main results are summarized as follows:

(i) A highly probable (within 95%) recovery process is derived from the annual MLR at high southern latitudes in the two stratospheric layers and, therefore, in the total column. It is also derived at high northern latitudes in the MUSt. However, ~~the effectiveness of the Montreal Protocol needs~~ a longer period of IASI measurements is needed ~~for being~~ to unequivocally demonstrate~~assured~~ a positive trend on annual basis in the IASI record. Only ~2-3 additional years of IASI measurements are required in the MUSt.

(ii) A likely O_3 decline (within 95%) is measured in the lower stratosphere at mid-latitudes, specifically, of the N.H., but it would require an additional ~7 years of IASI measurements to be categorically confirmed. Given the large contribution from the

LSt to the total column (~45-50% from LSt vs ~35% from the MUSt into TOCs), the decline is also calculated in total O_3 with ~4-6 years of additional measurements for the trend to be ~~being~~ unequivocal.

(iii) A significant O_3 recovery is categorically found in the two stratospheric layers (>~35°N/S in the MUSt and >~45°S in the LSt) as well as in the total column (>~45°S) during the winter/spring period, which confirms previous studies that showed healing in the Antarctic O_3 hole with a decrease of its areal extent. These results verify the ~~efficiency~~ efficacy of the ban on O_3 depleting substances imposed by~~of~~ the Montreal protocol ~~with the banning of ODS~~ and it's amendments, throughout the stratosphere and in the total column, from only one single satellite dataset for the first time.

(iv) The decline observed in LSt O_3 at northern mid-latitudes is unequivocal over the available IASI measurements in winter/spring of the N.H. The exact reasons for that decline are still unknown but O_3 changes in the LSt are estimated to be mainly attributable to dynamics ~~and it~~ which likely perturbs the healing of LSt and total O_3 in the N.H.

(v) A significant speeding up (within 95%) in that decline is measured in LSt and total O_3 over the last 10 years (from ~-0.7±0.2 DU/yr over 2008-2017 to ~-~~2.5~~2.8±~~1.5~~1.2 DU/yr over 2015-2017 in LSt O_3 on ~~latitudinal~~ zonal averages). Even if the acceleration cannot be categorically confirmed yet, ~~I~~it is of particular urgency to understand its causes for apprehending its possible impact on the O_3 layer and on future climate changes.

(vi) ~~-~~A clear and significant speeding up (within 95%) in stratospheric and total O_3 recovery is measured at southern latitudes (e.g. from ~1.5±0.~~3~~4 DU/yr over 2008-2017 to ~~~~6.5~~5.5±~~3.5~~2.5 DU/yr over 2015-2017 in the LSt), which ~~and~~ translate to trend values that ~~are~~ would be categorically detectable in the next few years on an annual basis. It demonstrates that we are currently progressing towards a substantial emergence in O_3 healing in the stratosphere over the whole year in the S.H..

Additional years of IASI measurements that will be provided by the operational IASI-C (2018) on flight and the upcoming IASI-Next Generation (IASI-NG) instrument onboard the Metop Second Generation (Metop-SG) series of satellites would be of particular interest to confirm and monitor, in the~~a~~ near future and over a longer period, the speeding up in the O_3 healing of the S.H. as well as in the LSt O_3 decline measured at mid-latitudes of the N.H. IASI-NG/Metop-SG is expected to extend~~t~~ the data record much further in the future (Clerbaux and Crevoisier, 2013; Crevoisier et al., 2014).

Data availability

The IASI O_3 data processed with FORLI-O_3 v0151001 can be downloaded from the Aeris portal at: http://iasi.aeris-data.fr/O3/ (last access: 14 July 2019).

Author contribution

C.W. performed the analysis, wrote the manuscript and prepared the figures. D.H. was responsible for the retrieval algorithm development and the processing of the IASI O_3 dataset. All authors contributed to the analysis and reviewed the manuscript.

Competing interests

The authors declare that they have no conflict of interest.

Acknowledgments

IASI has been developed and built under the responsibility of the Centre National d'Etudes Spatiales (CNES, France). It is flown onboard the Metop satellites as part of the EUMETSAT Polar System. The IASI L1 data are received through the EUMETCast near real time data distribution service. We acknowledge the financial support from the ESA O_3-CCI and Copernicus O_3-C3S projects. FORLI-O_3 is being implemented at Eumetsat with the support of the AC SAF project. The research in Belgium is also funded by the Belgian State Federal Office for Scientific, Technical and Cultural Affairs and the European Space Agency (ESA Prodex IASI Flow and B-AC SAF). We acknowledge Ingo Wohltmann (Alfred Wagner Institute, Postdam, Germany) as well as Beiping Luo (Institute for Atmosphere and Climate, ETH Zurich, Switzerland) and Larry Thomason (NASA Langley Research Center, Hampton, USA), for processing and providing datasets of volume of polar stratospheric clouds and of sulfuric acid extinction coefficients, respectively. We are also grateful to Maxime Prignon (Université de Liège, Liège, Belgium) for providing several years of BASCOE simulations.

908 **Table 1** List of the explanatory variables used in the multi-linear regression model applied on
909 IASI stratospheric O_3, their temporal resolution and their sources.
910

Proxy	Description (*resolution*)	Sources
F10.7	The 10.7 cm solar radio flux (*daily*)	NOAA National Weather Service Climate Prediction Center: ftp://ftp.ngdc.noaa.gov/STP/space-weather/solar-data/solar-features/solar-radio/noontime-flux/penticton/penticton_adjusted/listings/listing_drao_noontime-flux-adjusted_daily.txt
QBO^{10} **QBO^{30}**	Quasi-Biennial Oscillation index at 10hPa and 30hPa (*monthly*)	Free University of Berlin: www.geo.fu-berlin.de/en/met/ag/strat/produkte/qbo/
EPF	Vertical component of Eliassen-Palm flux crossing 100 hPa, averaged over 45°-75° for each hemisphere and accumulated over the 3 or 12 last months depending on the time period and the latitude (see text for more details) (*daily*)	Calculated at ULB from the NCEP/NCAR gridded reanalysis: https://www.esrl.noaa.gov/psd/data/gridded/data.ncep.reanalysis.html
AERO	Stratospheric volcanic aerosols; Vertically integrated sulfuric acid extinction coefficient at 12 µm over 150-25 hPa and 25-2hPa, averaged over the tropics and the extra-tropics north and south (see text for more details) (*monthly*)	Extinction coefficients processed at the Institute for Atmosphere and Climate (ETH Zurich, Switzerland; Thomason et al., 2018)
VPSC	Volume of Polar Stratospheric Clouds for the N.H. and the S.H. multiplied by the equivalent effective stratospheric chlorine (EESC) and accumulated over the 3 or 12 last months (see text for details) (*daily*)	Processed at the Alfred Wagner Institute (AWI, Postdam, Germany; Ingo Wolthmann, private communication) EESC taken from the Goddard Space Flight Center: https://acd-ext.gsfc.nasa.gov/Data_services/automailer/index.html
ENSO	Multivariate El Niño Southern Oscillation Index (MEI) (2-*monthly averages*)	NOAA National Weather Service Climate Prediction Center: http://www.esrl.noaa.gov/psd/enso/mei/table.html
NAO	North Atlantic Oscillation index for the N.H. (*daily*)	ftp://ftp.cpc.ncep.noaa.gov/cwlinks/norm.daily.nao.index.b500101.current.ascii
AAO	Antarctic Oscillation index for the S.H. (*daily*)	ftp://ftp.cpc.ncep.noaa.gov/cwlinks/norm.daily.aao.index.b790101.current.ascii
GEO	Geopotential height at 200 hPa (2.5°x2.5° gridded) (*daily*)	http://apps.ecmwf.int/datasets/data/interim-full-daily/?levtype=pl
PV	Potential vorticity at 200 hPa (2.5°x2.5° gridded) (*daily*)	

Figure captions

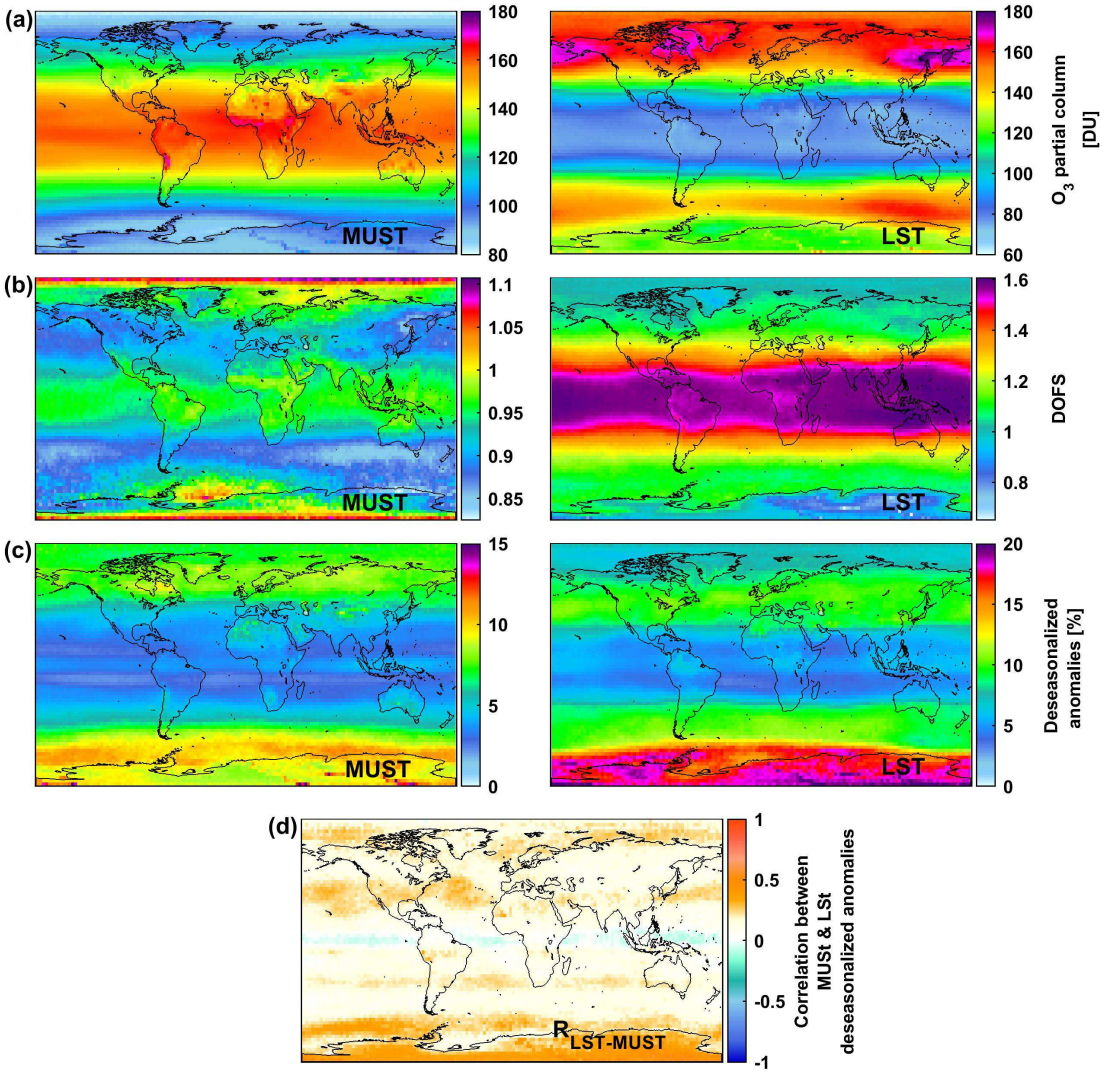

Fig.1. Global distribution of (a) daily O_3 columns (in Dobson Units - DU), (b) associated DOFS, (c) absolute deseasonalized anomalies (in %) averaged over January 2008 – December 2017 in the MUSt (Mid-Upper Stratosphere: >25 hPa; left panels) and in the LSt (Lower Stratosphere: 150-25hPa; right panels). (d) shows the correlation coefficients between the daily O_3 deseasonalized anomalies in the MUSt and in the LSt. Note that the scales are different between MUSt and LSt.

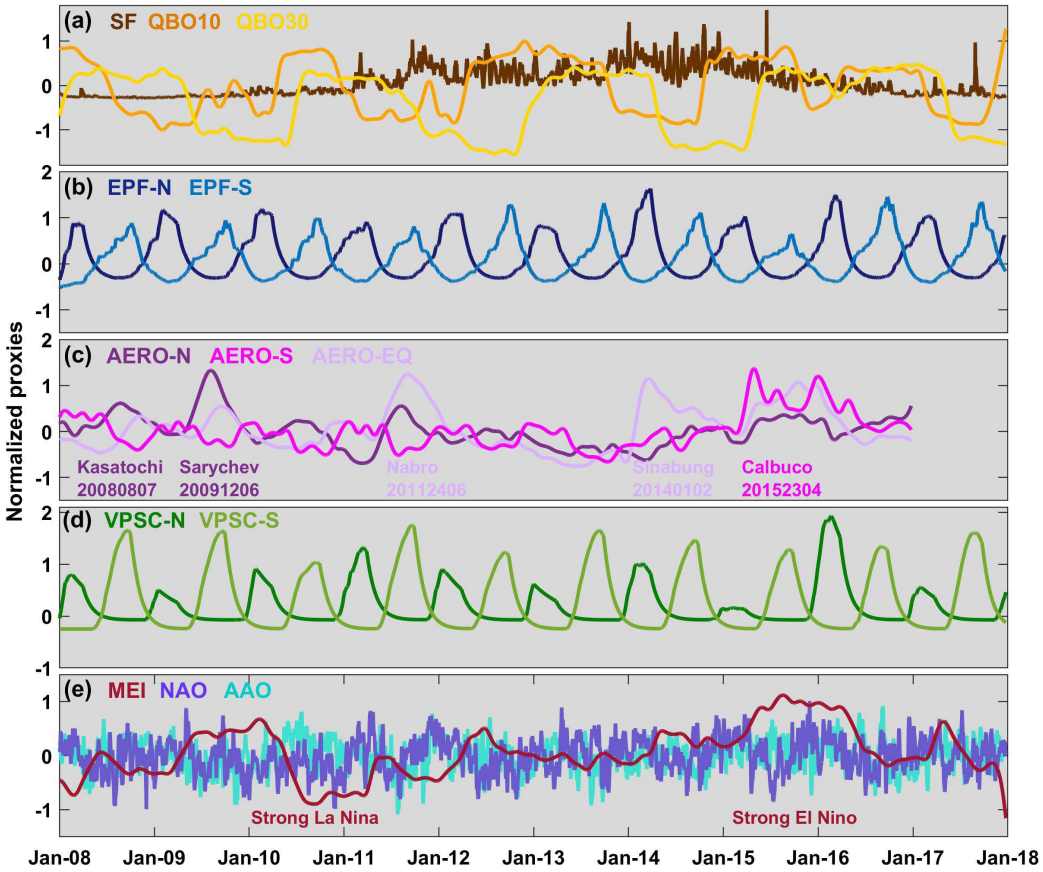

Fig.2. Normalized proxies as a function of time for the period covering January 2008 to December 2017 for (a) the F10.7 cm solar radio flux (SF) and the equatorial winds at 10 (QBO10) and 30 hPa (QBO30), respectively, (b) the upward components of the EP flux crossing 100 hPa accumulated over time and averaged over the 45°-75° latitude band for each hemispheres (EPF-N and EPF-S), (c) the extinction coefficients at 12 µm vertically integrated over the stratospheric O_3 column (from 150-2hPa) and averaged over the extra-tropics north and south (22.5°-90°N/S; AERO-N and AERO-S) and over the tropics (22.5°S-22.5°N; AERO-EQ) (the main volcanic eruptions are indicated), (d) the volume of polar stratospheric clouds multiplied by the equivalent effective stratospheric chlorine (EESC) and accumulated over time for the north and south hemispheres (VPSC-N and VPSC-S) and (e) the El Niño Southern (ENSO), North Atlantic (NAO) and Antarctic (AAO) oscillations.

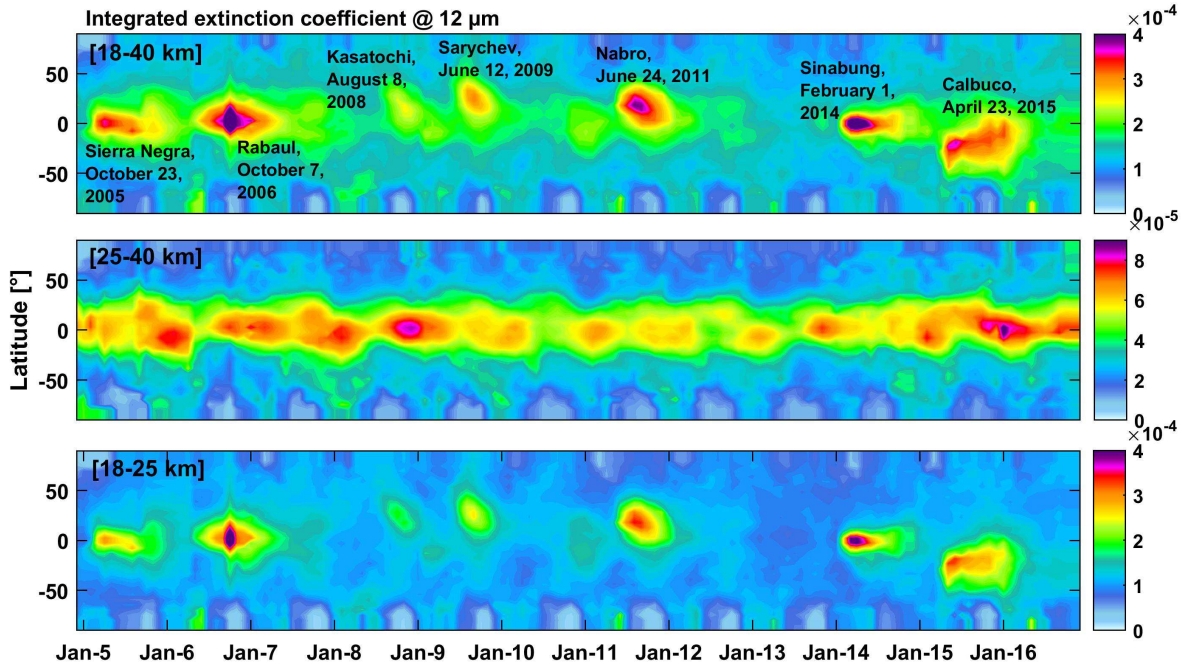

Fig.3: Latitudinal distribution of volcanic sulfuric acid extinction coefficient at 12 µm integrated over the stratosphere (top panel), over the middle stratosphere (middle panel) and the lower stratosphere (bottom panel) as a function of time from 2005 to 2017. The dataset consists of monthly mean aerosol data merged from SAGE, SAM, CALIPSO, OSIRIS, 2D-model-simulation and Photometer (processed at NASA Langley Research Center, USA and ETH Zurich, Switzerland).

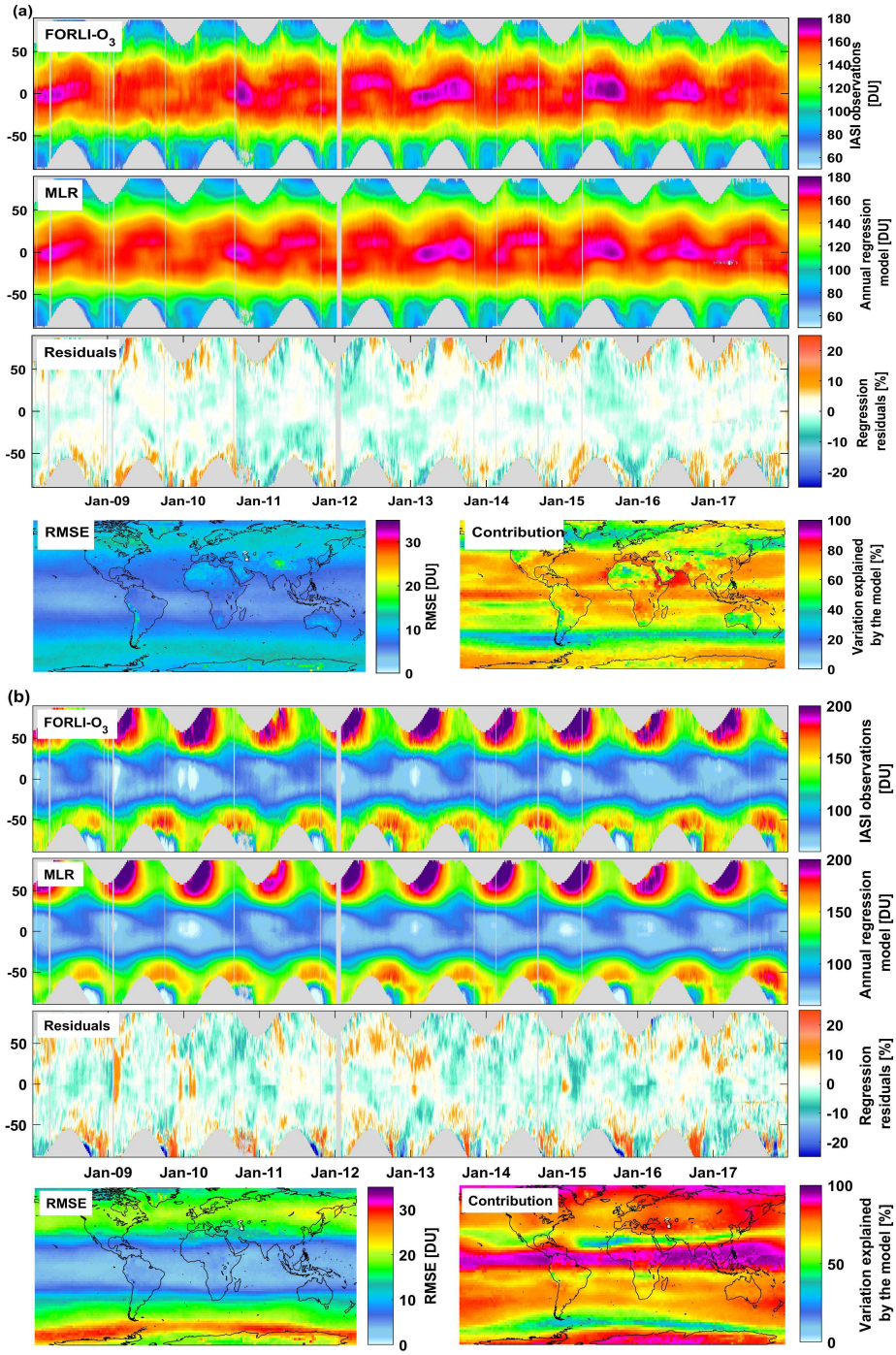

Fig.4: Latitudinal distribution of (a) MUSt O_3 column and (b) LSt O_3 columns as a function of time observed from IASI (in DU; top panels), simulated by the annual regression model (in DU, second panels) and of the regression residuals (in %; third panels). Global distribution of *RMSE* of the regression residual (in DU) and fraction of the variation in IASI data explained by the regression model calculated as $\left[100\times\left(\sigma\left(O_3^{Fitted\_model}(t)\right)/\sigma\left(O_3(t)\right)\right)\right]$ (in %; fourth panels).

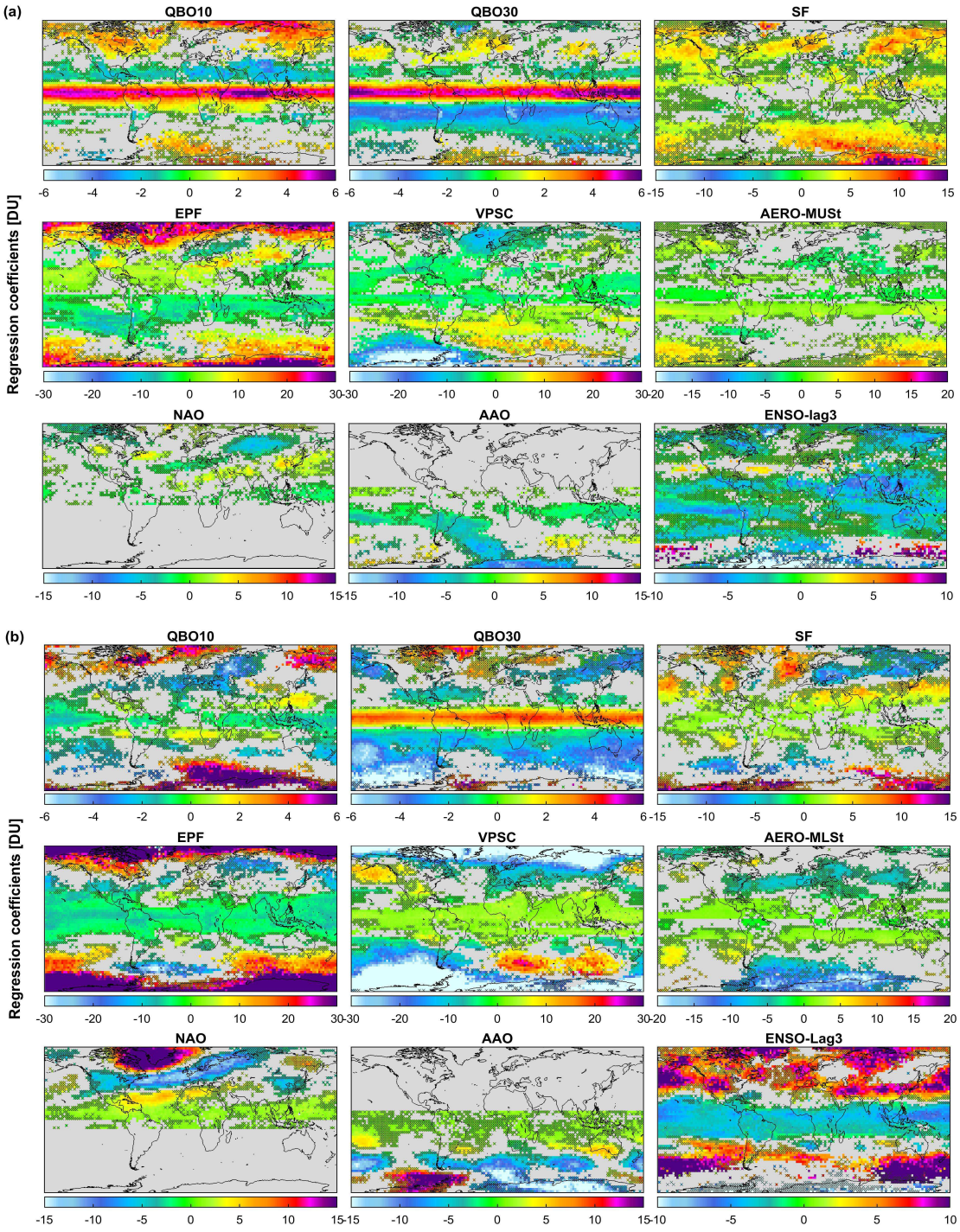

Fig.5: Global distribution of the annual regression coefficient estimates (in DU) for the main O_3 drivers in (a) MUSt and in (b) LSt: QBO10, QBO30, SF, EPF, VPSC, AERO, NAO, AAO and ENSO (ENSO-lag3 for both LSt and MUSt). Grey areas and crosses refer to non-significant grid cells in the 95% confidence limit. Note that the scales differ among the drivers.

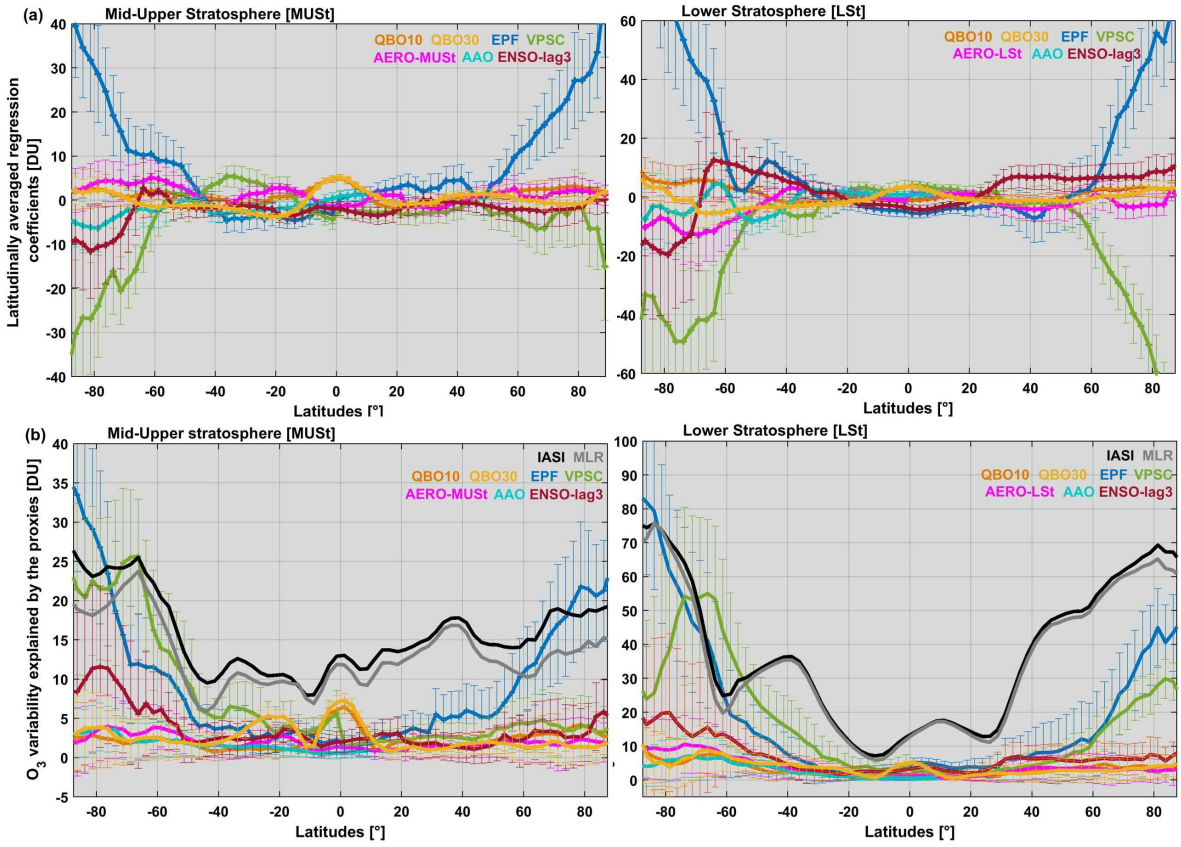

Fig.6: Latitudinal distributions (a) of fitting regression coefficients for various O_3 drivers (QBO10, QBO30, EPF, VPSC, AERO, AAO and ENSO-lag3; in DU) and (b) of 2σ O_3 variability due to variations in those drivers (in DU) from the annual MLR in MUSt and LSt (left and right panels respectively). Vertical bars correspond (a) to the uncertainty of fitting coefficients at the 2σ level and (b) to the corresponding error contribution into O_3 variation. Note that the scales are different.

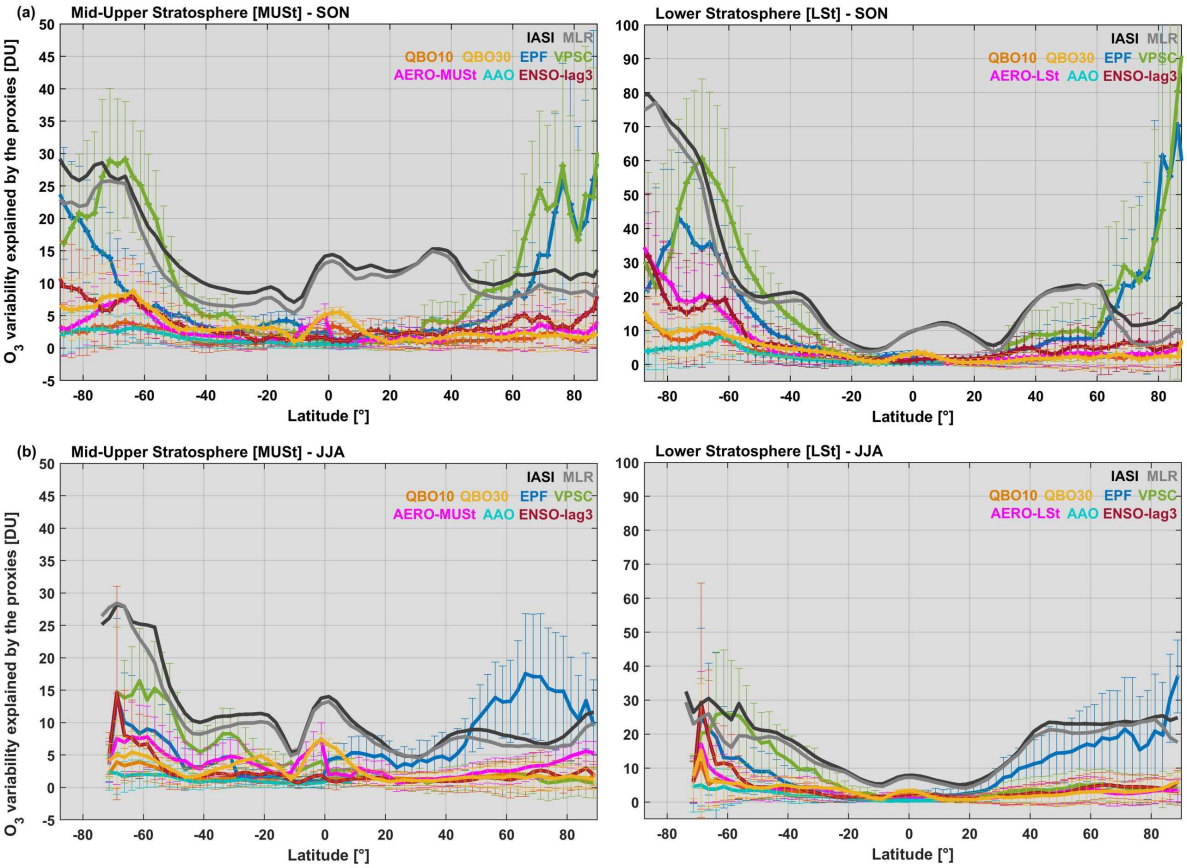

Fig.7: Same as Fig. 6b but for (a) the austral winter and (b) the austral spring periods (JJA and SON, respectively) from the seasonal MLR. Note that the scales are different.

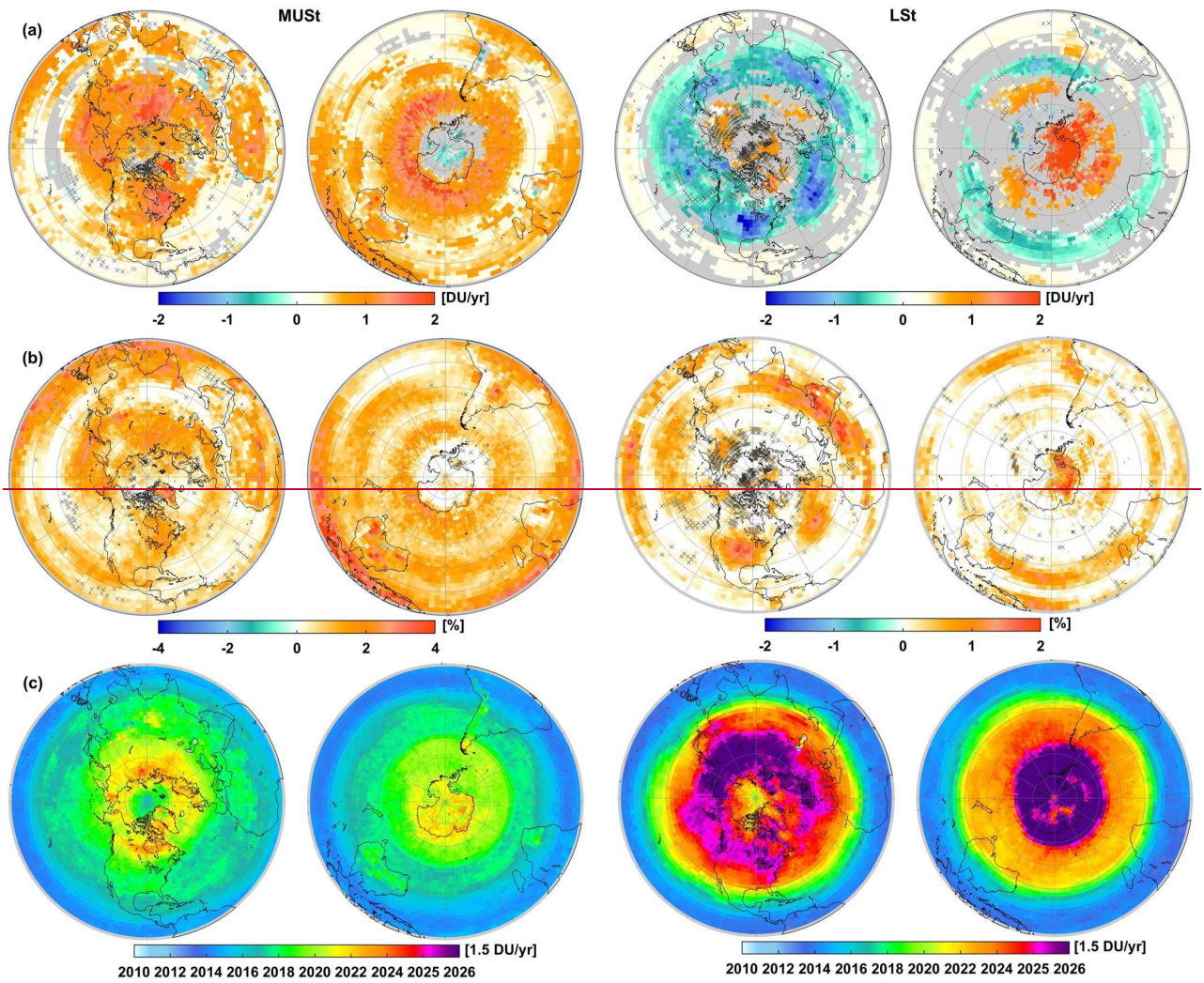
MUSt
LSt
(a)
[DU/yr]
-2 -1 0 1 2
(b)
[%]
-4 -2 0 2 4
-2 -1 0 1 2
(c)
[1.5 DU/yr]
2010 2012 2014 2016 2018 2020 2022 2024 2025 2026

996

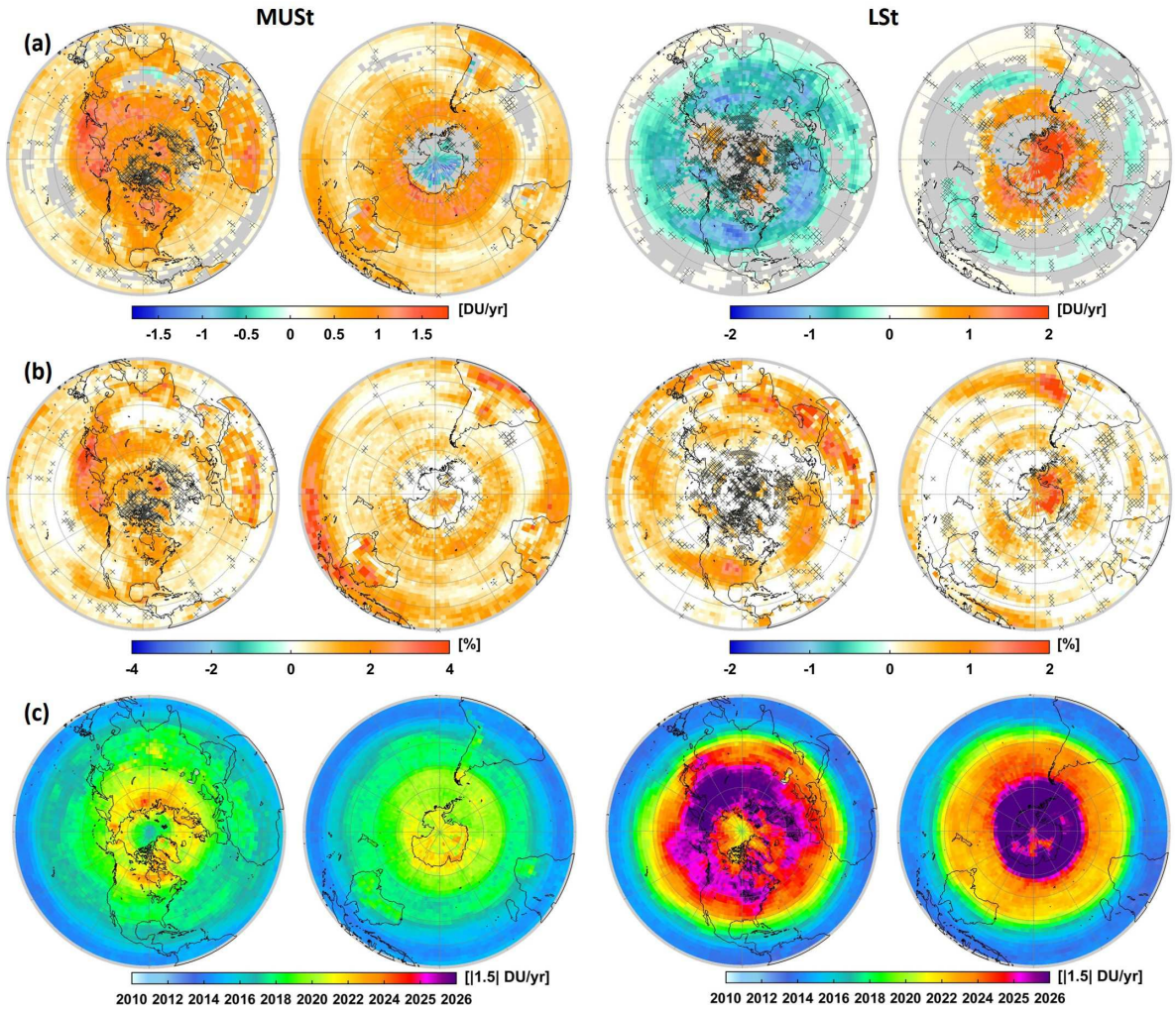

Fig. 8: Global distribution (a) of the estimated annual trends (in DU/yr; grey areas and crosses refer to non-significant grid cells in the 95% confidence limit), (b) of the IASI sensitivity to trend calculated as the differences between the *RMSE* of the annual MLR fits with and without linear trend term [$(RMSE_{\_w/o\_LT} - RMSE_{\_with\_LT})/RMSE_{\_with\_LT} \times 100$] (in %), (c) of the estimated year for a significant detection (with a probability of 90%) of a given trend of |1.5| DU/yr starting in January 2008 in MUSt and LSt O_3 columns (left and right panels, respectively). Note that the scales are different for the two layers.

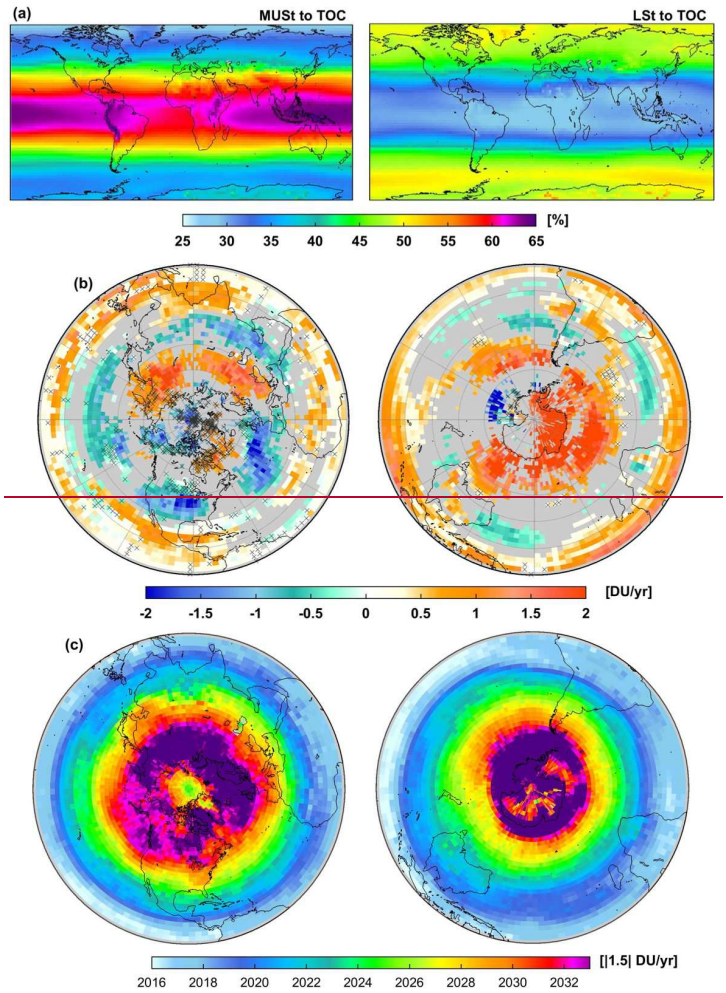
(a)
MUSt to TOC
LSt to TOC
[%]
25 30 35 40 45 50 55 60 65
(b)
[DU/yr]
-2 -1.5 -1 -0.5 0 0.5 1 1.5 2
(c)
[|1.5| DU/yr]
2016 2018 2020 2022 2024 2026 2028 2030 2032

1007

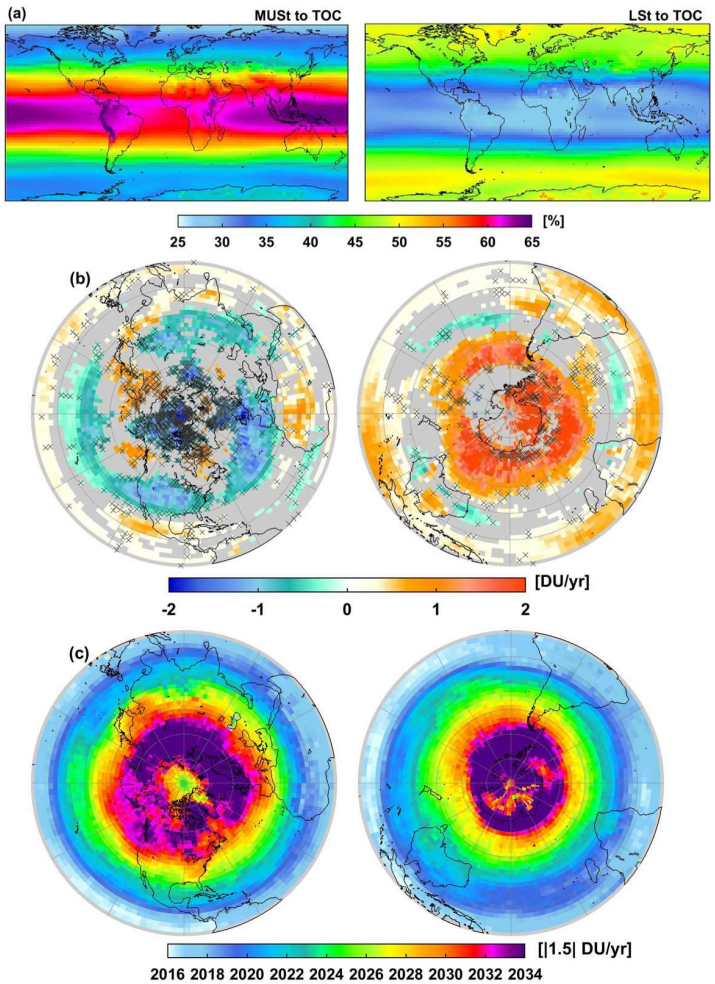

Fig.9: Global distribution of (a) the contribution (in %) of MUSt and LSt into the total O_3 (left and right panels respectively) averaged over January 2008 – December 2017, (b) fitted trends in total O_3 (in DU/yr; the grey areas and crosses refer to the non-significant grid cells in the 95% confidence limit) and (c) estimated year for the detection of a significant trend in total O_3 (with a probability of 90%) for a given trend of |1.5| DU/yr starting on January 2008.

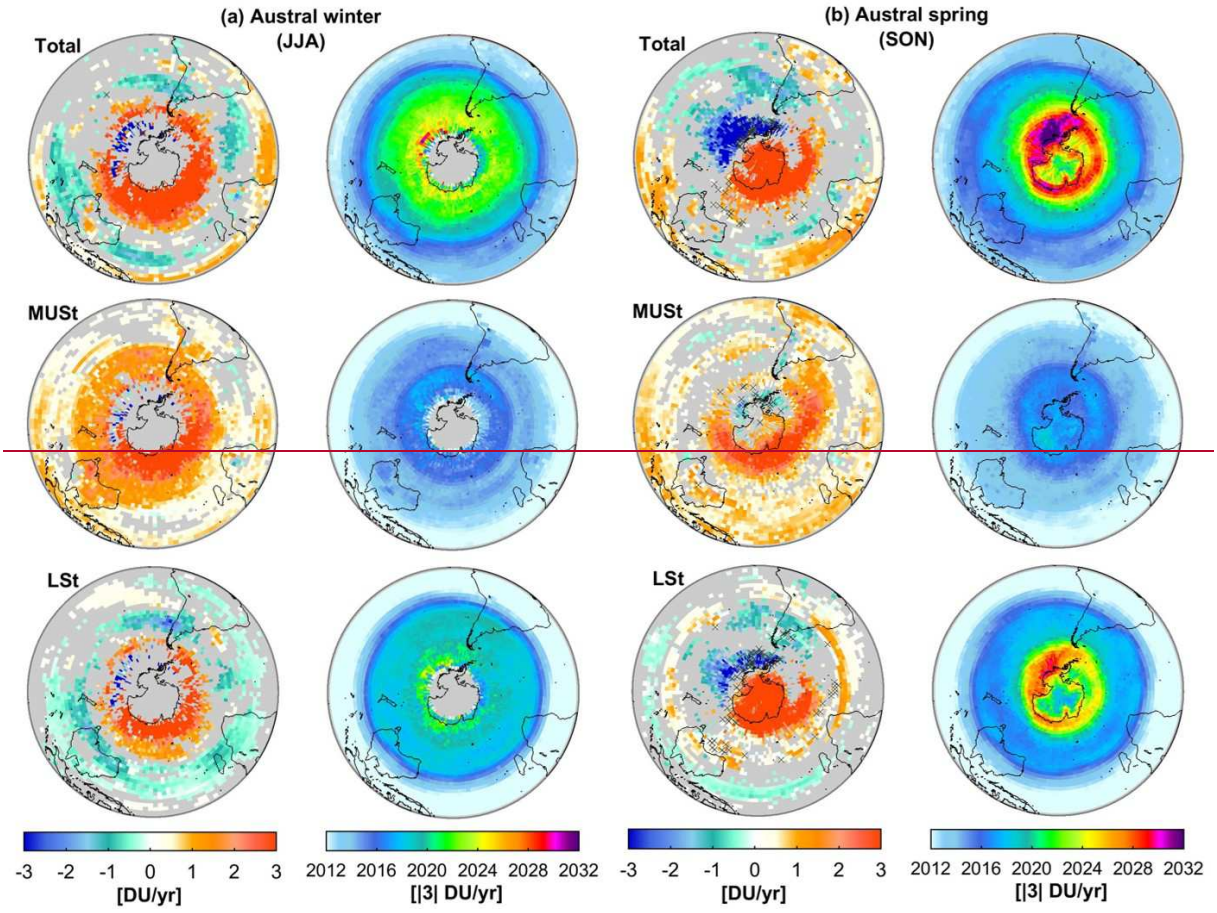
(a) Austral winter
(JJA)
(b) Austral spring
(SON)
Total
Total
MUSt
MUSt
LSt
LSt
-3 -2 -1 0 1 2 3
[DU/yr]
2012 2016 2020 2024 2028 2032
[|3| DU/yr]
-3 -2 -1 0 1 2 3
[DU/yr]
2012 2016 2020 2024 2028 2032
[|3| DU/yr]

1014

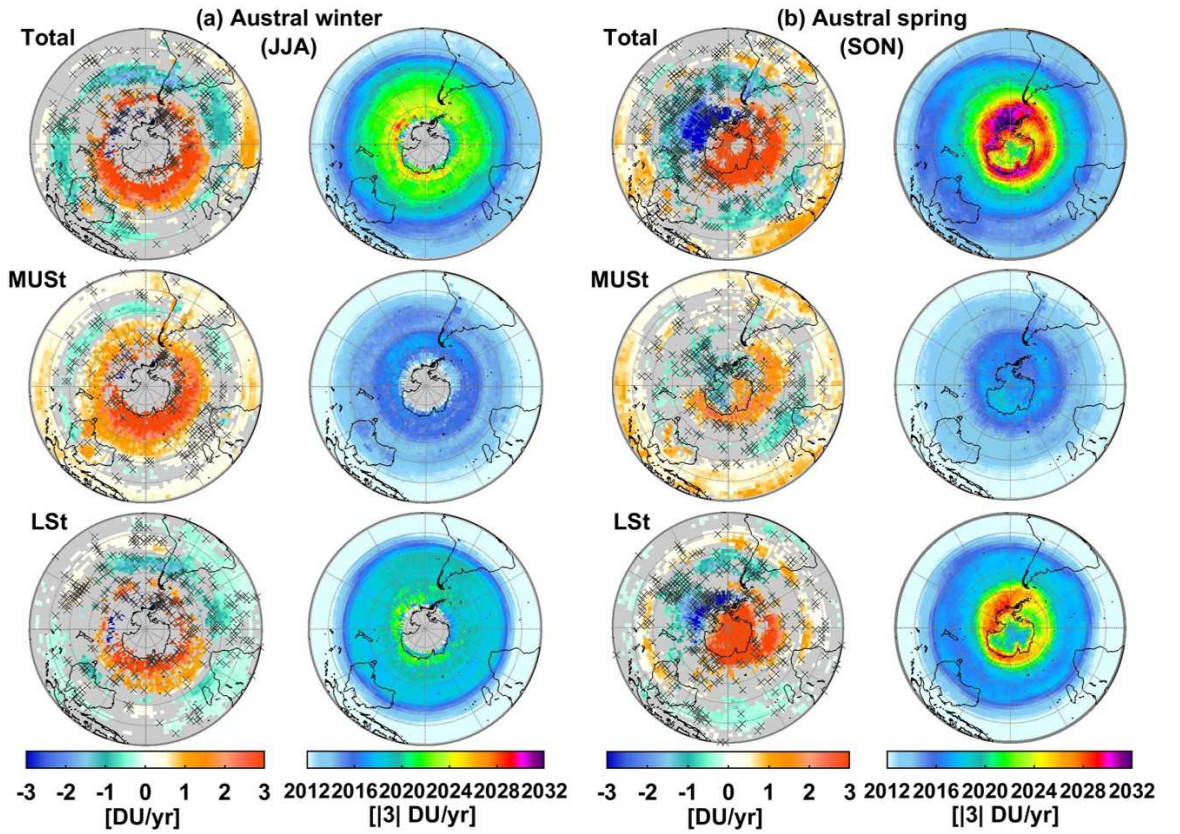

Fig.10: Hemispheric distribution (a) in austral winter (JJA) and (b) in austral spring (SON) of the estimated trends in total, MUSt and LSt O_3 columns (left panels: top, middle and bottom, respectively; in DU/yr; the grey areas and crosses refer to the non-significant grid cells in the 95% confidence limits) and of the corresponding estimated year for a significant trend detection (with a probability of 90%) of a given trend of |3| DU/yr starting at January 2008 (right panels: top, middle and bottom, respectively).

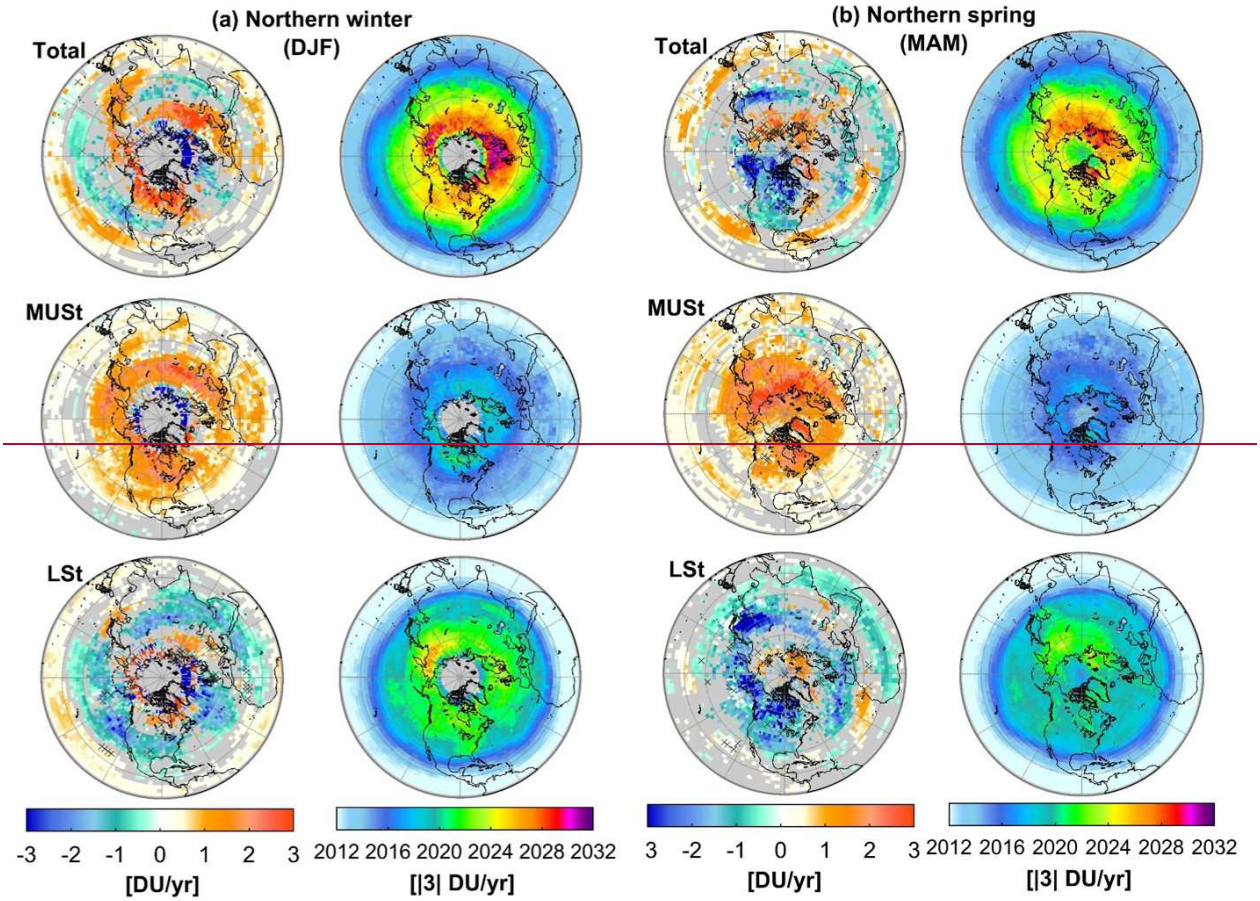
(a) Northern winter
(DJF)
(b) Northern spring
(MAM)
Total
Total
MUSt
MUSt
LSt
LSt
-3 -2 -1 0 1 2 3
[DU/yr]
2012 2016 2020 2024 2028 2032
[|3| DU/yr]
3 -2 -1 0 1 2 3
[DU/yr]
2012 2016 2020 2024 2028 2032
[|3| DU/yr]

1033

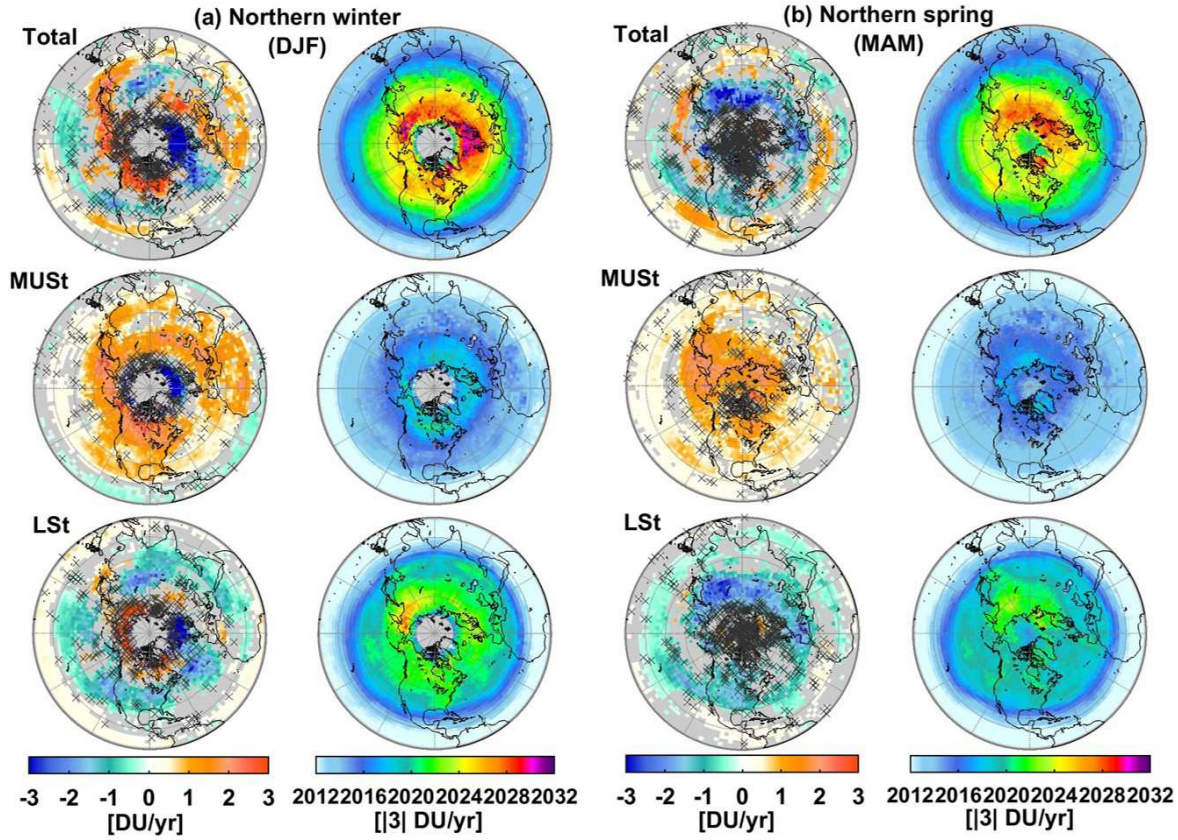

Fig. 11: Same as Fig. 10 but (a) for the winter (DJF) and (b) for the spring (MAM) of the northern Hemisphere.

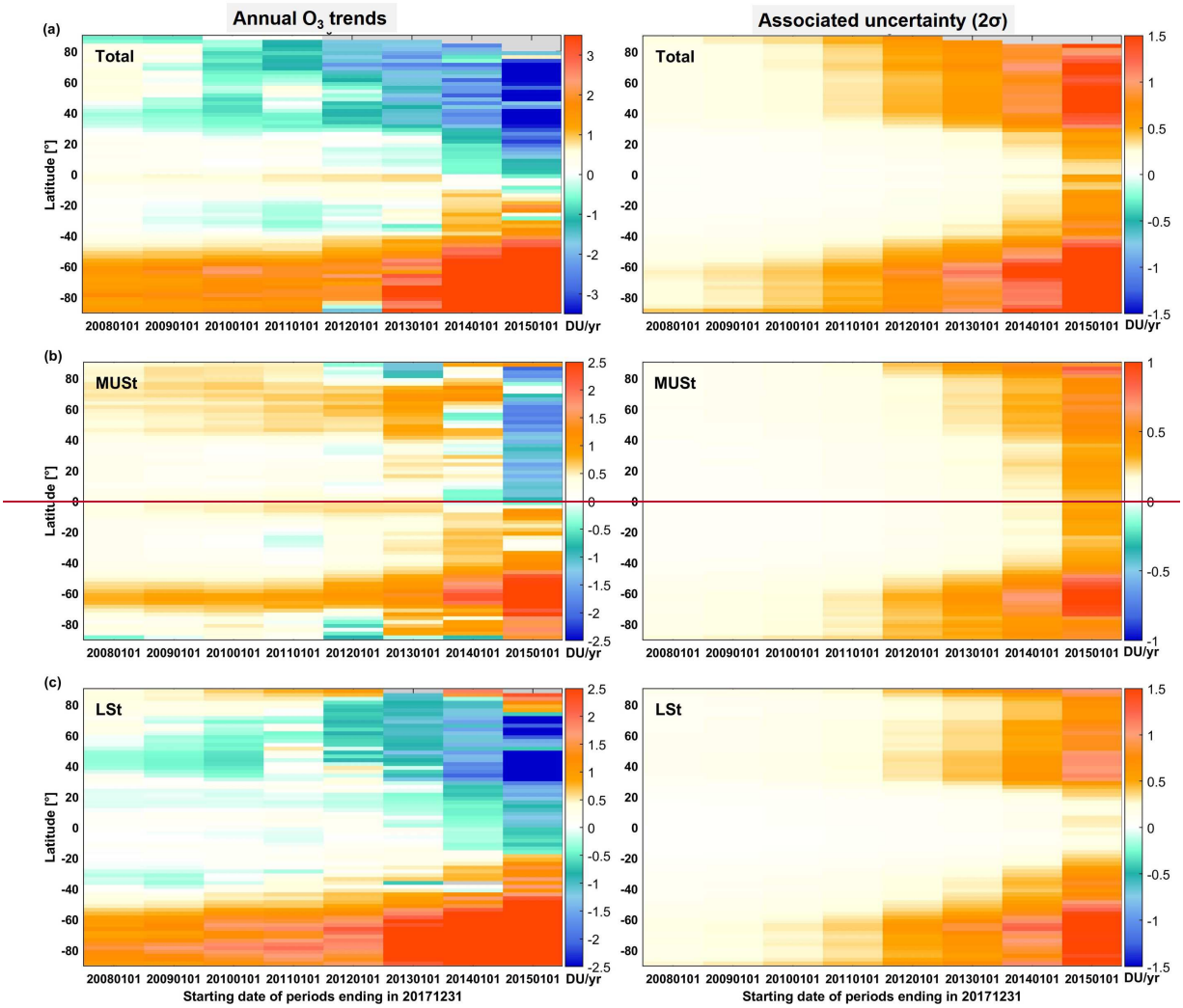
Annual O_3 trends
Associated uncertainty (2σ)
(a)
Total
(b)
MUSt
(c)
LSt
Latitude [°]
DU/yr
20080101 20090101 20100101 20110101 20120101 20130101 20140101 20150101
Starting date of periods ending in 20171231

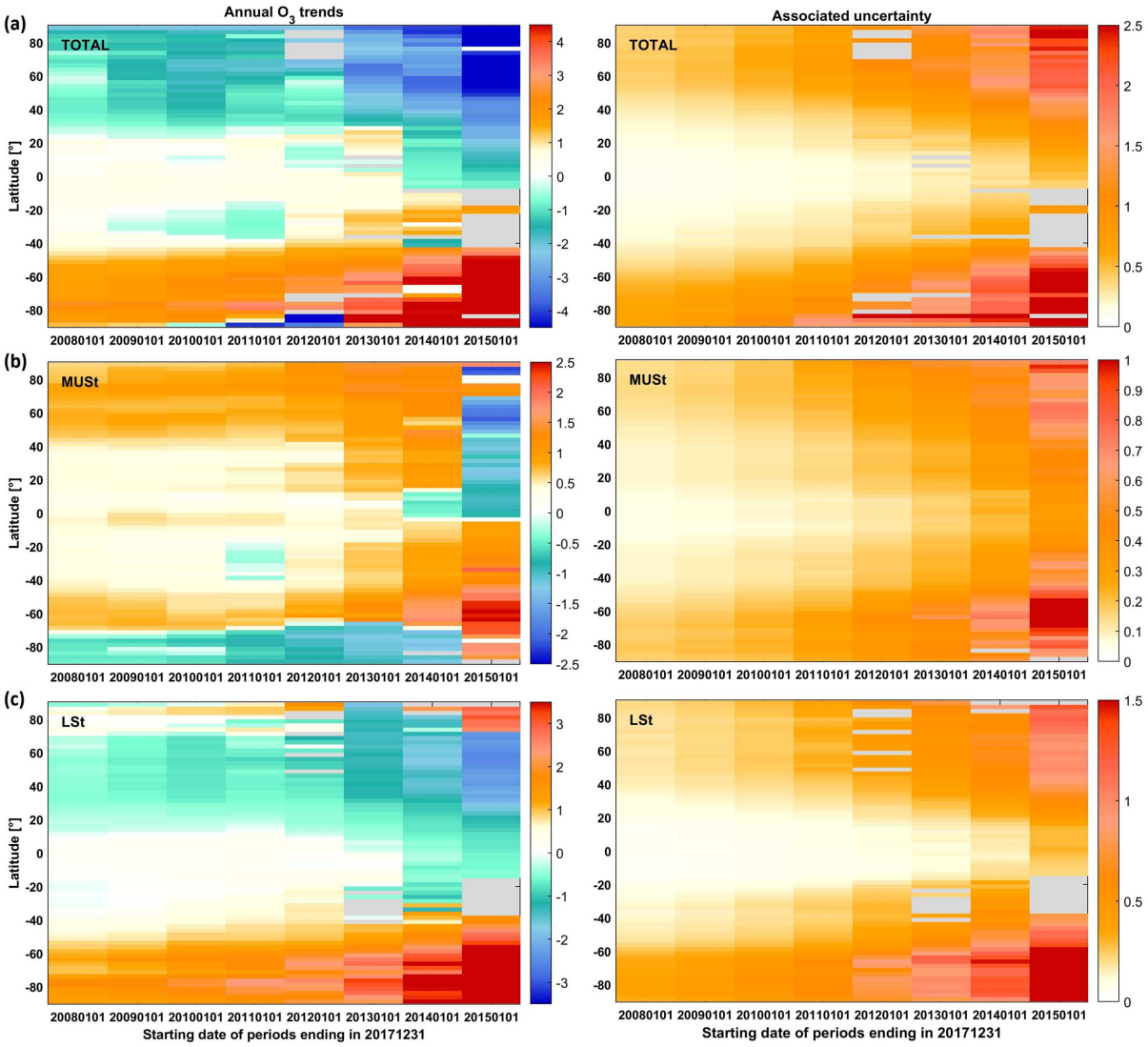

Fig.12: Evolution of estimated linear trend (DU/yr) and associated uncertainty accounting for the autocorrelation in the noise residuals (DU/yr; in the 95% confidence level) in (a) total, (b) MUSt and (c) LSt O_3 columns, as a function of the covered IASI measurement period ending in December 2017, with all natural contributions estimated from the whole IASI period (2008-2017). Note that the scales are different between the columns.

References

Anderson, J., Russell, J. M., Solomon, S., and Deaver, L. E.: Halogen Occultation Experiment confirmation of stratospheric chlorine decreases in accordance with the Montreal Protocol, J. Geophys. Res.-Atmos., 105, 4483–4490, https://doi.org/10.1029/1999JD901075, 2000.

Baldwin, M. P., L.J. Gray, T.J. Dunkerton, K. Hamilton, P.H. Haynes, W.J. Randel, J.R. Holton, M.J. Alexander, I. Hirota, T. Horinouchi, D.B.A. Jones, J.S. Kinnersley, C. Marquardt, K. Sato, and M. Takahashi: The quasi-biennial oscillation, Rev. Geophys., 39, 179–230, doi:10.1029/1999RG000073, 2001.

Ball, W. T., Alsing, J., Mortlock, D. J., Staehelin, J., Haigh, J. D., Peter, T., Tummon, F., Stübi, R., Stenke, A., Anderson, J., Bourassa, A., Davis, S. M., Degenstein, D., Frith, S., Froidevaux, L., Roth, C., Sofieva, V., Wang, R., Wild, J., Yu, P., Ziemke, J. R., and Rozanov, E. V.: Evidence for a continuous decline in lower stratospheric ozone offsetting ozone layer recovery, Atmos. Chem. Phys., 18, 1379–1394, https://doi.org/10.5194/acp-18-1379-2018, 2018.

Barnston, A. G. and Livezey, R. E.: Classification, seasonality and persistence of low-frequency atmospheric circulation patterns, Mon. Weather. Rev. 115: 1083–1126, 1987.

Boynard, A., D. Hurtmans, K. Garane, F. Goutail, J. Hadji-Lazaro, M. E. Koukouli, C. Wespes, C. Vigouroux, A. Keppens, J.-P. Pommereau, A. Pazmino, D. Balis, D. Loyola, P. Valks, R. Sussmann, D. Smale, P.-F. Coheur and C. Clerbaux: Validation of the IASI FORLI/Eumetsat O_3 products using satellite (GOME-2), ground-based (Brewer-Dobson, SAOZ, FTIR) and ozonesonde measurements, Atmos. Meas. Tech., 11, 5125–5152, 2018.

Brasseur, G.: The response of the middle atmosphere to long-term and short-term solar variability: A two-dimensional model, J. Geophys. Res., 98, 23 079–23 090, 1993.

Brönnimann, S., Luterbacher, J., Staehelin, J., Svendby, T. M., Hansen, G., and Svenøe, T.: Extreme climate of the global troposphere and stratosphere 1940–1942 related to El Nino, Nature, 431, 971–974, 2004.

Brunner, D., Staehelin, J., Maeder, J. A., Wohltmann, I., and Bodeker, G. E.: Variability and trends in total and vertically resolved stratospheric ozone based on the CATO ozone data set, Atmos. Chem. Phys., 6, 4985–5008, doi:10.5194/acp-6-4985-2006, 2006.

Buffet, L., Villaret, C., Jacquette, E., Vandermarcq, O., Astruc, P., and Anstötz, S.: Status of IASI instruments onboard Metop-A and Metop-B satellites, 4th IASI International Conference, Antibes Juan-Les-Pins, France, 11–15 April 2016, available at: https://iasi.cnes.fr/sites/default/files/drupal/201612/default/bpc_iasi-conference4-1_02_instruments_buffet.pdf (last access: 30 August 2018), 2016.

Butler, A. H., M. Polvani, and C. Deser: Separating the stratospheric and tropospheric pathways of El Niño–Southern Oscillation teleconnections, Environ. Res. Lett., 9, 2, 024014, doi:10.1088/1748-9326/9/2/024014, 2014.

Cagnazzo, C., E. Manzini, N. Calvo, A. Douglass, H. Akiyoshi, S. Bekki, M. Chipperfield, M. Dameris, M. Deushi, A. M. Fischer, H. Garny, A. Gettelman, M. A. Giorgetta, D. Plummer, E. Rozanov, T. G. Shepherd, K. Shibata, A. Stenke, H. Struthers and W. Tian: Northern winter stratospheric temperature and ozone responses to ENSO inferred from an ensemble of Chemistry Climate Models, Atmos. Chem. Phys., 9, 8935–8948, www.atmos-chem-phys.net/9/8935/2009/, 2009.

Chabrillat, S., Vigouroux, C., Christophe, Y., Engel, A., Errera, Q., Minganti, D., Monge-Sanz, B. M., Segers, A., and Mahieu, E.: Comparison of mean age of air in five reanalyses using the BASCOE transport model, Atmos. Chem. Phys., 18, 14715-14735, 2018.

Chipperfield, M. P., Kinnersley, J. S., and Zawodny, J.: A twodimensional model study of the QBO signal in SAGE II NO_2 and O_3, Geophys. Res. Lett., 21, 589–592, 1994.

Chubachi, S.: Preliminary results of ozone observations at Syowa Station from February 1982 to January 1983, in: Proc. Sixth Symposium on Polar Meteorology and Glaciology, edited by: Kusunoki, K., vol. 34 of Mem. National Institute of Polar Research Special Issue, 13–19, 1984.

Clarisse, L., Clerbaux, C., Franco, B., Hadji-Lazaro, J., Whitburn, S., Kopp, A. K., D. Hurtmans and P.-F. Coheur: A decadal data set of global atmospheric dust retrieved from IASI satellite measurements, J. Geophys. Res., 124, https://doi.org/10.1029/2018JD029701, 2019.

Coldewey-Egbers, M., D. G. Loyola R., P. Braesicke, M. Dameris, M. van Roozendael, C. Lerot, and W. Zimmer: A new health check of the ozone layer at global and regional scales, Geophys. Res. Lett., 41, 4363–4372, doi:10.1002/2014GL060212, 2014.

Clerbaux, C., A. Boynard, L. Clarisse, M. George, J. Hadji-Lazaro, H. Herbin, D. Hurtmans, M. Pommier, A. Razavi, S. Turquety, C. Wespes, and P.-F. Coheur: Monitoring of atmospheric composition using the thermal infrared IASI/MetOp sounder, Atmos. Chem. Phys., 9, 6041-6054, 2009.

Clerbaux, C. and Crevoisier, C.: New Directions: Infrared remote sensing of the troposphere from satellite: Less, but better, Atmos. Environ., 72, 24–26, 2013.

Cochrane, D. and Orcutt, G. H.: Application of least squares regression to relationships containing auto-correlated error terms, J. Am. Stat. Assoc., 44, 32–61, 1949.

Crevoisier, C., Clerbaux, C., Guidard, V., Phulpin, T., Armante, R., Barret, B., Camy-Peyret, C., Chaboureau, J.-P., Coheur, P.-F., Crépeau, L., Dufour, G., Labonnote, L., Lavanant, L., Hadji-Lazaro, J., Herbin, H., Jacquinet-Husson, N., Payan, S., Péquignot, E., Pierangelo, C., Sellitto, P., and Stubenrauch, C. : Towards IASI-New Generation (IASI-NG): impact of improved

spectral resolution and radiometric noise on the retrieval of thermodynamic, chemistry and climate variables, Atmos. Meas. Tech., 7, 4367-4385, 2014.

Crutzen, P. J.: Estimates of possible future ozone reductions from continued use of fluoro-chloro-methanes (CF2Cl2, CFCl3), Geophys. Res. Lett., 1, 205–208, https://doi.org/10.1029/GL001i005p00205, 1974.

Dhomse, S., Weber, M., Wohltmann, I., Rex, M., and Burrows, J. P.: On the possible causes of recent increases in northern hemispheric total ozone from a statistical analysis of satellite data from 1979 to 2003, Atm. Chem. Phys., 6, 1165–1180, 2006.

Dhomse, S. S., Chipperfield, P., Feng, W., Hossaini, R., Mann G. W., and Santee, M. L.: Revisiting the hemispheric asymmetry in midlatitude ozone changes following the Mount Pinatubo eruption: A 3-D model study, Geophys. Res. Lett., 42, 3038–3047, 2015.

Domeisen, D. I., Garfinkel, C. I., and Butler, A. H.: The teleconnection of El Niño Southern Oscillation to the stratosphere, Reviews of Geophysics, 57. https://doi.org/10.1029/2018RG000596, 2019.

Errera, Q., S. Chabrillat, Y. Christophe, J. Debosscher, D. Hubert, W. Lahoz, M. Santee, M. Shiotani, S. Skachko, T. von Clarmann, and K. Walker: Reanalysis of Aura MLS Chemical Observations submitted to Atms. Chem. Phys. Discuss., doi:10.5194/acp-2019-530, 2019.

Farman, J. C., Gardiner, B. G., and Shanklin, J. D.: Large losses of total ozone in Antarctica reveal seasonal ClOx/NOx interaction, Nature, 315, 207–210, doi:10.1038/315207a0, 1985.

Farmer, C. B., G. C. Toon, P. W. Shaper, J. F. Blavier, and L. L. Lowes, Stratospheric trace gases in the spring 1986 Antarctic atmosphere, Nature, 329, 126–130, 1987.

Fioletov, V. E. and Shepherd, T. G.: Seasonal persistence of midlatitude total ozone anomalies, Geophys. Res. Lett., 30, 1417, doi:10.1029/2002GL016739, 2003.

Fioletov, V. E. and Shepherd, T. G.: Summertime total ozone variations over middle and polar latitudes, Geophys. Res. Lett, 32, 4807, doi:10.1029/2004GL022080, 2005.

Fishman, J., J.K. Creilson, A.E. Wozniak, and P.J. Crutzen, The interannual variability of stratospheric and tropospheric ozone determined from satellite measurements, J. Geophys. Res., 110, D20306, doi:10.1029/2005JD005868, 2005.

Frossard, L., H.E. Rieder, M. Ribatet, J. Staehelin, J. A, Maeder, S. Di Rocco, A. C. Davison, T. Pete.: On the relationship between total ozone and atmospheric dynamics and chemistry at mid-latitudes – Part 1: Statistical models and spatial fingerprints of atmospheric dynamics and chemistry, Atmos. Chem. Phys., 13, 147–164, doi:10.5194/acp-13-147-2013, 2013.

Fusco, A. C. and Salby, M. L.: Interannual variations of total ozone and their relationship to variations of planetary wave activity, J. Clim., 12, 1619–1629, 1999.

Galytska, E., Rozanov, A., Chipperfield, M. P., Dhomse, Sandip. S., Weber, M., Arosio, C., Feng, W., and Burrows, J. P.: Dynamically controlled ozone decline in the tropical mid-stratosphere observed by SCIAMACHY, Atmos. Chem. Phys., 19, 767-783, https://doi.org/10.5194/acp-19-767-2019, 2019.

Gebhardt, C., Rozanov, A., Hommel, R., Weber, M., Bovensmann, H., Burrows, J. P., Degenstein, D., Froidevaux, L., and Thompson, A. M.: Stratospheric ozone trends and variability as seen by SCIAMACHY from 2002 to 2012, Atmos. chem. Phys., 14, 831–846, https://doi.org/10.5194/acp-14-831-2014, 2014.

Harris, N. R. P., Hassler, B., Tummon, F., Bodeker, G. E., Hubert, D., Petropavlovskikh, I., Steinbrecht, W., Anderson, J., Bhartia, P. K., Boone, C. D., Bourassa, A., Davis, S. M., Degenstein, D., Delcloo, A., Frith, S. M., Froidevaux, L., Godin-Beekmann, S., Jones, N., Kurylo, M. J., Kyrölä, E., Laine, M., Leblanc, S. T., Lambert, J.-C., Liley, B., Mahieu, E., Maycock, A., De Mazière, M., Parrish, A., Querel, R., Rosenlof, K. H., Roth, C., Sioris, C., Staehelin, J., Stolarski, R. S., Stübi, R., Tamminen, J., Vigouroux, C., Walker, K. A., Wang, H. J., Wild, J., and Zawodny, J. M.: Past changes in the vertical distribution of ozone – Part 3: Analysis and interpretation of trends, Atmos. Chem. Phys., 15, 9965-9982, https://doi.org/10.5194/acp-15-9965-2015, 2015.

Harrison, D. E., and Larkin, N. K.: El Niño-Southern Oscillation sea surface temperature and wind anomalies, 1946–1993, Rev. Geophys., 36, 353–399, doi:10.1029/98RG00715, 1998.

Hilton, F., R. Armante, T. August, et al. : Hyperspectral Earth Observation from IASI: Five Years of Accomplishments, Bulletin of the American Meteorological Society, vol. 93, issue 3, pp. 347-370, 2012.

Hofmann, D. J. and Solomon, S.: Ozone destruction through heterogeneous chemistry following the eruption of El Chichón, J. Geophys. Res., 94, 5029, https://doi.org/10.1029/JD094iD04p05029, 1989.

Hofmann, D. J., S. J. Oltmans, Antarctic ozone during 1992: Evidence for Pinatubo volcanic aerosol effects. J. Geophys. Res. 98, 18555–18561, doi:10.1029/93JD02092, 1993.

Hofmann, D. J., S. J. Oltmans, J. M. Harris, B. J. Johnson, and J. A. Lathrop: Ten years of ozonesonde measurements at the south pole: Implications for recovery of springtime Antarctic ozone, J. Geophys. Res., 102(D7), 8931– 8943, doi:10.1029/96JD03749, 1997.

Hood, L. L., McCormick, J. P., and Labitzke, K.: An investigation of dynamical contributions to midlatitude ozone trends in winter, J. Geophys. Res, 102, 13 079–13 093, 1997.

Hood, L. L., and B. E. Soukharev: Quasi-decadal variability of the tropical lower stratosphere: The role of extratropical wave forcing, J. Atmos. Sci., 60, 2389–2403, 2003.

Hood, L. L., and B. E. Soukharev: Solar induced variations of odd nitrogen: Multiple regression analysis of UARS HALOE data, Geophys. Res. Lett., doi:10.1029/2006GL028122, 2006.

Hubert, D., Lambert, J.-C., Verhoelst, T., Granville, J., Keppens, A., Baray, J.-L., Bourassa, A. E., Cortesi, U., Degenstein, D. A., Froidevaux, L., Godin-Beekmann, S., Hoppel, K. W., Johnson, B. J., Kyrölä, E., Leblanc, T., Lichtenberg, G., Marchand, M., McElroy, C. T., Murtagh, D., Nakane, H., Portafaix, T., Querel, R., Russell III, J. M., Salvador, J., Smit, H. G. J., Stebel, K., Steinbrecht, W., Strawbridge, K. B., Stübi, R., Swart, D. P. J., Taha, G., Tarasick, D. W., Thompson, A. M., Urban, J., van Gijsel, J. A. E., Van Malderen, R., von der Gathen, P., Walker, K. A., Wolfram, E., and Zawodny, J. M.: Ground-based assessment of the bias and long-term stability of 14 limb and occultation ozone profile data records, Atmos. Meas. Tech., 9, 2497-2534, https://doi.org/10.5194/amt-9-2497-2016, 2016.

Hurrell, J. W.: Decadal trends in the North Atlantic Oscillation regional temperatures and precipitation, Science, 269, 676–679, 1995.

Hurtmans, D., P. Coheur, C.Wespes, L. Clarisse, O. Scharf, C. Clerbaux, J. Hadji-Lazaro, M. George, and S. Turquety: FORLI radiative transfer and retrieval code for IASI, Journal of Quantitative Spectroscopy and Radiative Transfer, 113, 1391-1408, 2012.

Jackman, C., E. Fleming, and F. Vitt: Influence of extremely large solar proton events in a changing stratosphere, J. Geophys. Res., 105, 11 659–11 670, 2000.

Jonsson, A. I., de Grandpré, J., Fomichev, V. I., McConnell, J. C., and Beagley, S. R.: Doubled CO2-induced cooling in the middle atmosphere: photochemical analysis of the ozone radiative feedback, J. Geophys. Res., 109, D24103, https://doi.org/10.1029/2004JD005093, 2004.

Kalnay, E., M. Kanamitsu, R. Kistler, W. Collins, D. Deaven, L. Gandin, M. Iredell, S. Saha, G. White, J. Woollen, Y. Zhu, M. Chelliah, W. Ebisuzaki, W. Higgins, J. Janowiak, K.C. Mo, C. Ropelewski, J. Wang, A. Leetmaa, R. Reynolds, R. Jenne, and D. Joseph, 1996: The NCEP/NCAR 40-Year Reanalysis Project. Bull. Amer. Meteor. Soc., 77, 437–472, https://doi.org/10.1175/1520-0477, 1996.

Keeble, J., Brown, H., Abraham, N. L., Harris, N. R. P., and Pyle, J. A.: On ozone trend detection: using coupled chemistry–climate simulations to investigate early signs of total column ozone recovery, Atmos. Chem. Phys., 18, 7625-7637, https://doi.org/10.5194/acp-18-7625-2018, 2018.

Keppens, A., J.-C. Lambert, J. Granville, D. Hubert, T. Verhoelst, S. Compernolle, B. Latter, B. Kerridge, R. Siddans, A. Boynard, J. Hadji-Lazaro, C. Clerbaux, C. Wespes, D. R. Hurtmans, P.-F. Coheur, J. van Peet, R. van der A, K. Garane, M. E. Koukouli, D. S. Balis, A. Delcloo, R. Kivi, R. Stübi, S. Godin-Beekmann, M. Van Roozendael, C. Zehner: Quality assessment of the

Ozone_cci Climate Research Data Package (release 2017): 2. Ground-based validation of nadir ozone profile data products, in preparation for this QOS special issue.

Kyrölä, E., Laine, M., Sofieva, V., Tamminen, J., Päivärinta, S.-M., Tukiainen, S., Zawodny, J., and Thomason, L.: Combined SAGE II-GOMOS ozone profile data set for 1984–2011 and trend analysis of the vertical distribution of ozone, Atmos. Chem. Phys., 13, 10645–10658, https://doi.org/10.5194/acp-13-10645-2013, 2013.

Kodera, K. and Kuroda, Y.: Dynamical response to the solar cycle: Winter stratopause and lower stratosphere, J. Geophys. Res., 107, 4749, doi:310.1029/2002JD002224, 2002.

Kuttippurath, J., F. Lefèvre, J.-P. Pommereau, H. K. Roscoe, F. Goutail, A. Pazmiño, J. D. Shanklin, Antarctic ozone loss in 1979–2010: First sign of ozone recovery. Atmos. Chem. Phys. 13, 1625–1635, doi:10.5194/acp-13-1625-2013, 2013.

Kuttippurath, J., and P.J. Nair: The signs of Antarctic ozone hole recovery 2017, Scientific Reports, **7**, 585, doi:10.1038/s41598-017-00722-7, 2017.

Labitzke, K. and van Loon, H.: The QBO effect on the solar signal in the global stratosphere in the winter of the Northern Hemisphere, J. Atmos. Solar-Terr. Phys., 62, 621–628, 2000.

Mäder, J. A., J. Staehelin, D. Brunner, W.A. Stahel, I. Wohltmann, and T. Peter: Statistical modelling of total ozone: Selection of appropriate explanatory variables, J. Geophys. Res., 112, D11108, doi:10.1029/2006JD007694, 2007.

Mäder, J. A., J. Staehelin, T. Peter, D. Brunner, H. E. Rieder, and W. A. Stahel: Evidence for the effectiveness of the Montreal Protocol to protect the ozone layer, Atmos. Chem. Phys., 10, 24, 12,161–12,171, doi:10.5194/acp-10-12161-2010, 2010.

Manatsa, D. and G. Mukwada: A connection from stratospheric ozone to El Niño-Southern Oscillation, Scientific Reports, 7, *5558*, DOI:10.1038/s41598-017-05111-8, 2017.

Manzini, E., Giorgetta, M. A., Esch, M., Kornblueh, L., and Roeckner, E.: The influence of sea surface temperatures on the northern winter stratosphere: Ensemble simulations with the MAECHAM5 model, J. Climate, 19, 3863–3881, 2006.

McCormack, J. P., D. E. Siskind, and L. L. Hood: Solar-QBO interaction and its impact on stratospheric ozone in a zonally averaged photochemical transport model of the middle atmosphere, *J. Geophys. Res.*, 112, D16109, doi:10.1029/2006JD008369, 2007.

McPeters, R. D., G.J. Labow, and J.A. Logan: Ozone climatological profiles for satellite retrieval algorithms, J. Geophys. Res.-Atmos., 112, D05308, doi:10.1029/2005JD006823, 2007.

Molina, M. J. and Rowland, F. S.: Stratospheric sink for chlorofluoromethanes: Chlorine atom-catalysed destruction of ozone, Nature, 249, 810–812, 1974.

Nair, P. J., Froidevaux, L., Kuttippurath, J., Zawodny, J. M., Russell, J. M., Steinbrecht, W., Claude, H., Leblanc, T., van Gijsel, J. A. E., Johnson, B., Swart, D. P. J., Thomas, A., Querel, R., Wang, R., and Anderson, J.: Subtropical and midlatitude ozone trends in the stratosphere: Implications for recovery, J. Geophys. Res.-Atmos., 120, 7247–7257, https://doi.org/10.1002/2014JD022371, 2015.

Newchurch, M. J., Yang, E.-S., Cunnold, D. M., Reinsel, G. C., Zawodny, J. M., and Russell III, J. M.: Evidence for slowdown in stratospheric ozone loss: First stage of ozone recovery, J. Geophys. Res., 108, 4507, doi:10.1029/2003JD003471, 2003.

Newman, P. A., Nash, E. R., Kawa, S. R., Montzka, S. A., and Schauffler, S. M.: When will the Antarctic ozone hole recover?: Geophys. Res. Lett., 33, L12814, doi:10.1029/2005GL025232, 2006.

Oman, L. D., Douglass, A. R., Ziemke, J. R., Rodriguez, J. M., Waugh, D. W., and Nielsen, J. E.: The ozone response to ENSO in Aura satellite measurements and a chemistry–climate simulation, J. Geophys. Res.-Atmos., 118, 965–976, 2013.

Pawson, S., Steinbrecht, W., Charlton-Perez, A J Fujiwara, M., Karpechko, A. Y., Petropavlovskikh, I., Urban, J., and Weber, M.: Update on Global Ozone: Past, Present, and Future, in: Scientific Assessment of Ozone Depletion: 2014, World Meteorological Organization, Global Ozone Research and Monitoring Project – Report No. 55, chap. 2, World Meteorological Organization/UNEP, 2014.

Portmann, R. W., S. Solomon, R. R. Garcia, L. W. Thomason, L. R. Poole, M. P. McCormick, Role of aerosol variations in anthropogenic ozone depletion in the polar regions. J. Geophys. Res. 101, 22991–23006, doi:10.1029/96JD02608, 1996.

Knudsen, B. M. and Grooss, J.: Northern midlatitude stratospheric ozone dilution in spring modeled with simulated mixing, J. Geophys. Res., 105, 6885–6890, 2000.

Randel, W. J. and Cobb, J. B.: Coherent variations of monthly mean total ozone and lower stratospheric temperature, J. Geophys. Res.-Atmos., 99, 5433–5447, 1994.

Randel, W. J. and F. Wu: Isolation of the ozone QBO in SAGE II data by singular-value decomposition, J. Atmos. Sci., 53, 2546– 2559, 1996.

Randel, W. J., F. Wu, and R. Stolarski: Changes in column ozone correlated with the stratospheric EP flux, J. Meteorol. Soc. Jpn., 80, 849–862, 2002.

Randel, W. J., Garcia, R. R., Calvo, N., and Marsh, D.: ENSO influence on zonal mean temperature and ozone in the tropical lower stratosphere, Geophys. Res. Lett., 36, L15822, https://doi.org/10.1029/2009GL039343, 2009.

Randel, W. J., and A. M. Thompson: Interannual variability and trends in tropical ozone derived from SAGE II satellite data and SHADOZ ozonesondes, J. Geophys. Res., 116, D07303, doi:10.1029/2010JD015195, 2011.

Reinsel, G. C., Miller, A. J., Weatherhead, E. C., Flynn, L. E., Nagatani, R. M., Tiao, G. C., and Wuebbles, D. J.: Trend analysis of total ozone data for turnaround and dynamical contributions, J. Geophys. Res., 110, D16306, doi:10.1029/2004JD004662, 2005.

Revell, L. E., Stenke, A., Luo, B., Kremser, S., Rozanov, E., Sukhodolov, T., and Peter, T.: Impacts of Mt Pinatubo volcanic aerosol on the tropical stratosphere in chemistry–climate model simulations using CCMI and CMIP6 stratospheric aerosol data, Atmos. Chem. Phys., 17, 13139-13150, 2017.

Rex, M., Salawitch, R. J., von der Gathen, P., Harris, N. R. P., Chipperfield, M. P., and Naujokat, B.: Arctic ozone loss and climate change, Geophys. Res. Lett., 32, L04116, doi:10.1029/2003GL018844, 2004.

Rieder, H. E., Frossard, L., Ribatet, M., Staehelin, J., Maeder, J. A., Di Rocco, S., Davison, A. C., Peter, T.,Weihs, P., and Holawe, F.: On the relationship between total ozone and atmospheric dynamics and chemistry at mid-latitudes – Part 2: The effects of the El Nino/Southern Oscillation, volcanic eruptions and contributions of atmospheric dynamics and chemistry to long-term total ozone changes, Atmos. Chem. Phys., 13, 165–179, 2013.

Rind, D., Perlwitz, J., and Lonergan, P.: AO/NAO response to climate change: 1. Respective influences of stratospheric and tropospheric climate changes, J. Geophys. Res., 110, D12107, doi: 10.1029/2004JD005103, 2005.

Rodgers, C. D.: Inverse Methods for Atmospheric Sounding: Theory and Practice, World Scientific, Series on Atmospheric, Oceanic and Planetary Physics, 2, Hackensack, N. J., 2000.

Salby, M., E. Titova, and L. Deschamps: Rebound of Antarctic ozone, *Geophys. Res. Lett.*, *38*, L09702, doi:10.1029/2011GL047266, 2011.

Schnadt, C. and Dameris, M.: Relationship between North Atlantic Oscillation changes and stratospheric ozone recovery in the Northern Hemisphere in a chemistry-climate model, J. Geophys. Res., 30, 1487, doi:10.1029/2003GL017006, 2003.

Shepherd, T. G., Plummer, D. A., Scinocca, J. F., Hegglin, M. I., Fioletov, V. E., Reader, M. C., Remsberg, E., von Clarmann, T., and Wang, H. J.: Reconciliation of halogen-induced ozone loss with the total-column ozone record, Nat. Geosci., 7, 443–449, https://doi.org/10.1038/ngeo2155, 2014.

Sioris, C. E., McLinden, C. A., Fioletov, V. E., Adams, C., Zawodny, J. M., Bourassa, A. E., Roth, C. Z., and Degenstein, D. A.: Trend and variability in ozone in the tropical lower

stratosphere over 2.5 solar cycles observed by SAGE II and OSIRIS, Atmos. Chem. Phys., 14, 3479–3496, https://doi.org/10.5194/acp-14-3479-2014, 2014.

Sofieva, V. F., Kyrölä, E., Laine, M., Tamminen, J., Degenstein, D., Bourassa, A., Roth, C., Zawada, D., Weber, M., Rozanov, A., Rahpoe, N., Stiller, G., Laeng, A., von Clarmann, T., Walker, K. A., Sheese, P., Hubert, D., van Roozendael, M., Zehner, C., Damadeo, R., Zawodny, J., Kramarova, N., and Bhartia, P. K.: Merged SAGE II, Ozone_cci and OMPS ozone profile dataset and evaluation of ozone trends in the stratosphere, Atmos. Chem. Phys., 17, 12533–12552, https://doi.org/10.5194/acp-17-12533-2017, 2017.

Solomon, S., R. R. Garcia, F. S. Rowland, and D. J. Wuebbles, On the depletion of Antarctic zone, Nature, 321, 755–758, 1986.

Solomon, S., Portman, R. W., Garcia, R. R., Thomason, L. W., Poole, L. R., and McCormack, M. P.: The role of aerosol variations in anthropogenic ozone depletion at northern midlatitudes, J. Geophys. Res., 101, 6713–6727, 1996.

Solomon, S.: Stratospheric ozone depletion: A review of concepts and history. Rev. Geophys. 37, 275–316, doi:10.1029/1999RG900008, 1999.

Solomon, P., Barrett, J., Mooney, T., Connor, B., Parrish, A., and Siskind, D. E.: Rise and decline of active chlorine in the stratosphere, Geophys. Res. Lett., 33, L18807, https://doi.org/10.1029/2006GL027029, 2006.

Solomon, S., Ivy, D. J., Kinnison, D., Mills, M. J., Neely, R. R., and Schmidt, A.: Emergence of healing in the Antarctic ozone layer, Science, 353, 269–274, https://doi.org/10.1126/science.aae0061, 2016.

Stolarski, R. S., A. J. Krueger, M. R. Schoeberl, R. D. Mc-Peters, P. A. Newman, and J. C. Alpert, Nimbus 7 satellite measurements of the springtime Antarctic ozone decrease, Nature, 322, 808–811, 1986.

Soukharev, B. E. and L. L. Hood: Solar cycle variation of stratospheric ozone: Multiple regression analysis of long-term satellite data sets and comparisons with models, J. Geophys. Res., 111, D20314, doi:10.1029/2006JD007107, 2006.

Steinbrecht, W., H. Claude, U. Köhler, and K. P. Hoinka: Correlations between tropopause height and total ozone: Implications for long-term changes, *J. Geophys. Res.*, *103*, 19,183–19,192, doi:10.1029/98JD01929, 1998.

Steinbrecht, W., B. Hassler, H. Claude, P. Winkler, and R. S. Stolarski: Global distribution of total ozone and lower stratospheric temperature variations, Atmos. Chem. Phys., 3, 1421–1438, 2003.

Steinbrecht, W., et al.: Interannual variation patterns of total ozone and lower stratospheric temperature in observations and model simulations, *Atmos. Chem. Phys.*, *6*, 349–374, doi:10.5194/acp-6-349-2006, 2006

Steinbrecht, W., Froidevaux, L., Fuller, R., Wang, R., Anderson, J., Roth, C., Bourassa, A., Degenstein, D., Damadeo, R., Zawodny, J., Frith, S., McPeters, R., Bhartia, P., Wild, J., Long, C., Davis, S., Rosenlof, K., Sofieva, V., Walker, K., Rahpoe, N., Rozanov, A., Weber, M., Laeng, A., von Clarmann, T., Stiller, G., Kramarova, N., Godin-Beekmann, S., Leblanc, T., Querel, R., Swart, D., Boyd, I., Hocke, K., Kämpfer, N., Maillard Barras, E., Moreira, L., Nedoluha, G., Vigouroux, C., Blumenstock, T., Schneider, M., García, O., Jones, N., Mahieu, E., Smale, D., Kotkamp, M., Robinson, J., Petropavlovskikh, I., Harris, N., Hassler, B., Hubert, D., and Tummon, F.: An update on ozone profile trends for the period 2000 to 2016, Atmos. Chem. Phys., 17, 10675–10690, doi:10.5194/acp-17-10675-2017, 2017.

Thomason, L. W., Ernest, N., Millán, L., Rieger, L., Bourassa, A., Vernier, J.-P., Manney, G., Luo, B., Arfeuille, F., and Peter, T.: A global space-based stratospheric aerosol climatology: 1979–2016, Earth Syst. Sci. Data, 10, 469-492, https://doi.org/10.5194/essd-10-469-2018, 2018.

Thompson, D. W. J. and J.M. Wallace: Annular modes in the extratropical circulation. Part I: month-to-month variability, J. Climate, 13, 1000–1016, 2000.

Thompson, D. W. J. and Solomon, S.: Interpretation of Recent Southern Hemisphere Climate Change, Science, 296, 895-899, 2002.

Tian, W., M.P. Chipperfield, L.J. Gray, and J.M. Zawodny: Quasi-biennial oscillation and tracer distributions in a coupled chemistry-climate model, J. Geophys. Res., 111, D20301, doi:10.1029/2005JD006871, 2006.

Tiao, G. C., G. C. Reinsel, D. Xu, J. H. Pedrick, X. Zhu, A. J. Miller, J. J. DeLuisi, C. L. Mateer, and D. J. Wuebbles, Effects of autocorrelation and temporal sampling schemes on estimates of trend and spatial correlation, J. Geophys Res., 95, 20,507-20,517, 1990.

Tweedy, O. V., Waugh, D. W., Randel, W. J., Abalos, M., Oman, L. D. and Kinnison, D. E.: The impact of boreal summer ENSO events on tropical lower stratospheric ozone, J.Geophys. Res., Atmospheres, 123, 9843–9857, doi:10.1029/2018JD029020, 2018.

Valks, P., N. Hao, S. Gimeno Garcia, D. Loyola, M. Dameris, P. Jöckel, and A. Delcloo: Tropical tropospheric ozone column retrieval for GOME-2, Atmos. Meas. Tech., 7, 2513–2530, doi:10.5194/amt-7-2513-2014, 2014.

Vigouroux, C., Blumenstock, T., Coffey, M., Errera, Q., García, O., Jones, N. B., Hannigan, J. W., Hase, F., Liley, B., Mahieu, E., Mellqvist, J., Notholt, J., Palm, M., Persson, G., Schneider, M.,Servais, C., Smale, D., Thölix, L., and De Mazière, M.: Trends of ozone total columns and vertical distribution from FTIR observations at eight NDACC stations around the globe, Atmos. Chem. Phys., 15, 2915–2933, https://doi.org/10.5194/acp-15-2915-2015, 2015.

Weatherhead, E.C., G. C. Reinsel, G. C. Tiao, X.-L. Meng, D. Choi, W.-K. Cheang, T. Keller, J. DeLuisi, D. J. Wuebbles, J. B. Kerr, A. J. Miller, S. J. Oltmans and J. E. Frederick: Factors affecting the detection of trends: Statistical considerations and applications to environmental data, J. Geophys. Res. Atmos., 103, 17149–17161, 1998.

Weber, M., Dikty, S., Burrows, J. P., Garny, H., Dameris, M., Kubin, A., Abalichin, J., and Langematz, U.: The Brewer-Dobson circulation and total ozone from seasonal to decadal time scales, Atmos. Chem. Phys., 11, 11221-11235, https://doi.org/10.5194/acp-11-11221-2011, 2011.

Weber, M., Coldewey-Egbers, M., Fioletov, V. E., Frith, S. M., Wild, J. D., Burrows, J. P., Long, C. S., and Loyola, D.: Total ozone trends from 1979 to 2016 derived from five merged observational datasets – the emergence into ozone recovery, Atmos. Chem. Phys., 18, 2097–2117, https://doi.org/10.5194/acp-18-2097-2018, 2018.

Wespes, C., D. Hurtmans, L.K. Emmons, S. Safieddine, C. Clerbaux, D.P. Edwards, and P.-F. Coheur: Ozone variability in the troposphere and the stratosphere from the first six years of IASI observations (2008-2013), Atmos. Chem. Phys., 16, 5721-5743, 2016.

Wespes, C., D. Hurtmans, C. Clerbaux, and P.-F. Coheur: O_3 variability in the troposphere as observed by IASI over 2008–2016 — Contribution of atmospheric chemistry and dynamics, J. Geophys. Res. Atmos., 122, 2429–2451, doi:10.1002/2016JD025875, 2017.

Wespes, C., Hurtmans, D., Clerbaux, C., Boynard, A., and Coheur, P.-F.: Decrease in tropospheric O_3 levels in the Northern Hemisphere observed by IASI, Atmos. Chem. Phys., 18, 6867–6885, https://doi.org/10.5194/acp-18-6867-2018, 2018.

Witte, J. C., M.R. Schoeberl, A.R. Douglass, and A.M. Thompson: The Quasi-biennial Oscillation and annual variations in tropical ozone from SHADOZ and HALOE, Atmos. Chem. Phys., 8, 3929–3936, 2008.

World Meterological Organization (WMO): Scientific Assessment of Ozone Depletion: 2006, Global Ozone Research and Monitoring Project, Report No. 50, Geneva, Switzerland, 2007.

World Meterological Organization (WMO): Scientific Assessment of Ozone Depletion: 2010, Global Ozone Research and Monitoring Project, Report No. 52, Geneva, Switzerland, 2011.

World Meterological Organization (WMO): Scientific Assessment of Ozone Depletion: 2014, Global Ozone Research and Monitoring Project, Report No. 55, Geneva, Switzerland, 2014.

World Meterological Organization (WMO): Scientific Assessment of Ozone Depletion: 2018, Global Ozone Research and Monitoring Project, Report No. 58, Geneva, Switzerland, 2018.

Wohltmann, I., R. Lehmann, M. Rex, D. Brunner, and J. A. Maeder: A process-oriented regression model for column ozone, *J. Geophys. Res.*, *112*, D12304, doi:10.1029/2006JD007573, 2007.

Yang, E.-S., D. M. Cunnold, M. J. Newchurch, R. J. Salawitch, M. P. McCormick, J. M. Russell III, J. M. Zawodny, S. J. Oltmans: First stage of Antarctic ozone recovery. J. Geophys. Res. 113, D20308, doi:10.1029/2007JD009675, 2008.

Zerefos, C. S., Tourpali, K., Bojkov, R., Balis, D., Rognerund, B., and Isaksen, I.: Solar acticity – total ozone relationships: observations and model studies with heterogeneous chemistry, J. Geophys. Res., 102, 1561–1569, 1997.

Ziemke, J. R., A.R. Douglass, L.D. Oman, S.E. Strahan, and B.N. Duncan: Tropospheric ozone variability in the tropics from ENSO to MJO and shorter timescales, Atmos. Chem. Phys., 15, 8037–8049, 2015.

Supplementary Information
for

~~**Speeding up in the stratospheric O_3 recovery of the Southern Hemisphere contrasting with the O_3 decline of the Northern Hemisphere as seen by IASI over 2008-2017**~~

Is the recovery of stratospheric O_3 speeding up in the Southern Hemisphere?
An evaluation from the first IASI decadal record

C. Wespes[1], D. Hurtmans[1], S. Chabrillat[2], G. Ronsmans[1], C. Clerbaux[1,3] and P.-F. Coheur[1]

[1] Chimie Quantique et Photophysique, Université Libre de Bruxelles, Brussels, Belgium
[2] Belgian Institute for Space Aeronomy, Brussels, Belgium
[3] LATMOS/IPSL, Sorbonne Université, UVSQ, CNRS, Paris, France

Contents of this file

Figure S1 displays the latitudinal distribution of MUSt O_3 columns as a function of time observed from IASI in comparison with that simulated by the BASCOE CTM with its standard chemical mechanism (smoothed by the IASI averaging kernels), as well as the IASI-BASCOE differences for the MUSt and the LSt O_3 columns (Fig. S1 a et b, respectively). Note that the BASCOE simulations are driven by offline meteorological fields from ERA-Interim and performed after a 1 year spin-up with a horizontal resolution of 2.0°×2.5° and 60 levels in the vertical. Details on chemical mechanisms and parameterizations can be found in Huijnen et al., (2016) and Chabrillat et al. (2018). The purpose of this comparison is not to perform a proper validation/comparison exercise but to highlight and to estimate the "Jump" amplitude that affects the IASI MUSt O_3 time series and for which the exact reasons are still unknown. The "jump" in the IASI time series is clearly visible in the IASI-BASCOE difference panel on 15th September 2010 in the MUSt (see black narrow in Fig. S1a), while not in the LSt, as previously reported in the validation paper of Boynard et al. (2018). Based on that IASI-BASCOE comparison, the jump is estimated as reaching ~1-2 DU in the 55°S–55°N band and ~3-4 DU in the 55°–90° bands. These values are considered when analyzing trends in the MUSt O_3 time series in Sections 4.1 to 4.3 of the paper.

Figure S2 represents three typical examples of gridded daily time series of O_3 measured by IASI in the LSt over the period 2008-2017, after the natural variations fitted from MLR over the full

IASI period have been removed. The significant fitted trends calculated over varying time periods from a single linear regression are superimposed. The trend values with associated uncertainties (in the 95% confidence level; in DU/yr) are indicated.

3 Figure S3

Figure S3 illustrates the time evolution of the lowest amplitude of the estimated trends in (a) total, (b) MUSt and (c) LSt O_3 columns over varying time periods that all end in December 2017, by subtracting the associated uncertainty (accounting for the autocorrelation in the noise residual; in the 95% confidence level) from the absolute value of the linear trends.

Figure caption

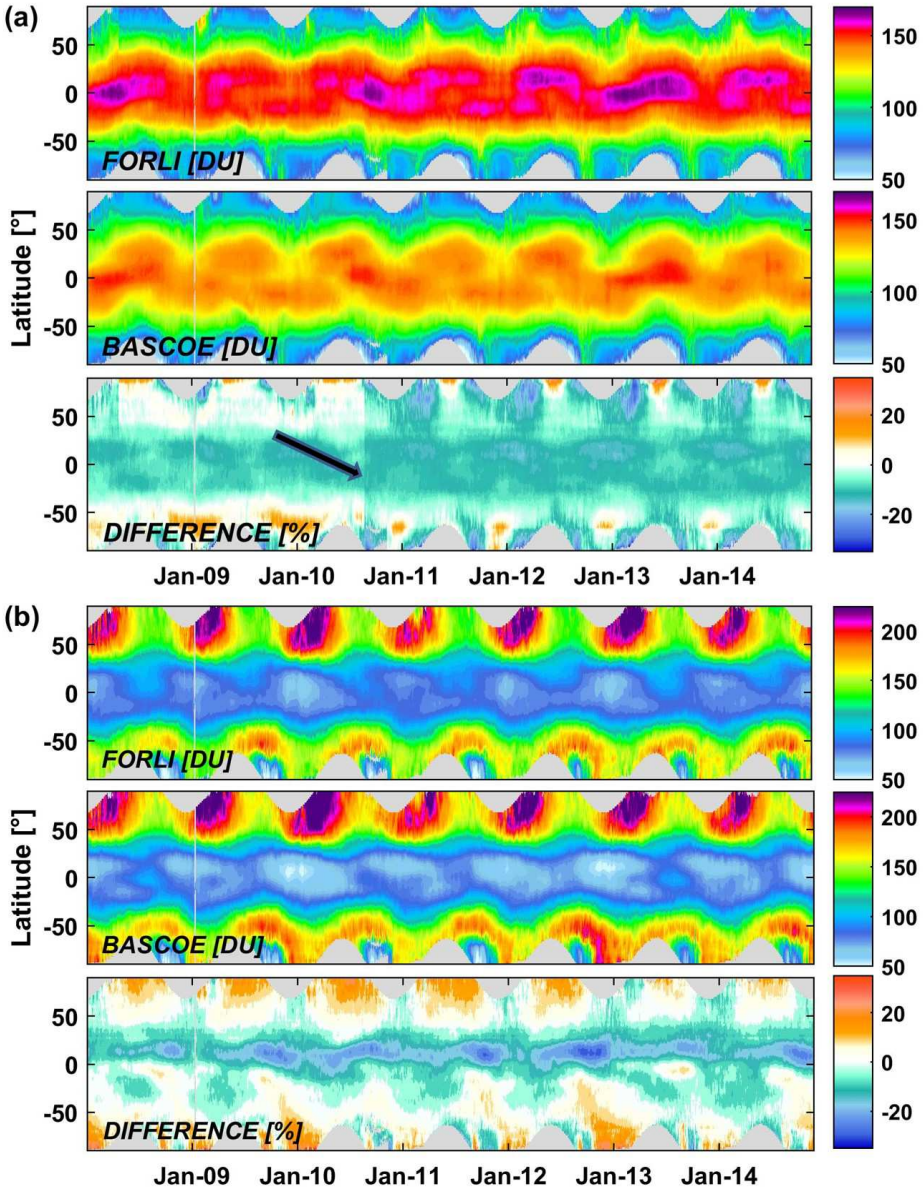

Fig.S1: Latitudinal distribution of (a) MUSt and (b) LSt O_3 columns as a function of time observed from IASI (in DU; top panels), simulated by BASCOE (in DU; middle panels) and of the IASI-BASCOE differences (in %; bottom panels). The black narrow in the difference panel for the MUSt highlights a jump on 15th September 2010.

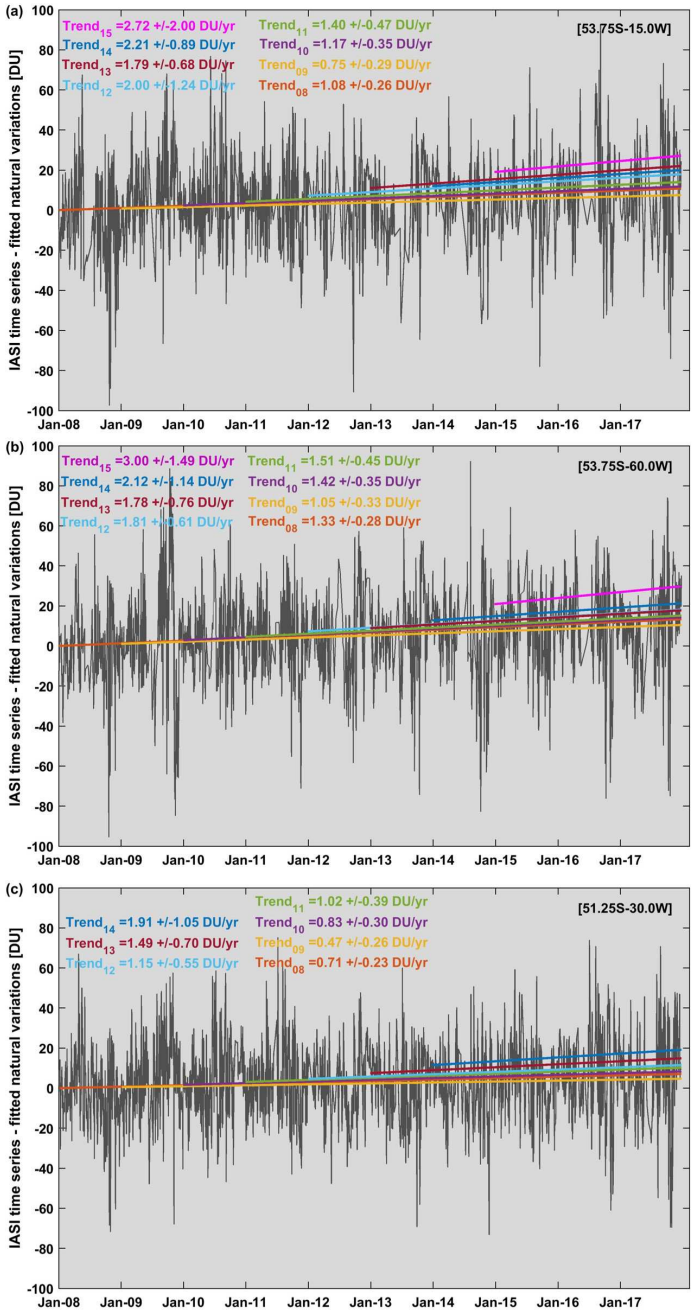

Fig. S2: Examples of gridded daily time series of O_3 measured by IASI in the LSt over the period 2008-2017 with all contributions to O_3 variations adjusted from MLR over the full IASI period removed, except for the trend (in DU). The significant fitted trends calculated over varying time periods from a single linear regression are superimposed. The trend values with associated uncertainties (in the 95% confidence level; in DU/yr) are indicated.

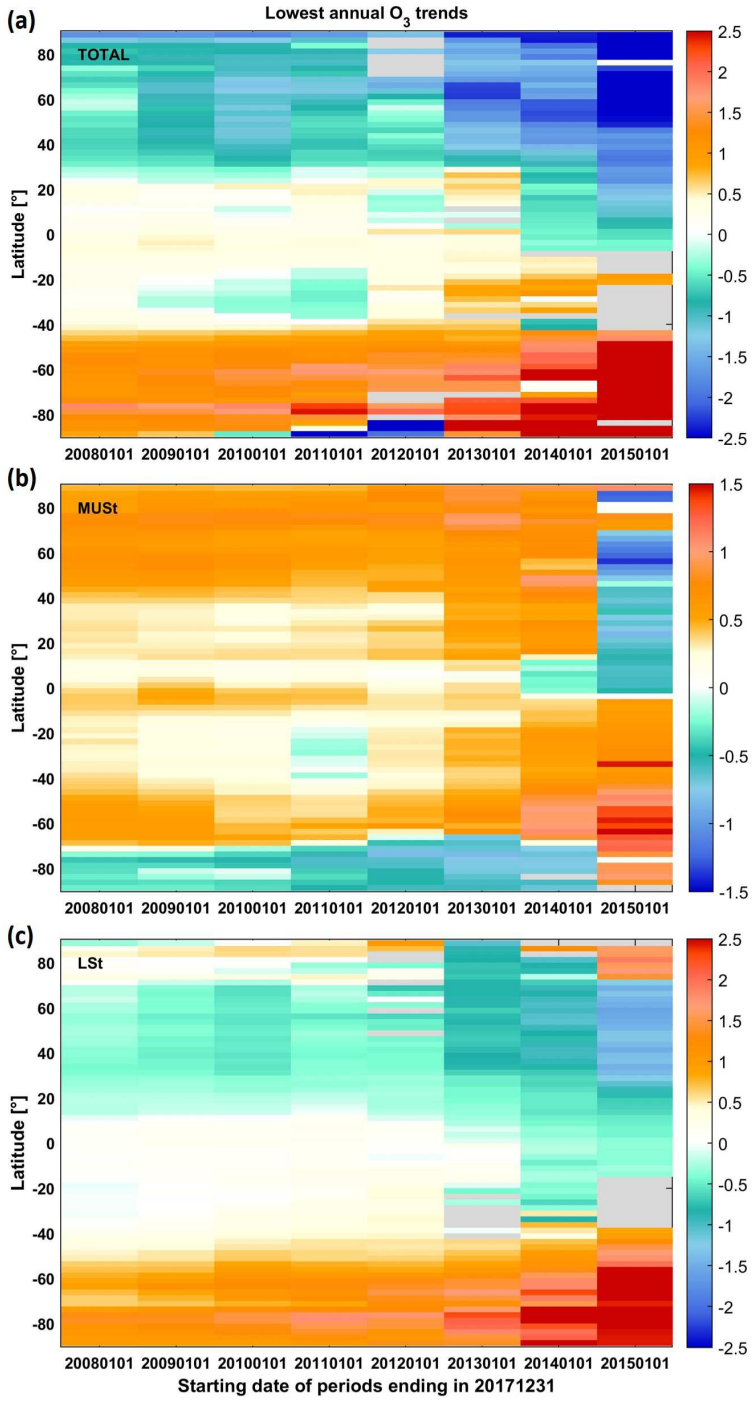

Fig. S3: Evolution of estimated linear trend minus the associated uncertainty accounting for the autocorrelation in the noise residual (DU/yr; in the 95% confidence level) in (a) the total, (b) the MUSt and (c) the LSt O_3 columns, as a function of the covered IASI measurement period ending in December 2017, with all natural contributions estimated over the full IASI period (2008-2017).